# PHYTOLITH EVIDENCE FOR THE PRESENCE AND ABUNDANCE OF WILD RICE (*ZIZANIA* spp.) FROM CENTRAL MINNESOTA LAKE SEDIMENTS

by

Chad L Yost

B.S., University of Minnesota, Minneapolis, 1995

A Thesis

Submitted to the Graduate Faculty

of

St. Cloud State University

in Partial Fulfillment of the Requirements

for the Degree

Master of Science

St. Cloud, Minnesota

May, 2007

This thesis submitted by Chad L Yost in partial fulfillment of the requirements for the Degree of Master of Science at St. Cloud State University is hereby approved by the final evaluation committee.

_____
Chairperson

_____

_____

_____

_____
Dean
School of Graduate Studies

PHYTOLITH EVIDENCE FOR THE PRESENCE AND ABUNDANCE OF WILD RICE (*ZIZANIA* spp.) FROM CENTRAL MINNESOTA LAKE SEDIMENTS

Chad L. Yost

The purpose of this study was to develop phytolith analysis as a tool to better understand the presence, abundance and paleodistribution of wild rice (*Zizania* spp. L.) from paleo lake sediment cores. Thirty-seven dominant study area plant species, divided into 180 plant-parts, were investigated for phytolith production, with extra emphasis on *Zizania* and *Leersia*. *Zizania palustris* was found to produce 23 locally diagnostic phytolith morphotypes that were used to calculate concentration and influx of wild rice phytoliths in modern and paleo lake sediments.

Methodologies optimized for the extraction, concentration and quantification of the phytolith fraction from highly organic lake sediments were developed, utilizing novel and established limnological techniques new to phytolith analysis.

Analysis of 21 modern sediment samples collected along transects across three different wild rice lakes indicated that *Zizania* phytolith deposition is spatially correlated with stand location and density of wild rice. However, lake morphology and bathymetry can have an effect on depositional patterns.

Analysis of 47 paleo lake sediment samples from two Lake Ogechie cores indicated that wild rice may have first appeared in Lake Ogechie approximately 4000 cal yr BP and persisted in relatively low numbers until an apparent population explosion starting approximately 1600 cal yr BP, which peaked at around 800 to 1000 cal yr BP. The archaeological record and oral histories by the Mille Lacs Band of Ojibwe suggest that Lake Ogechie was covered with wild rice; however, wild rice has almost completely disappeared from the lake. Phytolith data indicates that wild rice maintained relatively high abundance for several hundred years and then rapidly declined to present day levels.

This study demonstrated that multiplicity and redundancy of basic phytolith typologies in the Poaceae did not limit the establishment of locally diagnostic phytolith morphotypes when three-dimensional observation and descriptors are used.

Methods developed during this study can now be used to better understand the timing of the entry and speciation of *Zizania* in North America.

_____
Month Year

Approved by Research Committee:

_____
Mikhail S. Blinnikov Chairperson

ACKNOWLEDGEMENTS

I would like to thank Dr. Richard Rothaus and the Office of Sponsored programs for providing financial support, logistical and field assistance, and NSF grant assistance; without which, this research would not have been possible. I would also like to acknowledge Dr. Matthew Julius, Department of Biology, who generously provided lab space and technical assistance critical to the successful outcome of this thesis. Dr. Mikhail Blinnikov deserves recognition in his ability to inspire and encourage my creation of the original thesis proposal and NSF grant proposal which lead to this thesis. Dr. Susan Mulholland, Duluth Archaeology Center, and Dr. Linda Scott-Cummings, Paleo Research Institute, were also generous in sharing some of their hard earned phytolith knowledge and laboratory procedures. I finally wish to acknowledge Dr. James Huber, Huber Consulting, for his interest in the antiquity of wild rice utilization in the upper Great Lakes region. His Ph.D. dissertation: "Palynological investigations related to archaeological sites and the expansion of wild rice (*Zizania aquatica* L.) in northeast Minnesota" inspired me to develop phytolith analysis as a wild rice paleoecological tool.

Storms, hails, different things that might destroy,
That's why we act.
We fear, yet we're not sure of this crop,
Until we receive it in our hands.

And life, it gives us strength.
Beware!
Anything could happen between now and then,
That we are 'bout ready to receive it from the great Natural,
We should say thanks.

- Paul Buffalo, Leech Lake Ojibway

The moment one gives close attention to anything,
Even a blade of grass, it becomes a mysterious, awesome,
Indescribably magnificent world in itself.

- Henry Miller

TABLE OF CONTENTS

LIST OF TABLES

Table Page

Table Page

LIST OF FIGURES

Figure Page

Figure Page

# Chapter I

# INTRODUCTION

## Climate and Cultural Change Since the Last Glacial Maximum

It is widely acknowledged that American wild rice (*Zizania* spp.) has played an important role as a source of sustenance and cultural significance for past and present inhabitants of Minnesota and the greater Great Lakes region. Ethnographic evidence (Jenks, 1900; Yarnell, 1964; Dore, 1969; Vennum, 1998; Bois Fort Tribal Council, 2001) and the archaeological record (Johnson, 1969a, 1969b; Ford and Brose, 1975; Gibbon, 1976; Rajnovich, 1984; Lofstrom, 1987; Yourd, 1988; Thompson and others, 1994; Moffat, 2000; Valppu and Rapp, 2000) indicate at least 2000 years of wild rice utilization in the Great Lakes region. Despite these studies and the current grass pollen paleoecological work of McAndrews (1969, 2000, 2005) and Huber (1996, 2001a, 2001b, 2006), direct unequivocal evidence for the presence and abundance of wild rice during the late Pleistocene/early Holocene is incomplete. Thus, the antiquity of wild rice availability and utilization for the Great Lakes region has not yet been fully resolved.

The Late-Wisconsinan glacial period (30,000 to 10,000 BP) produced a complex sequence of ice movement and glacial lake formation in Minnesota; however,

portions of central and northeastern Minnesota stayed relatively ice-free from 13,000 BP to present (Teller, 1987; MGS, 1997; Mulholland and others, 1997). The precise spatial and compositional assemblage of the vegetation immediately following deglaciation is unknown and is actively debated by paleoecologists and biogeographers. This uncertainty is largely due to the fact that no modern pollen assemblage exits today that is analogous with those found in recent deglaciated areas during the late Pleistocene and early Holocene (Birks, 1976; Grimm, 1983, 2001; Yu and Wright, 2001; Wright and others, 2004). The oldest pollen zone in northeastern Minnesota is described by several researchers as the Compositae-Cyperaceae assemblage zone (Cushing, 1967; Huber, 2001a). This zone is interpreted as being sub-arctic and tundra-like; however, through the insect and plant macrofossil work of Ashworth and others (1981) and the climatic modeling of Yu and Wright (2001), an open boreal type of environment with herbaceous vegetation is suggested. In fact, Yu and Wright (2001) make a case for the existence of a late-glacial climate that favored the admixture of boreal and temperate taxa.

With wild rice being found in both boreal and temperate biomes, the potential exists for the presence of wild rice in Minnesota since the late Pleistocene. It is also thought that due to local variations in conditions and species response time, a mosaic of ecological niches would have existed throughout the Holocene, resulting in more varied food resources for the earliest human occupants of the region (Lofstrom, 1984; Mulholland and others, 1997; Mulholland, 2000).

Central and northeastern Minnesota has had a long history of human occupation, extending probably at least 10,000 years BP (Mulholland and others, 1997; Mulholland, 2000). Although date boundaries vary by researcher and geographic location, the Minnesota Office of the State Archaeologist summarizes the archaeological sequence for Minnesota as follows: Paleoindian, ca. 12,000 to 8,000 BP; Archaic, ca. 8000 to 2800 BP; Woodland, ca. 2800 to historic contact.

Mulholland and others (1997) summarize the following vegetation sequence in northeastern Minnesota: 1) shrub tundra-like (open boreal forest?) to approximately 12,000 BP; 2) forest/shrub tundra from 12,000 BP in the south and 10,500 BP in the north; 3) mixed pine-spruce forest by 8,300 BP; 4) mixed conifer-hardwood forest after 7,000 BP.

In the Lake Mille Lacs area of central Minnesota, a mixed pine forest was already established by 10,000 BP and dominated the landscape until 7,800 BP when a dry and warm oak savanna became dominant until around 4,000 BP. From 4,000 to 2,300 BP, slightly wetter conditions allowed a mixed oak and mesic deciduous forest to exist until cooler conditions gave rise to the expansion of white pine (McAndrews, 2000).

Pollen data suggests that wild rice was present throughout the Holocene in Minnesota with major expansion of its distribution 4,000 to 2,000 years ago (Farnham and others, 1964; McAndrews, 1969, 2000; Huber, 1996, 2001a, 2001b, 2006). However, over the last 100 years, Minnesota has seen a reduction in harvestable acres of wild rice (MNDNR, 2007; Figure 1). In some once prolific wild rice lakes, such as

Lake Ogechie in Minnesota's Mille Lacs Kathio State Park, wild rice has almost completely disappeared.

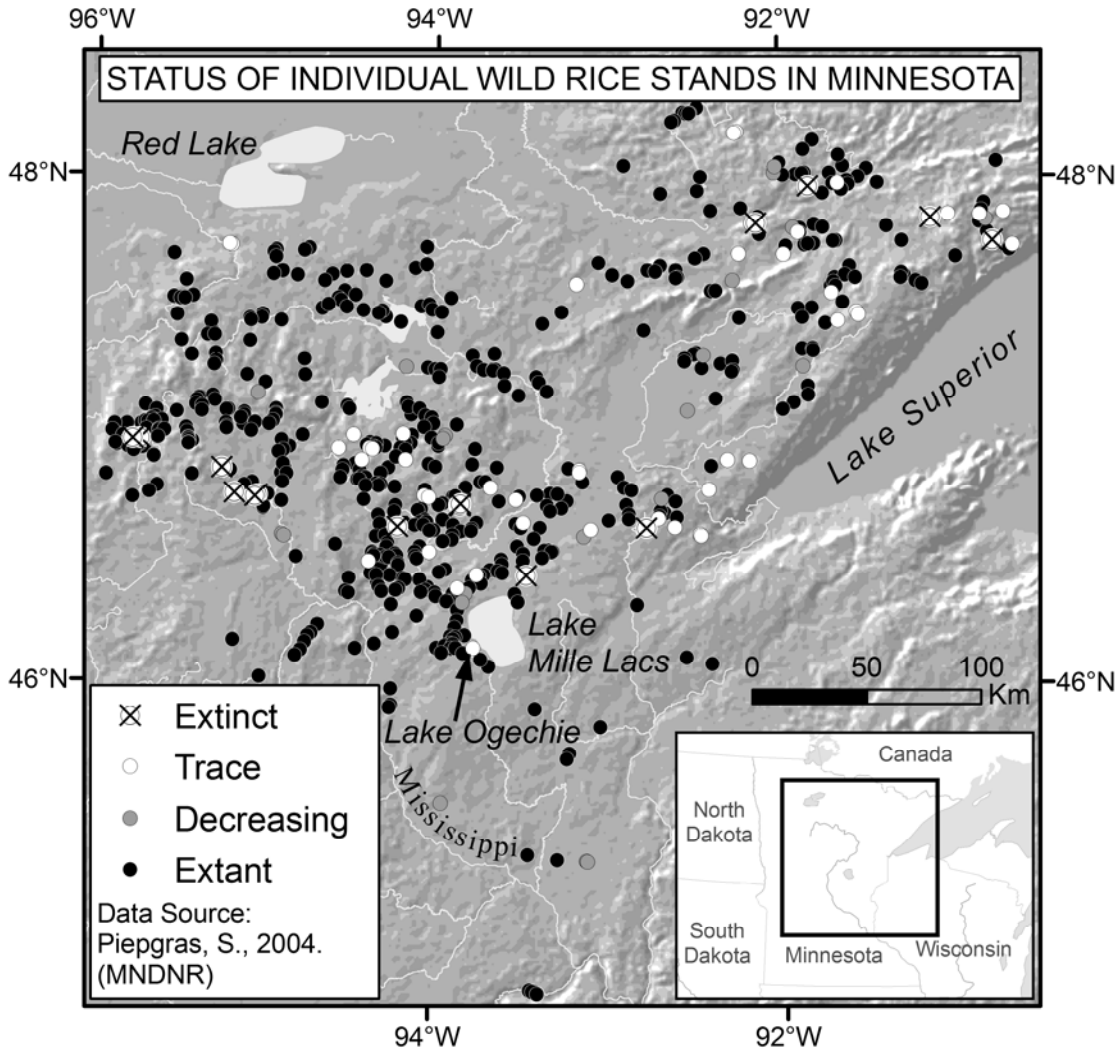


Figure 1

Point Map of the Distribution and Status of Wild Rice Stands in Minnesota
The status of individual wild rice stands was based on current, historic and anecdotal accounts of present and past occurrence of wild rice. This data was derived from a 1999-2001, Minnesota Department of Natural Resources wildlife staff statewide survey (Amy Geisen, MN DNR, 2004, personal communication; Piepgras, 2004).

Since presence or absence of wild rice today does not necessarily indicate past occurrence or abundance, an understanding of the paleodistribution of wild rice is of special interest to archaeologists and plant ecologists. There is a high probability that many archaeological sites are spatially related to past populations of wild rice (Johnson, 1969b; Rajnovich, 1984; Lofstrom, 1987; Yourd, 1988; McAndrews, 2000; Huber, 2001a; Lee and others, 2004). Further, in understanding where and when wild rice historically occurred, land management agencies can better assess current conditions, impacts of climate change and better manage for possible restoration in areas that have seen reductions in wild rice.

## Diagnostic Holocene Wild Rice Macrofossil Evidence

Plant macrofossils (leaf, needle, stem debris) are typically diagnostic indicators of local flora and vegetation (Birks, 2000). Wild rice macrofossils in both archaeological and paleoecological settings are extremely rare. The oldest known wild rice macrofossils in Minnesota (and some of the oldest in North America) are from sediment cores obtained at Wolf Creek, near Lake Mille Lacs in east central Minnesota, and date between 9,000 and 10,000 BP (Birks, 1976). In an archaeological context, the oldest know evidence for human utilization of wild rice in Minnesota comes from the Big Rice Lake site, St. Louis County. The charred wild rice seed dates to around 2,000 BP (Valppu and Rapp, 2000). Outside of Minnesota, Warner and others (1987) report possible *Zizania palustris* leaf and spikelet macrofossils from sediments along the Goulais River, southeastern Lake Superior, Ontario. These

sediments were deposited during the Nipissing transgression of the Wisconsinan and date between approximately 5,300 to 6,600 BP. Although wild rice macrofossil remains are diagnostic indicators of wild rice presence, rarity of recovery makes presence and abundance estimation difficult to quantify.

## Prior Paleolimnological Studies used to Infer Probable Presence of Wild Rice

Detection of the presence and abundance of wild rice pollen microfossils in lake core sediment has been reported by some (Farnum and others, 1964; Janssen, 1966; McAndrews, 1969, 2000; Birks, 1976; Yourd, 1988; Orson, 1992; Huber, 1996, 2001a, 2001b, 2006), but is still relatively understudied. Diagnostic wild rice identification through pollen analysis is possible; however, it requires the use of scanning electron microscopy to view pollen surface sculpturing and may not be practical in many situations (Yourd, 1988; Lee and others, 2004). Two proxy methods have commonly been used to infer the likely presence of wild rice in the paleoecological record: grass pollen spikes and pollen grain size analysis.

The first method is to compare the percent abundance of grass pollen, Poaceae (Gramineae), in the pollen profile to control cores (see Figure 1 for example; McAndrews, 1969, 2000; Yourd, 1988; Huber, 2001a). This proxy method assumes that typical Poaceae pollen values for Minnesota during the mid-Holocene range from <5% to 15% and late-Holocene values do not exceed 5%. Further, Poaceae values between 25% and 30% are high for most coring sites in Minnesota. Thus, Poaceae values exceeding 35% to 40% are thought to be a result of local influx (Yourd, 1988).

In this same study, Yourd (1988), and further study by Huber (1996, 2001a), indicated that lake bathymetry and basin size influence on Poaceae pollen values. Surface samples taken from relatively deep open water away from wild rice beds can contain Poaceae values of 1% to 5%, even in lakes with large, harvestable quantities of wild rice (Yourd, 1988; Huber 1996, 2001a). Thus, high Poaceae values alone cannot reliably infer the presence of wild rice.

The second method used to determine the presence of wild rice in the paleoecological record is by Poaceae pollen grain size distribution and frequency of occurrence (McAndrews, 1969, 2000; Yourd, 1988; Huber, 2001a, 2001b, 2006; Lee and others, 2004). In this method, wild rice pollen grain size is measured and compared with grass pollen grains from other modern taxa to determine the probability of recovered Poaceae grains belonging to wild rice (see Figure 3 for example). Lee and others (2004) studied this method further, and by employing a new method, determined that for their study area on the southwest shore of Lake Ontario, wild rice fossil pollen may not be of the same size as modern wild rice, making the grain size frequency method alone unreliable for the identification of wild rice. They were able to determine this by using scanning electron microscopy (SEM) to identify surface sculpturing unique to wild rice pollen grains. Although they were successful in identifying wild rice pollen grains from modern and recovered Poaceae pollen grains, they do concede that the SEM technique is time consuming and may not be accessible to everyone.

Huber (2001a) noted that the size range of his reference collection of wild rice pollen grains from Big Rice Lake in northeastern Minnesota were larger than McAndrews' size range for wild rice pollen from Rice Lake in west central Minnesota. Huber (2001a) hypothesizes that perhaps environmental conditions influence pollen grain size. It also seems possible that different varieties of *Zizania* may exhibit different pollen grain sizes. Comparative pollen collections should include not only different species, but also the recognized varieties of *Zizania*.

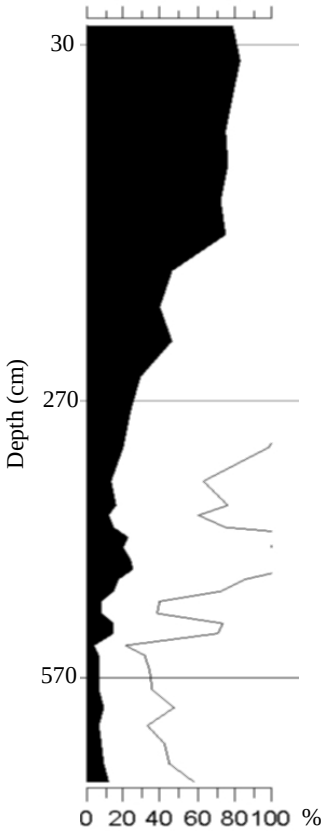


Figure 2

Example of Poaceae Pollen Relative Abundance Graph (McAndrews, 2000)

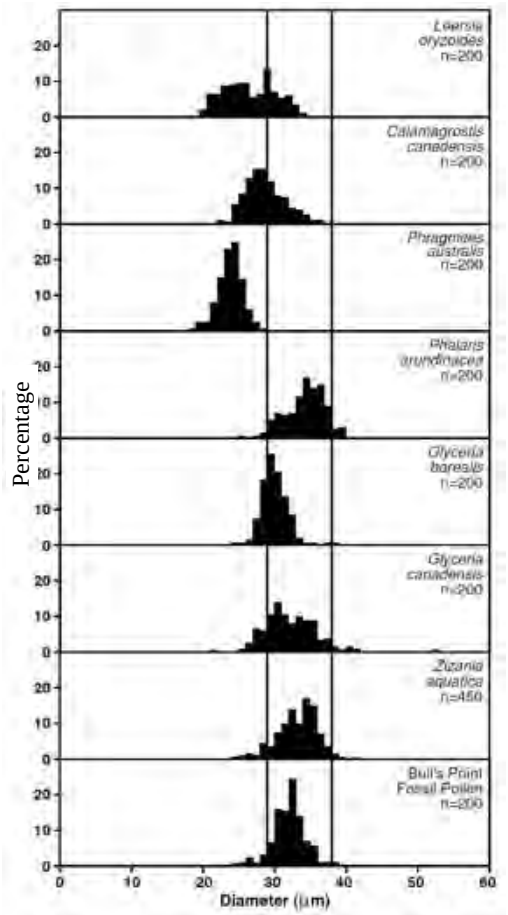


Figure 3

Example of pollen grain size analysis (Lee and others, 2004)

By employing a combination of the aforementioned techniques, these authors can infer some aspects of the paleodistribution of wild rice; however, the use of direct evidence, such as wild rice phytoliths, has the highest potential to identify the presence of wild rice in situations where other evidence cannot. Further, by understanding modern deposition of wild rice phytoliths, a measure of past quantity may be achieved with more certainty and precision than what can be achieved by proxy through pollen analysis.

## Classification and Biogeography of *Zizania* (wild rice)

Wild rice (*Zizania*) is an annual wind-pollinated emergent aquatic macrophyte, and is North America's only native cereal grain (Figures 4 & 5). Wild rice prefers clear, shallow, slow moving waters of lakes and rivers with organic muddy sediments (Fassett, 1924; Stover, 1928; Rogosin, 1954; Dore, 1969). Few studies concerning the paleoecological and archaeological record of wild rice have taken into account the three species and four varieties of wild rice that can be found in North America. This is especially true throughout Minnesota and the Great Lakes region where two species with three varieties are sympatric in some areas (Terrell and others, 1997).

Taxonomic classification within the Poaceae varies by author, but mostly deals with subfamily, tribe and sub-tribe groupings (Clayton and Renvoize, 1986; Watson and Dallwitz, 1992; Terrell and others, 1997; GPWG, 2001). I have adopted the GPWG (2001) classification for the Poaceae and Terrell and others (1997) classification for the genus *Zizania*. The three species and four varieties of wild rice in

North America are: *Zizania aquatica* L. var. *aquatica*, *Zizania aquatica* L. var. *brevis* Fassett, *Zizania palustris* L. var. *palustris*, *Zizania palustris* L. var. *interior* (Fassett) Dore, and *Zizania texana* Hitchc. One species, *Zizania latifolia* (Griseb.) Turcz. ex Stapf., is disjunct with its North American counterparts and is found in parts of Russia, China and southeast Asia.

It should be noted that *Zizania texana* is an endangered species and only occurs along a 2.5 km length of the headwaters along the San Marcos River, within the city limits of San Marcos, in south central Texas (Terrell and others, 1978, 1997).

The GPWG (2001) has placed *Zizania* in the subfamily Erhartoideae, tribe Oryzeae. It should be noted that many older herbarium specimens that are labeled *Zizania aquatica* may be in fact *Zizania palustris*. Further, many researchers, especially archaeologists, continue to use the *Zizania aquatica* name, when in fact, they are working with *Zizania palustris* (e.g. Huber, 1996, 2001a, 2001b, 2006; Valppu and Rapp, 2000).

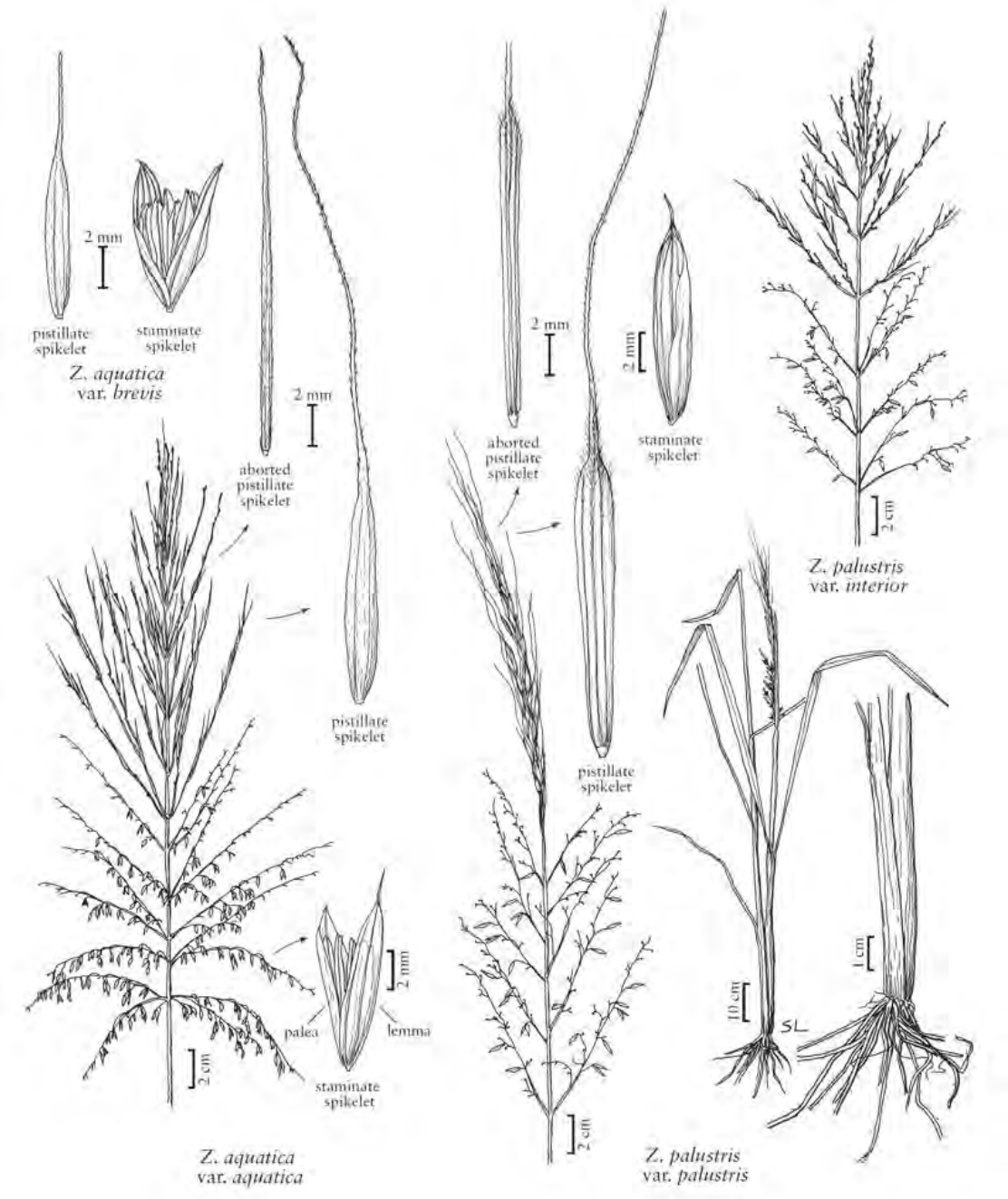


Figure 4

*Zizania aquatica* and *Z. palustris* Illustrations

Illustrations by Sandy Long and obtained and used with permission from Utah State University (copyright Utah State University).

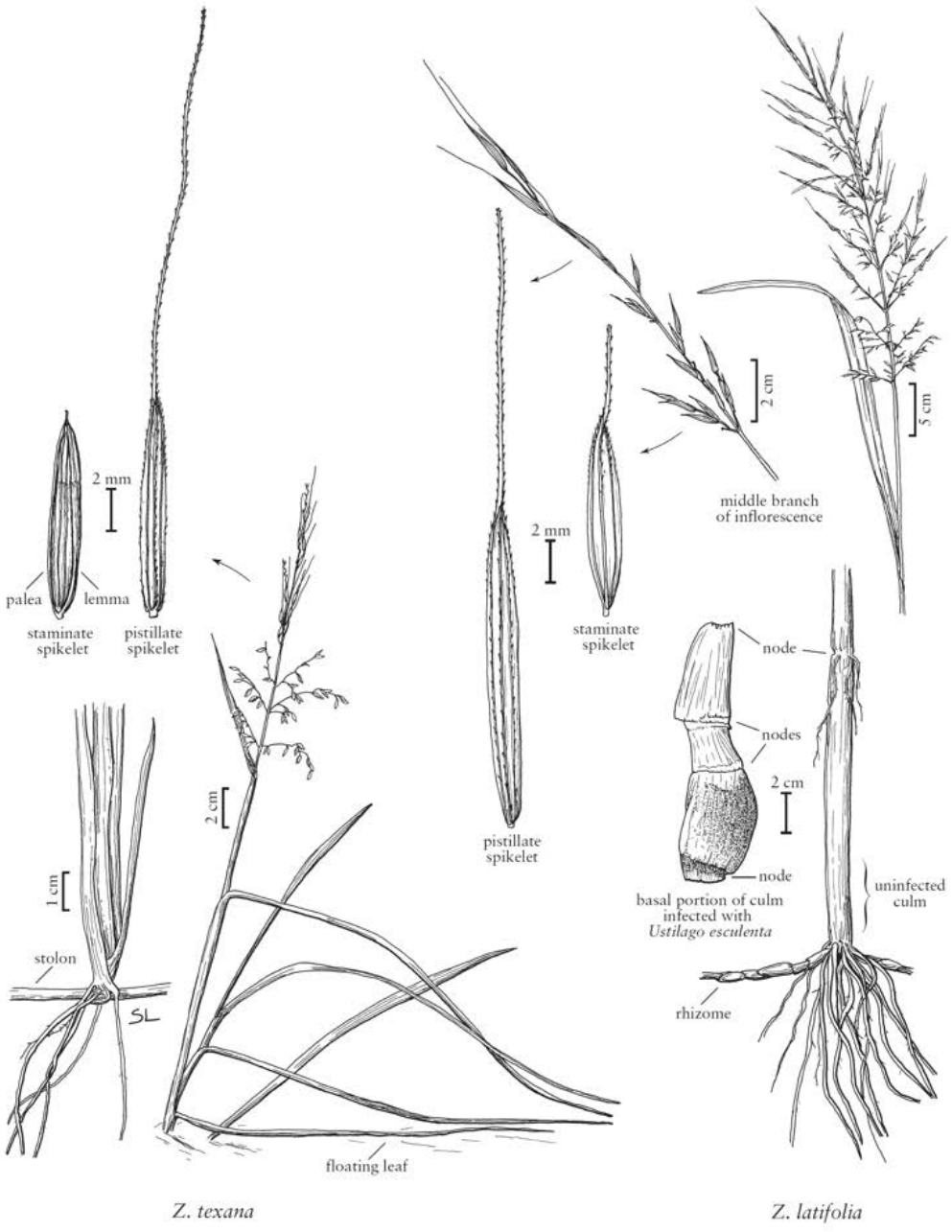


Figure 5

*Zizania texana* and *Z. latifolia* Illustrations

In Minnesota, *Zizania palustris* var. *palustris* (northern wild rice) is distributed throughout the state, and *Zizania palustris* var. *interior* (interior wild rice) is found everywhere except northeastern Minnesota. *Zizania aquatica* var. *aquatica*, at present, does not occur in Minnesota, but at one time may have been found in the Red Wing area and south along the lower Mississippi River (Figure 6).

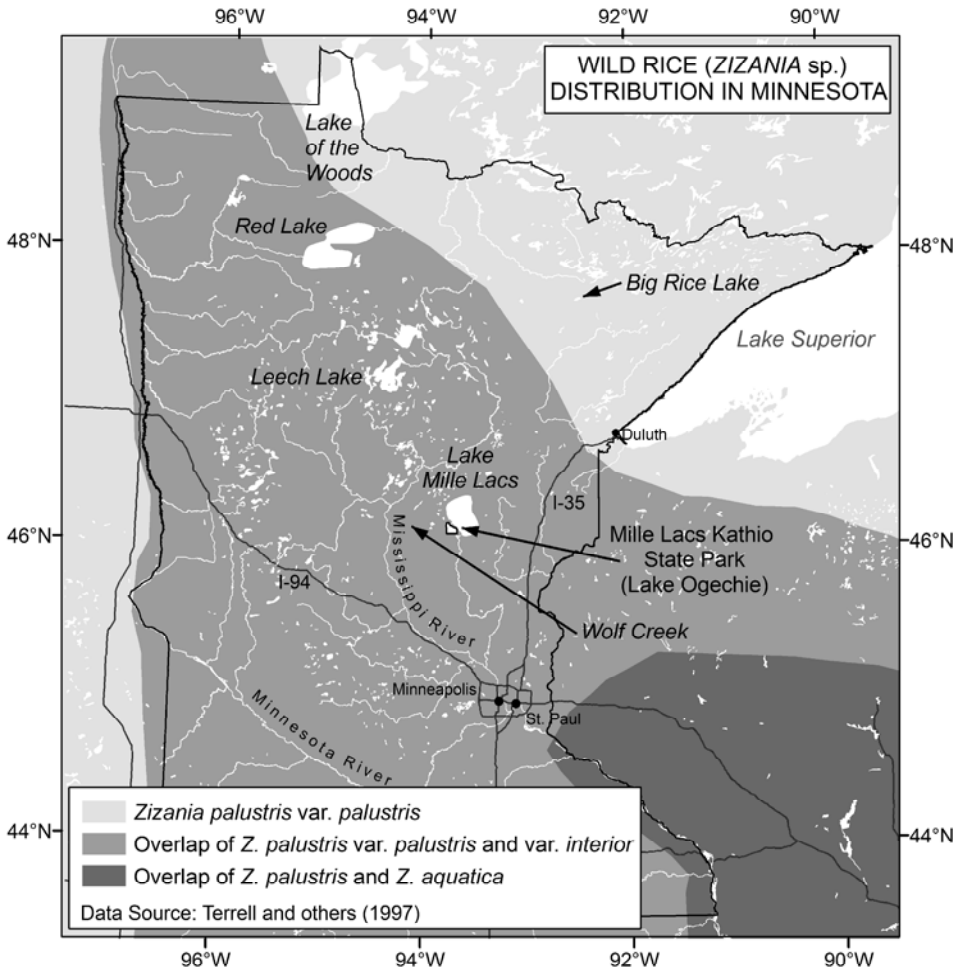


Figure 6

Generalized Range Map for *Zizania* in Minnesota
*Zizania aquatica* has not been collected in Minnesota, but may have once been found in the southeastern portion of the state.

Since the time of Linnaeus, many botanists have been interested in the close floristic relationship and disjunct occurrence of many plant taxa between eastern Asia and eastern North America (Hsu and others, 1983; Qian and others, 1999). Wild rice is a member of this disjunct group and is regarded as being a relict of the Tertiary flora (Qian and others, 1999). Horne and Khan (1997) determined through genetic analysis that *Z. palustris* is more closely related to *Z. texana* than to *Z. aquatica*, and theorize that *Z. texana* is a relict population of an ancestral zizanid that was compacted southward during the Pleistocene (Figures 7 & 8; see also Duvall & Biesboer, 1998). They also hypothesize that speciation has occurred within the last 18,000 years as a result of migration northward and eastward. However, they do concede that it is possible that *Z. aquatica* had already evolved prior to recent glaciations and then migrated up the Atlantic coast as the ice melted.

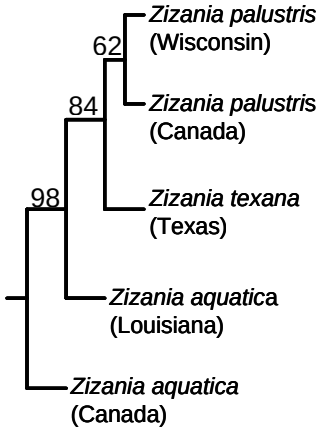


Figure 7

Phylogenetic Tree for the Three Species of North American *Zizania*
Bootstrap values (numbers) are confidence values ranging from 0 to 100 with values greater than 70 indicating strong support for the branching (Horne and Kahn, 1997). It is unclear whether the *Zizania palustris* seeds from Canada and Wisconsin used to grow tissue for the isozyme analysis are either variety *palustris* or *interior*.

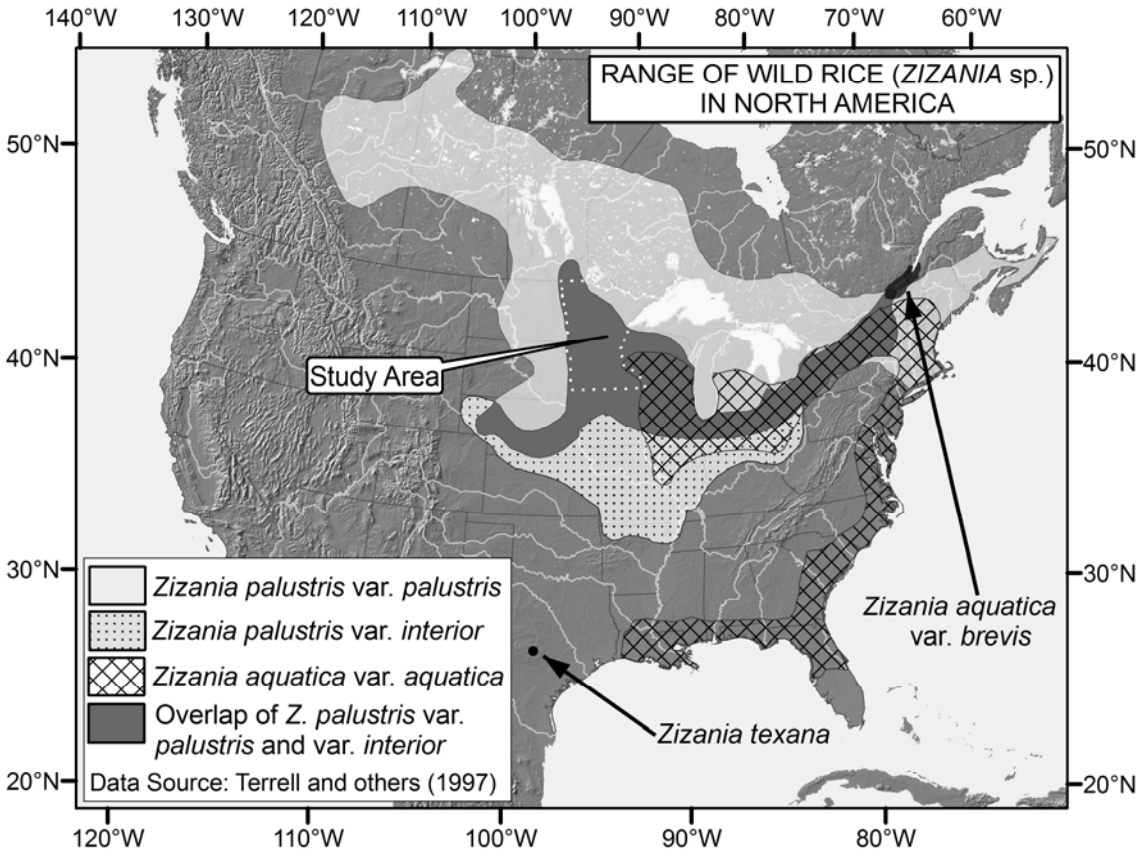


Figure 8

Generalized Range Map for North American Species and Varieties of *Zizania* Range boundaries redrawn from Terrell and others (1997). *Zizania latifolia* occurs in parts of Russia, China and southeastern Asia. *Z. texana* is an endangered species, restricted to a 2.4 km section of the San Marcos River in Texas. *Z. aquatica* var. *brevis* occurs only in tidal mud flats along the upper St. Lawrence River.

Plant Opal Phytolith Analysis

Plant phytoliths are microscopic opal silica bodies typically 5 to 200 μm (.005 to .2 mm) in size. They were first observed in living plants by the German botanist Struve in 1835 and first observed in soils by Ehrenberg, a German microbiologist, in 1841. Another German scientist, Netolitzky, was the first to describe their removal

from plants in 1929 (Piperno, 2006). Phyoliths form in plant tissues after soluble silica, in the form of monosilicic acid ($H_4SiO_4$) is taken up from the soil. Some of that silica is then deposited as solid, hydrogenated silicon dioxide ($SiO_2$) infillings of cell walls, cell interiors (lumina), and intercellular spaces (Piperno, 2006). The shape and abundance of phytoliths in any given plant group are largely under genetic control (Piperno, 1993a). Genetic loci that control phytolith traits have been identified in several major crop species: tga1 in corn, Hr1 in squash, and several genes in rice (Piperno, 2006).

When plant material decomposes, phytoliths are released to the soil and subjected to geologic sedimentation processes. Phytolith deposition is a highly localized, in situ decay-in-place mechanism (Piperno, 2006). Many plant taxa produce distinctive forms that retain cell shape after organic tissue has decayed or burned away. Because they are inorganic, they are not subject to the forces of decay that can destroy pollen grains. They are routinely recovered in Miocene age deposits (Stromberg, 2004, 2005) and have been observed in Cretaceous deposits (Prasad and others, 2005). When compared to grass pollen evidence, grass silica phytoliths can often be interpreted with greater taxonomic precision, better represent local flora (Carter, 2002) and enhance information from pollen analysis (Lu and others, 2006).

## ~~Prospects for the Establishment of Diagnostic~~ Wild Rice Phytolith Morphotypes

Wild rice (*Zizania*) is placed in the Poaceae subfamily Erhartoideae (GPWG, 2001) and tribe Oryzeae (*Hygroryza*, *Leersia*, *Luziola*, *Oryza*, *Zizaniopsis*). Phytoliths

from the Erhartoideae have certain diagnostic shapes (e.g. oryzoid-type crosses and bilobates), not found or rare in other subfamilies (Wang and others, 19998; Piperno & Sues, 2005; Prasad & Stromberg, 2005). Only one other member of the Erhartoideae, Indian cut-grass (*Leersia* sp.), occurs in my study region and is the closest relative to *Zizania*. Two other Erhartoideae, *Luziola* and *Zizaniopsis*, are native to Texas and the southeastern states. *Oryza* has been introduced to the southeastern states and is considered a noxious weed.

According to Susan Mulholland (personal communication, 2005), differentiation based on phytolith morphology between *Zizania* and other plants in the area, with the exception of *Leersia*, should pose no great difficulty. After establishing a locally derived comparative collection of other common grasses, regional diagnostics may be possible. Studies of epidermal features and SEM studies of silica bodies (Weatherwax, 1929; Hawthorn, 1970; Terrell and Robinson, 1984; Terrell and Wergin, 1981; Darbyshire and Aiken, 1986; Duvall and Biesboer, 1988) indicate significant taxonomic differences between all four species of *Zizania*. In a study that looked at epidermal features of spikelets in *Leersia*, Terrell and others (1983) identified specialized silica body epidermal features on the lemmas that are different from those found on lemmas of *Zizania*. Dore (1969) has a wild rice leaf epidermal peel micrograph showing bilobates *in situ* over leaf veins. The previously cited works and the early work of Metcalfe (1960) provide good baseline material for possible establishment of a regionally based diagnostic morphology of *Zizania*.

## Prospects of Wild Rice Phytolith Analysis as a Paleolimnological Tool

The paucity of phytolith analysis in a paleolimnological context is perhaps a legacy of the early archaeological emphasis for the discipline. However, a few classic studies clearly demonstrate how phytoliths can complement pollen data and provide additional information, especially in regards to the Poaceae. Piperno (1993b) in her study of deep lake cores from Panama, used phytolith and charcoal data to reconstruct anthropogenic effects on vegetation at several scales. Fearn (1998) used a phytolith ratio derived from a dry prairie to salt marsh transect to refine pollen based interpretations of an estuarine sediment core. Carter (2002), with one of the longest continuous phytolith records (197 meters, basal date around 115,000 Years BP), demonstrated how phytoliths from a New Zealand lake core gave a strong local environmental signal that *contrasted* pollen based interpretations. The pollen signal was apparently more reflective of regional than local change. Blinnikov and others (2001) complemented the Columbia Basin, Washington record of Carp Lake pollen analysis with phytolith analysis.

~~Wild rice phytolith lacustrine studies~~. Wild rice phytolith bodies from lake sediment samples are virtually unstudied, with apparently not a single peer-reviewed journal article on the subject. Davidson (2003), in an undergraduate thesis from the University of Toronto, undertook a serious attempt to detect wild rice phytoliths in fossil sediments from Cootes Paradise, Lake Ontario, Canada. Since wild rice no longer grows there, she acquired five plants (*Zizania aquatica*) 180 km west of her

study area. Unfortunately, no spikelets (seed and husk) remained. She identified 17 morphotypes that included lightly silicified epidermal long cells and more robust silica short cells, and then determined the phytolith assemblage for the partial plant. She tested length and width measurements, and found minimal within and between sample variation. She then processed four fossil sediment samples, two from within a likely wild rice zone, and two from outside the likely wild rice zone. She was successful in recovering and identifying wild rice morphotypes from the wild rice zone, but was unsuccessful in establishing an assemblage correspondence between reference plants and sediment for the entire suite of morphotypes. She did find better correspondence with only short cell types. It is unclear what the sediments were like, but minimalist lake sediment processing would suggest low organics and clays. Overall, Davidson (2003) was successful in developing a presence/absence methodology for basic wild rice phytolith typologies; however, full resolution of all silica short cell morphotypes was not achieved. Further, a detailed comparative collection of other local wetland grasses was not conducted; of particular concern is *Leersia*, an oryzoid with phytoliths that are virtually identical if using basic typological descriptions.

An important aspect of this study is the collection and analysis of modern lake sediment samples from wild rice and non-wild rice lakes. The deposition, re-suspension and possible sediment focusing of phytolith material based on lake bathymetry and morphometry has not been investigated; however, these studies have been looked at in regards to pollen sedimentation (Davis, 1973; Downing and Rath, 1988; Blais and Kalff, 1995). It is thought that phytolith deposition from wild rice

should remain fairly localized, making core placement of critical importance. Any estimates of abundance from the paleoecological record will have to take into account proximity to past wild rice stand location.

Wild rice phytolith archaeological studies. Only two refereed journal articles that directly deal with American wild rice (*Zizania*) phytoliths were found (Thompson and others, 1994; Hart and others, 2003), with Robert Thompson conducting the phytolith work for both. In Thompson and others (1994) wild rice rondels were recovered from pottery food residues from north central Minnesota. Further, Thompson obtained and analyzed, from the University of Minnesota Herbarium, five *Zizania palustris* pistillate spikelet samples from spatially and temporally varying locations. He found the phytolith assemblage for all five samples to be dominated by a distinctly indented rondel.

In Hart and others (2003), Thompson developed a detailed rondel taxonomy to describe maize and wild rice phytoliths. Only one reference sample of *Zizania aquatica* spikelet material was examined. This was acquired from the University of Minnesota Herbarium and was collected from Lake George, New York. He then compared recovered rondel assemblages with reference collection assemblages for food residue identification. He also stated that previous examination of *Zizania palustris* rondel assemblages ruled out this species as a possible source of the wild rice rondels. Exactly what the observed differences are between *Z. palustris* and *Z. aquatica* spikelet assemblages are not mentioned in the paper. Terrell and others

(1997) list *Zizania aquatica* var. *aquatica*, *Zizania palustris* var. *palustris* and *Zizania palustris* var. *interior* as occurring in New York.

Serpa and Phil (2005), in their study of cultigens from the American Northeast, examined reference material from the Rochester Academy of Science Herbarium, New York, and included *Zizania palustris* and *Zizania aquatica* in their analysis. They used simple typological terminology in describing a few morphotypes observed in fixed media. They mention the possible presence of double-peaked glume cells diagnostic of *Oryza*, but could not confirm this based on microscopy limitations. They also observed possible differences in leaf epidermal silicification between *Z. palustris* and *Z. aquatica*; however, this was not quantified or illustrated in the paper.

By developing a methodology specific to lacustrine wild rice phytolith analysis, this thesis has the potential to provide direct evidence for the presence and abundance of wild rice throughout the Holocene, resulting in a better understanding of the spatial and temporal paleodistribution of wild rice in central Minnesota and beyond. While the aforementioned wild rice phytolith studies show promise, they are in no way comprehensive in their examination and analysis of phytolith production in *Zizania*. This thesis is the first study to systematically look for distinguishing characteristics within and between *Zizania* and *Leersia* species. Further, the establishment of a phytolith morphotype comparative collection for wild rice and other wetland plants will be of significant benefit to the paleoecological and archaeological communities.

Hypotheses

1) Wild rice plants produce distinctive phytolith body morphotypes that can be distinguished from other aquatic grasses (and possibly other species of *Zizania*), either directly or by percent composition of morphotypes, in lake sediments.

2) As wild rice abundance (stand size and density) increases, wild rice phytolith abundance values in both modern lakebed and lake core sediment samples increase.

3) Rises in wild rice phytolith abundance values should correlate to some degree with rises in grass pollen abundance and wild rice pollen grain size frequency values that imply the presence of wild rice.

Research Questions

1) What is the phytolith evidence for the presence and abundance of wild rice, and at what taxonomic level can *Zizania* be resolved from *Leersia* and other grasses in lake sediment records from central Minnesota?

2) How do lake morphology and distance from a wild rice stand influence phytolith abundance in modern lake sediments?

3) What is the correlation between phytolith evidence for wild rice presence and abundance and that inferred from the pollen record for a wild rice lake?

Study Area: Mille Lacs Kathio State Park

Mille Lacs Kathio State Park has over 9,000 years of human history and is one of the most significant archeological areas in Minnesota with 19 individual archeological sites identified. The oldest site dates to the Archaic period and shows evidence of copper tool manufacture associated with the Old Copper Tradition. Early European explorers and traders such as Daniel Greysolon Sieur duLuth and Father Louis Hennepin visited local Dakota (Mdewakanton) villages during the late 1600's, located on Lake Ogechie and the Rum River (Jim Cummings, Mille Lacs Kathio State Park, personal communication, 2005). Lake Mille Lacs, source of the Rum River, borders the park on the north, with Lake Ogechie and Shakopee Lake within Park boundaries. The Rum River flows out of the southeast corner of the park, into Lake Onamia (Figures 9 & 10).

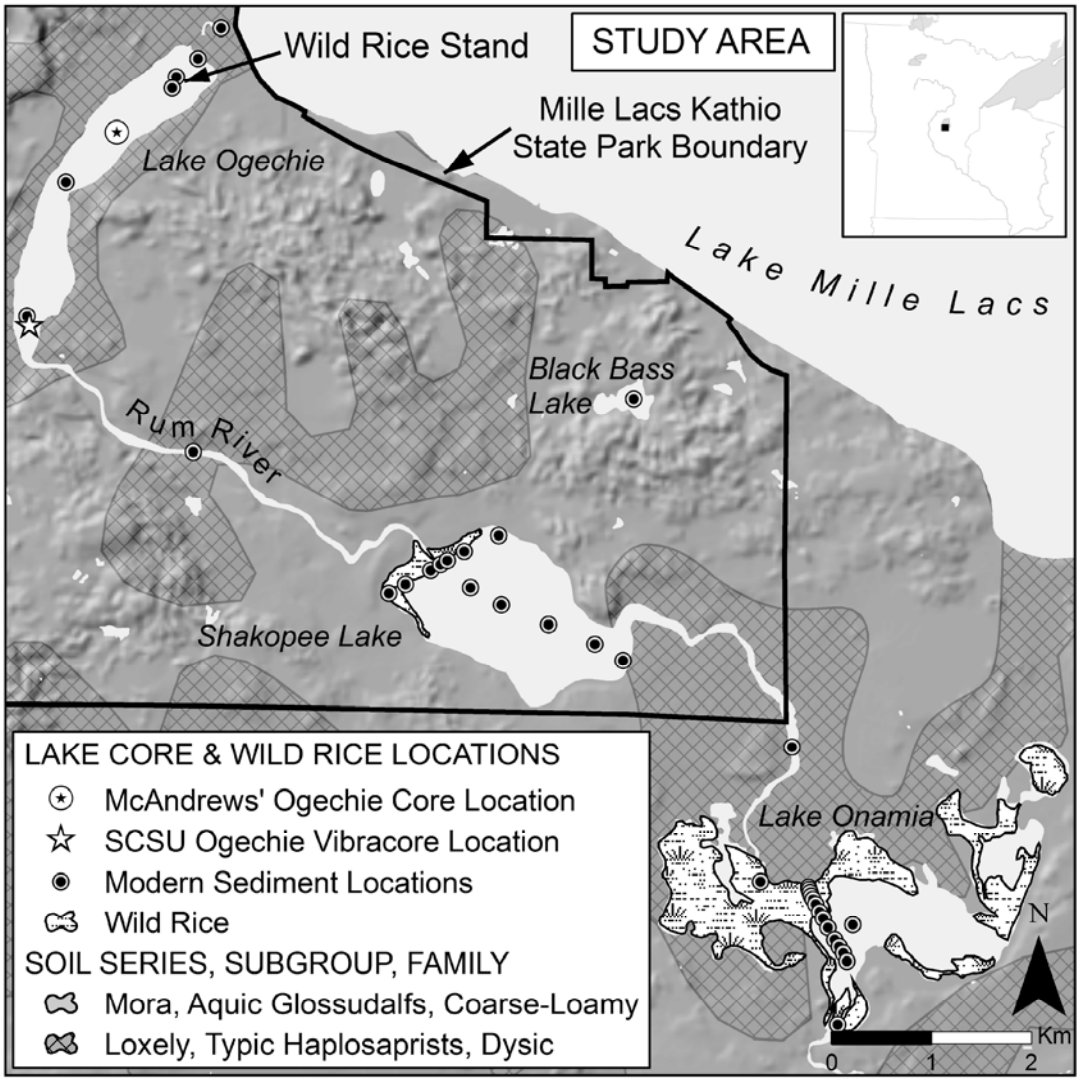


Figure 9

Map of Study Area: Mille Lacs Kathio State Park and Surroundings
Map of study area using a shaded digital elevation model layer from MNDNR Data Deli (2007) and a soils layer from NRCS (2006).

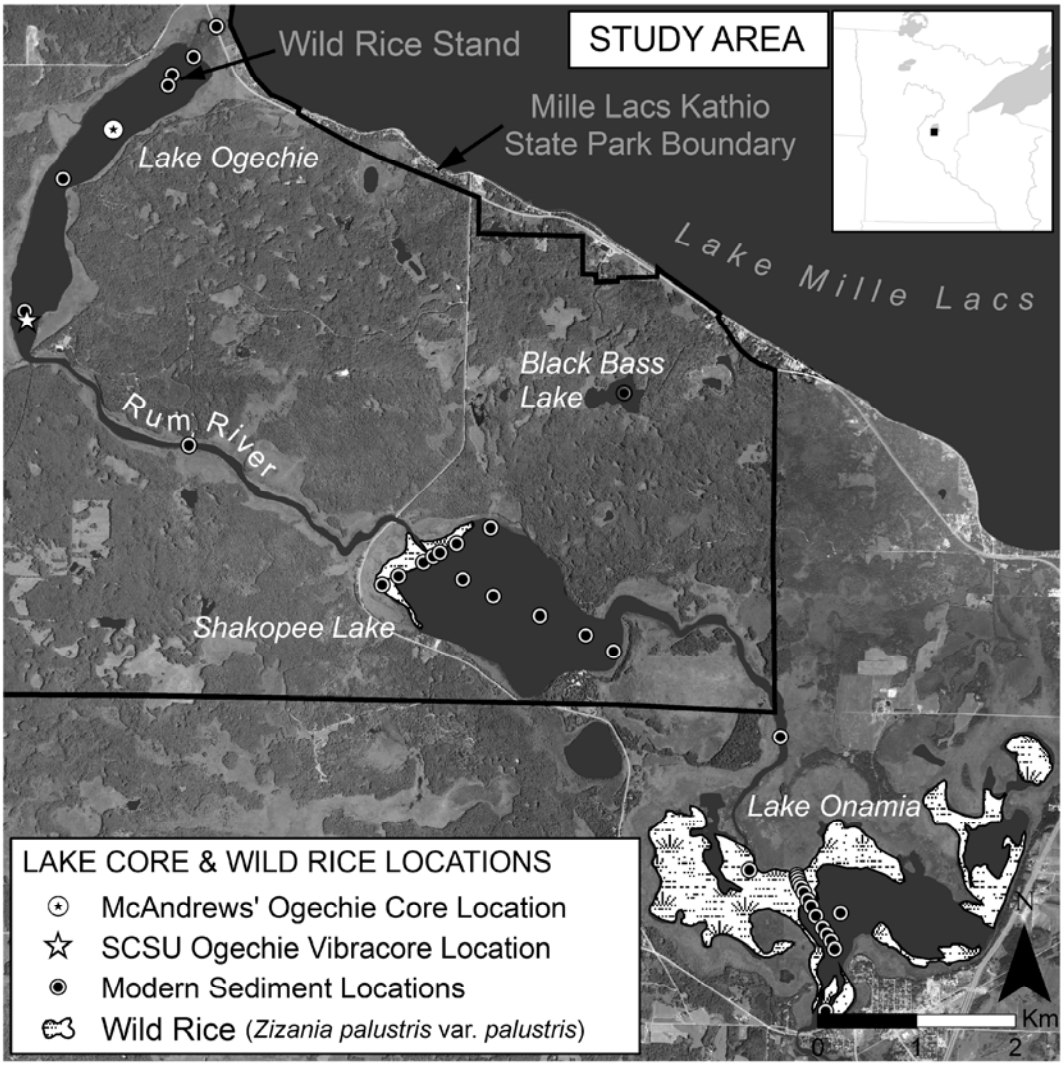


Figure 10

Map of Study Area with Airphoto Basemap

Map of study area using a 2004 NAIP aerial photograph layer from LMIC (2006).

Wild rice was once prolific on Lake Ogechie (historically called Rice Lake by local residents) and was an important source of subsistence for Native populations in the area. As early as 1852, the Mille Lacs Band of Ojibway had noticed a substantial decline in wild rice abundance and attributed this decline to the construction of

logging dams in the area (Rothaus, 2000; White, 2000). By the end of the 1930's, wild rice had all but disappeared from Lake Ogechie and may have been reduced on Shakopee Lake and Lake Onamia (Vennum, 1998, p. 27). Presently, only a few wild rice culms periodically appear in a small area on the north end of the lake.

The headwaters of the Rum River contain a nice variety of lakes with varying wild rice abundance and varying lake morphologies (Table 1). Black Bass Lake, a seepage lake with no inlet or outlet, is likely to never have supported a self sustaining stand of wild rice and serves as a control lake for this study.

Table 1

Study Area Lake Information

| Lake | Max Depth (m) | Area (ha) | Wild Rice (ha) | % Wild Rice Coverage |
|---|---|---|---|---|
| Onamia | 3.0 | 432 | 244 | 57.0 |
| Shakopee | 4.5 | 257 | 21 | 8.3 |
| Ogechie | 1.8 | 129 | 1 | 0.9 |
| Black Bass | 7.0 | 13 | 0 | 0.0 |

Rum River Watershed

The study area is located near the head of the Rum River watershed, with Lake Mille Lacs, the second largest lake in Minnesota, as the main headwaters (Figures 11 & 12). Lake Mille Lacs has an area of approximately 53,823 hectares and serves as a natural reservoir that tends to regulate stream flow in the upper part of the river. Evaporation from the large surface of Mille Lacs during summer historically caused periods of zero flow in the Rum River at Onamia (Maki, 1970); however, artificial water control features have altered natural hydrology. From Lake Mille Lacs to Lake

Onamia, the fall is about 4 feet. The watershed is constrained by the relatively short tributaries to the Rum River.

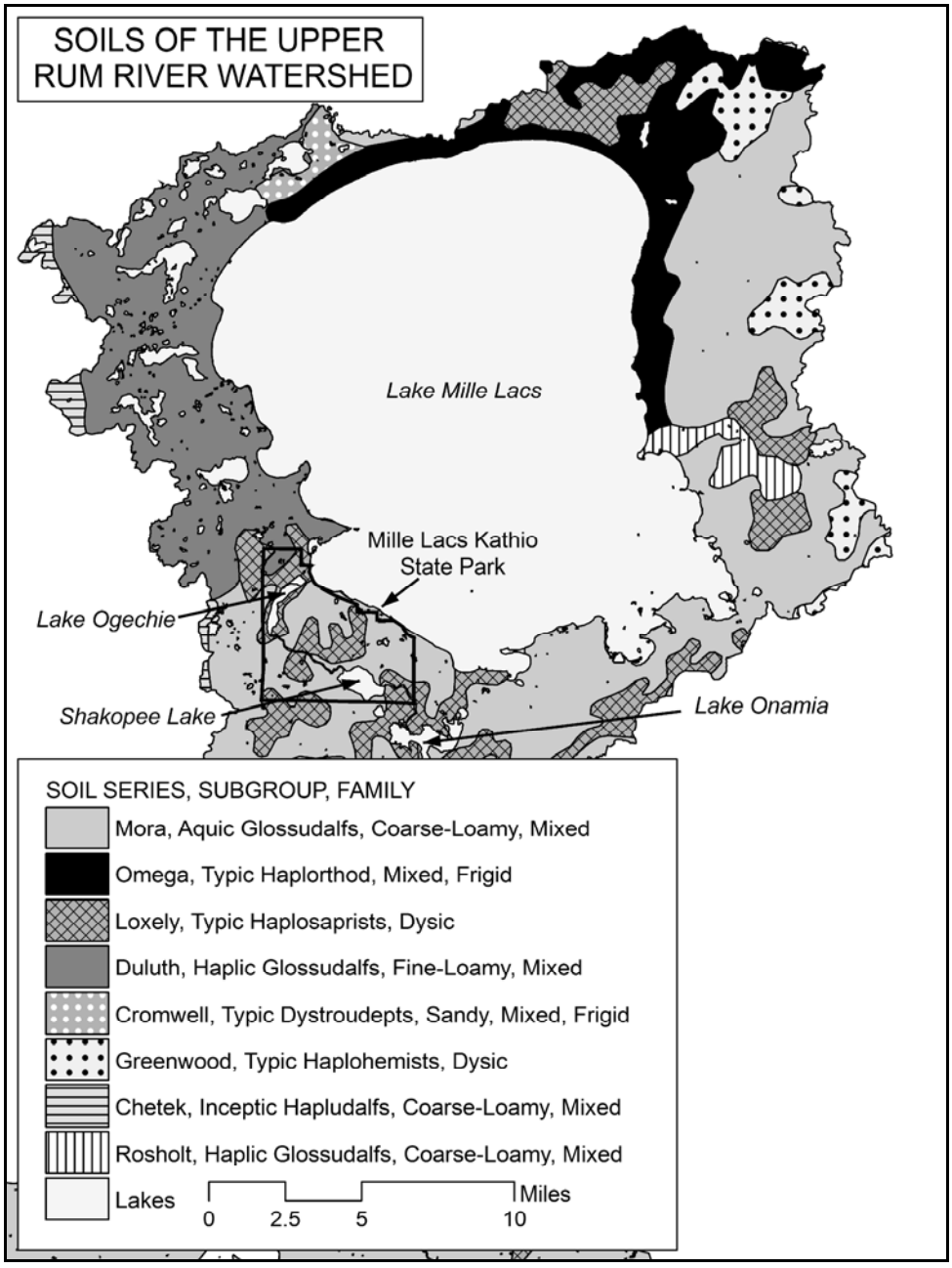


Figure 11

Soils of the Upper Rum River Watershed. GIS layer source: NRCS (2006).

The soils of the upper Rum River Watershed are an important factor when considering potential erosion and inheritance of phytoliths from upland areas (Figure 11). The Mora and Loxely series are poorly drained, moderately to highly acidic soils and have low to moderate surface runoff potential. The Loxely series Oe1 mucky peat horizon from 0 to 5 inches has a pH of 3.5. The Duluth and Omega series are well drained soils with moderate to high surface runoff potential and are fairly acidic. Surface runoff in the immediate vicinity of the study area is likely not much of a factor.

Starting around 1847, much of the area surrounding the study area was logged for white pine and red pine. By 1900, most of the large pines had been cleared (Maki, 1970). Using survey notes and sketches from the Public Land Survey 1847 – 1907, Francis J. Marschner created the Natural Vegetation Map of Minnesota. This map provides a glimpse of the dominant vegetation that existed before European settlement in the vicinity of the study area for at least the past several hundred years (Figure 12).

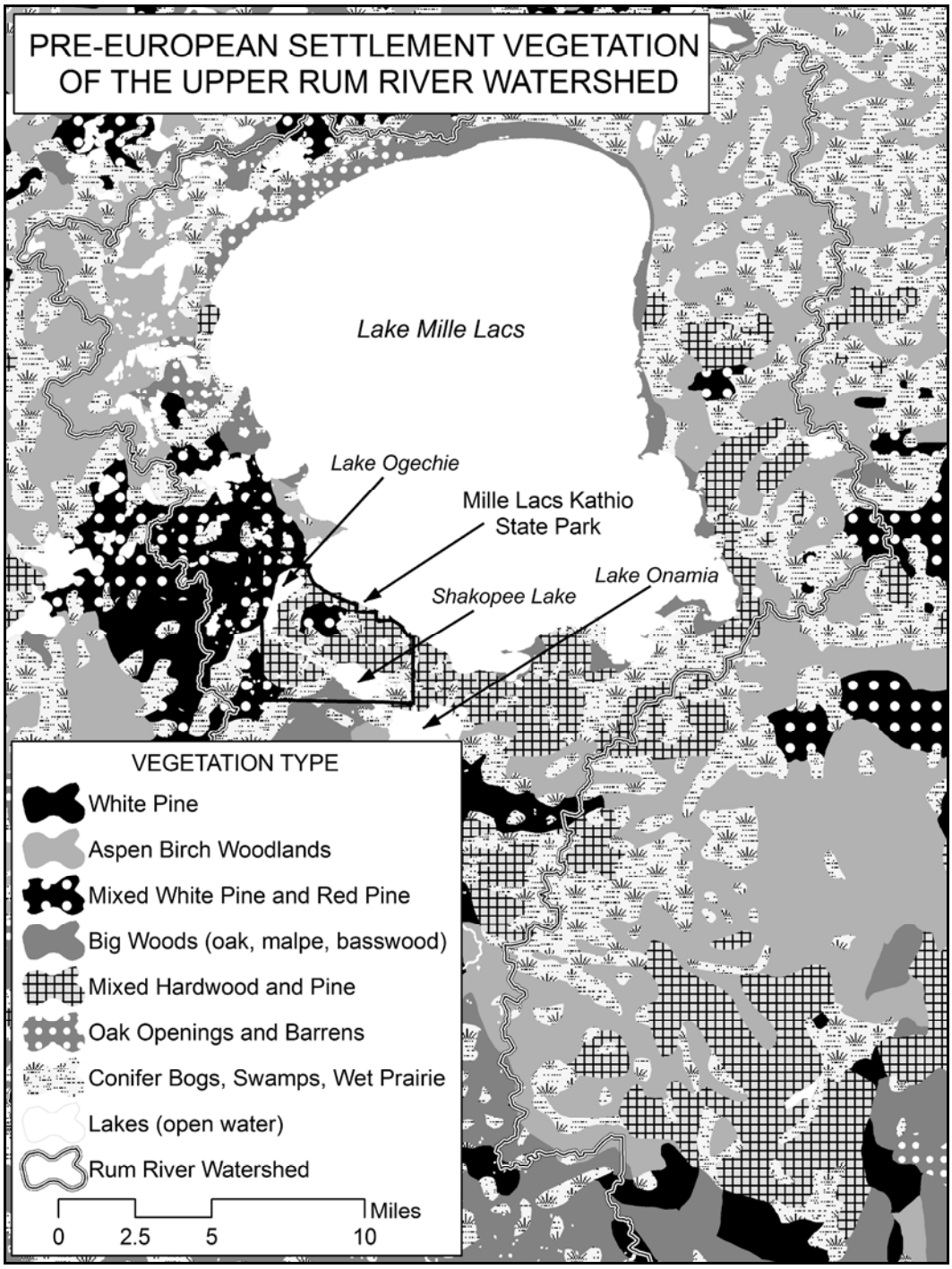


Figure 12

Pre-European Settlement Vegetation for Study Area
GIS layer digitized from Marschner's Natural Vegetation Map of Minnesota and obtained from MNDNR Data Deli (2007).

Scientific Merit for this Thesis

Northern wild rice, *Zizania palustris* is considered by many to be superior to southern wild rice, *Zizania aquatica*, in taste and quality as a food source. Understanding the spatial and temporal paleodistribution of wild rice species, as well as having a wild rice phytolith morphotype classification, would be of great interest to archaeologists. This research also develops tools that could potentially be utilized by biogeographers to study the entry and speciation of *Zizania* into North America. Wild rice phytolith analysis of lake sediments and soils has the potential to unlock many of these questions. This is especially true in the arid West, where pollen density in sediment is low and extraction requires considerable expertise (Linda Scott-Cummings, personal communication, 2007). In addition, when compared to indirect grass pollen evidence, grass plant silica phytoliths offer direct evidence and can often be interpreted with greater taxonomic precision. Thus, wild rice phytolith analysis would prove a useful tool in advancing our understanding of the biogeography of wild rice. Further, this research would undoubtedly advance the method of phytolith analysis for both paleoecological and archaeological investigation.

# Chapter II

# METHODOLOGY

The ability to determine the presence and abundance of wild rice in both modern and paleo lake sediments requires a sequence of steps and procedures that incorporate methods from several different fields of study. The multidisciplinary implications of this research are reflected in the diversity of methods detailed in this chapter. I will first describe a novel quantification technique modified from well established paleolimnological methodology that allows for the calculation of phytolith estimates of absolute abundance in lake sediments and from plant matter. Secondly, while borrowing some methods from the existing phytolith literature, I will detail plant collection and phytolith extraction techniques from plant matter. I will next describe modern and lake sediment collection methods and strategy, and the lake sediment phytolith extraction techniques that I developed through a trial and error approach. Finally, I will detail the equations used to calculate presence and abundance of wild rice and present data from intermediate step that are vital to correct quantification of wild rice abundance.

Preparation of an Exotic Diatom Spike

An exotic diatom spike, used to calculate estimates of absolute phytolith abundance in lake sediments, was created by using a small sub-sample of a Pleistocene diatomite deposit from Japan (Julius and others, 2006). This diatomite is comprised of approximately 99% *Pliocaenicus omarensis* and 1% *Stephanodiscus kusuensis*, both of which are now extinct.

Step 1) Approximately 1 gram of diatomite was added to a 200 ml beaker with 50 ml of 35% $H_2O_2$ and boiled at 110º C for 4 hours. The sample was then removed from the hotplate, filled with distilled water, and placed in an ultrasonic water bath for 1 hour and allowed to settle overnight. The supernatant was decanted and the diatom slurry was transferred to a 50 ml centrifuge tube, filled with distilled water, centrifuged and decanted.

Step 2) The diatom slurry was then transferred to a 1 liter agarose colloidal suspension solution prepared by using approximately 5 grams of SeaPlaque (FMC BioProducts, catalog no. 50101) in 1 liter of distilled water. The diatom spike solution was sonicated for 1 hour and stirred with a magnetic stir bar for several hours. The diatom spike solution concentration was then calibrated using a Battarbee evaporation tray (Battarbee, 1973).

Calibration of an Exotic Diatom Spike

Step 1) One round 18 mm cover slip was added to each well in each tray (4 wells per tray, 2 trays poured and counted). One milliliter of diatom spike

solution was added to 50 ml distilled water, mixed and poured into each tray and allowed to evaporate at room temperature until completely dry (usually 4 or 5 days).

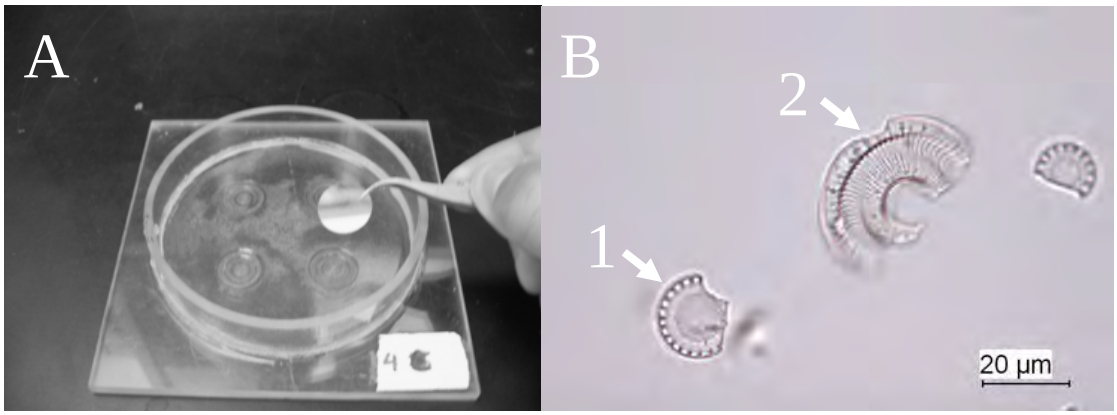


Figure 13

Battarbee Evaporation Tray & Exotic Diatom Spike
A) Battarbee evaporation tray (95 mm diameter settling chamber) with 4 round 18 mm cover slip wells. B) Exotic diatom spike: 1) *Pliocaenicus omarensis* and 2) *Stephanodiscus kusuensis.*

Step 2) When trays were visibly dry, each round cover slip was placed on an aluminum plate atop a hotplate, dried for 4 hours and then removed from heat. Each cover slip was then flipped over using tweezers, mounted on a microscope slide with a small drop of immersion oil and lined with nail polish.

Step 3) In order to test within tray and between tray variation in diatom settling, three diatom transects were counted per cover slip (12 per tray, 24 total) resulting in a diatom density calculation for each transect. Between tray

variation was then statistically evaluated using an independent-samples *t* test (SPSS ver. 12). The difference in means between each tray were not statistically significant (*p* value = .842); as a result, total diatoms in 1 ml of spike stock solution and 95% confidence intervals were then calculated based on the mean diatom density for all 24 transects.

Diatom Transect Density Equations:

1) transect distance (mm) / field of view diameter (mm) = # of transect fields viewed

2) # of transect fields viewed X field area ($mm^2$) = total transect area viewed ($mm^2$)

3) diatoms counted / total transect area viewed ($mm^2$) = transect diatoms per $mm^2$

Final Diatom Spike Calculation:

1) mean diatom density (43.8281 per $mm^2$) X total tray area (7088.2184 $mm^2$)

= 310,663 +/- 19,916 diatoms per ml of stock spike solution

Table 2

Independent-samples *t* Test Group Statistics for Tray 1 and 2 Transect Diatom Densities (t=.041, df=22, sig. two-tailed=.941)

| | TRAY | N | Mean | Std. Deviation | Std. Error Mean |
|---|---|---|---|---|---|
| DENSITY | 1.00 | 12 | 43.9316 | 6.89879 | 1.99151 |
| | 2.00 | 12 | 43.7246 | 6.70529 | 1.93565 |

Table 3

Diatom Spike Calibration Transect Counts and Calculations

| Battarbee Tray | Slide | Transect* | Distance (mm) | Diatom Count | Diatom Density/mm$^2$ |
|---|---|---|---|---|---|
| 1 | A | M | 16.8 | 283 | 34.7475 |
| 1 | A | T | 15.0 | 282 | 38.7797 |
| 1 | A | B | 14.6 | 213 | 30.0935 |
| 1 | B | M | 17.0 | 343 | 41.6190 |
| 1 | B | T | 15.1 | 339 | 46.3094 |
| 1 | B | B | 14.9 | 305 | 42.2241 |
| 1 | C | M | 17.2 | 441 | 52.8880 |
| 1 | C | T | 14.7 | 332 | 46.5873 |
| 1 | C | B | 15.1 | 392 | 53.5495 |
| 1 | D | M | 17.0 | 384 | 46.5939 |
| 1 | D | T | 13.6 | 317 | 48.0803 |
| 1 | D | B | 13.9 | 308 | 45.7070 |
| 2 | A | M | 17.0 | 364 | 44.1671 |
| 2 | A | T | 14.8 | 314 | 43.7638 |
| 2 | A | B | 15.7 | 331 | 43.4886 |
| 2 | B | M | 16.8 | 305 | 37.4487 |
| 2 | B | T | 14.7 | 223 | 31.2921 |
| 2 | B | B | 14.1 | 235 | 34.3792 |
| 2 | C | M | 16.8 | 428 | 52.5510 |
| 2 | C | T | 13.7 | 310 | 46.6754 |
| 2 | C | B | 14.4 | 337 | 48.2741 |
| 2 | D | M | 17.3 | 351 | 41.8512 |
| 2 | D | T | 14.7 | 341 | 47.8502 |
| 2 | D | B | 13.4 | 344 | 52.9542 |

* M = middle, T = top, B = bottom

Comparative Plant Phytolith Extraction

Plant material from a total of 37 different plant species (trees, shrubs, herbs and aquatic) were collected for phytolith extraction (Appendix A). These are species that are found within close approximation to study area lakes and that are the most likely contributors of opal silica phytoliths to study area lake sediments. Extra

emphasis was placed the collection of wetland grasses that grow in similar habitats and abundance as wild rice.

The vast majority of reference plant material was gathered from areas adjacent to Lake Ogechie in Mille Lacs Kathio State Park, Mille Lacs County, Minnesota. A few plants were collected from lakes and rivers in northeastern Minnesota. Additional plant material was acquired from herbarium specimens collected from central Minnesota. All fresh plant material was collected during the 2005 and 2006 growing season and identified by myself using various plant keys and reference material from the Saint Cloud State University Herbarium. Unless otherwise stated, only entire, mature plants with seed were collected. Plant material was processed for phytolith extraction using standard pre-treatment (Pearsall, 2000; Piperno, 2006) and dry ashing techniques (Parr and others, 2001a, 2001b) with some modifications.

Phytolith Extraction from Plants

Step 1) Plant material was cut into ½ inch to 1 inch sections, placed inside a Buchner funnel, rinsed with copious amounts of distilled water, and then transferred to appropriately sized beakers with 1% liquinox cleaning detergent. Each sample beaker was sonicated (ultrasonic water bath) for a ½ hour to 1 hour. Exact sonication time varied depending on the amount of extraneous material adhering to plants. Extra dirty plant material required several changes of liqinox solution during sonication. Plant material was then soaked in liquinox solution overnight, sonicated for another ½ hour the next day, rinsed with copious amounts of distilled water and then dried overnight at around 80º C. These sonication steps were extremely important when working with

aquatic plants such as *Zizania*. These plants have a considerable amount of algae (diatoms) and sediments with non-*Zizania* phytoliths lodged between culm and sheath material.

Step 2) Dried plant material was weighed, placed in crucibles and ashed in a muffle furnace for 6 hours at 500º C. Samples were allowed to cool overnight and then removed from furnace.

Step 3) Depending on the amount of ash material, samples were transferred to 15 or 50 ml centrifuge tubes using 10% hydrochloric acid (HCl) and heated for 1 hour at around 80º C. The addition of HCl helped to remove calcium carbonate and calcium oxalate, both of which can be abundant in aquatic plant material. The samples were then rinsed with distilled $H_2O$ and returned to heat (80º C) with 35% hydrogen peroxide ($H_2O_2$). The addition of $H_2O_2$ helped to remove additional organics and trace metals.

Step 4 ) Samples were twice rinsed with distilled water (centrifuge 3 minutes, 3000 rpm, then decant) and transferred to pre-weighed and dried 1-dram glass vials using 95% ETOH. Samples were then placed in drying oven for at least 24 hours and weighed.

Collection of Modern Lake Sediments

Surface samples were collected along transects from the densest part of a wild rice stand to areas away from and into deeper water for Lake Onamia, Shakopee Lake and Lake Ogechie (Table 4). Black Bass Lake is a non-wild rice lake and serves as a control. Transect placement was determined based on locations of wild rice observed

during the fall of 2005 and were collected at that time. Modern sediments were collected from a canoe using a modified Hongve-type gravity collector built by myself (see Figure 14) and based on mini gravity corer schematics from Wright (1990) and Glew (1991). The collector was lowered by rope slowly into the water until it came in contact with the surface of the sediment. Another rope, attached to the top, was pulled up, simultaneously closing the top and raising the collector. The sediment was held in place by suction and emptied into plastic containers. Every effort was made to only collect the top 2 or 3 centimeters, but some grabs may have been as deep as 4 cm. Because of the low bulk density and high organic content of modern lake sediments from the study area, volumetric sampling of wet sediment was virtually impossible. Sediments were dried completely in a drying oven and then stored in plastic bags.

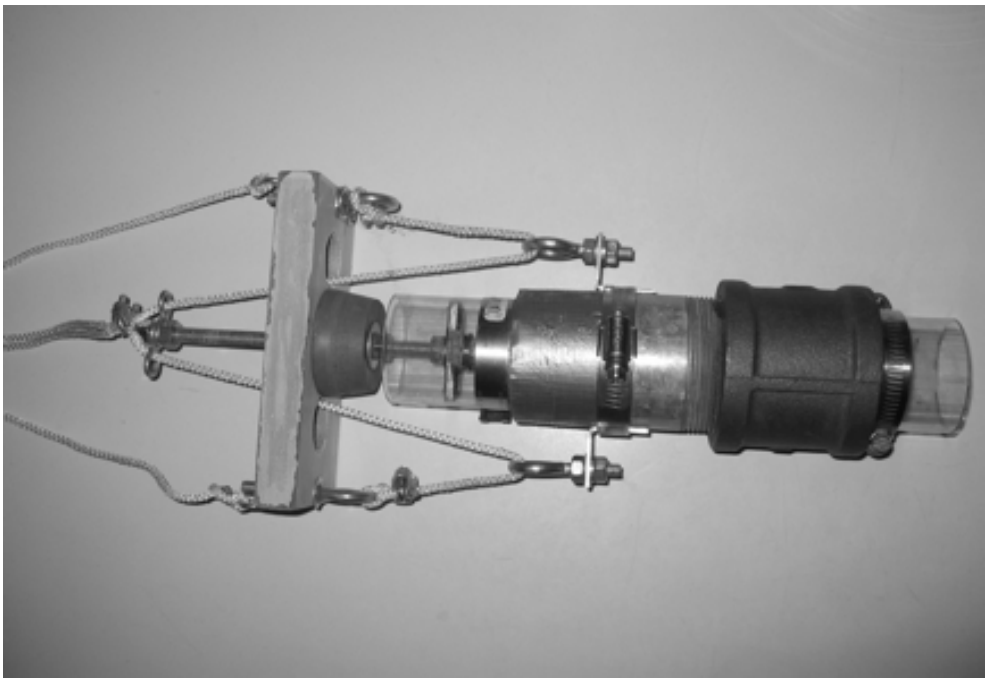

Figure 14

Modern Sediment Collector (Hongve-type Gravity Corer)

Table 4

Modern Lake Sediment Collection Locations

| Lake | Sample Code | Water Depth (meters) | Wild Rice Culms/$m^2$ | UTM Coord. (NAD 83) Northing | Easting | Comments |
|---|---|---|---|---|---|---|
| Ogechie | ML1 | 1.8 | 0 | 5112145 | 0441504 | sandy till |
| Ogechie | OGT1P1 | 0.8 | 0 | 5111840 | 0441270 | |
| Ogechie | OGT1P2 | 1.2 | 0 | 5111656 | 0441053 | |
| Ogechie | OGT1P3 | 1.2 | 15 | 5111542 | 0441013 | wild rice |
| Ogechie | OGT1P4 | 1.7 | 0 | 5110601 | 0439949 | |
| Ogechie | OGT1P5 | 1.4 | 0 | 5109264 | 0439559 | |
| Shakopee | ST1P1 | 0.9 | 120 | 5106486 | 0443183 | wild rice |
| Shakopee | ST1P2 | 0.9 | 0 | 5106575 | 0443348 | |
| Shakopee | ST1P3 | 0.9 | 100 | 5106716 | 0443602 | wild rice |
| Shakopee | ST1P4 | 1.3 | 0 | 5106774 | 0443780 | |
| Shakopee | ST1P5 | 1.1 | 100 | 5106814 | 0443769 | wild rice |
| Shakopee | ST1P6 | 1.2 | 0 | 5106905 | 0443938 | |
| Shakopee | ST1P7 | 1.0 | 0 | 5107065 | 0444283 | |
| Shakopee | ST2P1 | 3.7 | 0 | 5106543 | 0444000 | |
| Shakopee | ST2P2 | 4.3 | 0 | 5106372 | 0444308 | |
| Shakopee | ST2P3 | 3.3 | 0 | 5106175 | 0444782 | |
| Shakopee | ST2P4 | 3.5 | 0 | 5105979 | 0445246 | |
| Shakopee | ST2P5 | 1.0 | 0 | 5105812 | 0445526 | sandy till |
| Onamia | OT1P1 | 0.9 | 50 | 5103546 | 0447384 | wild rice |
| Onamia | OT1P2 | 0.9 | 40 | 5103520 | 447390 | wild rice |
| Onamia | OT1P3 | 1.1 | 20 | 5103492 | 447399 | wild rice |
| Onamia | OT1P4 | 1.0 | 40 | 5103455 | 0447412 | wild rice |
| Onamia | OT1P5 | 1.1 | 40 | 5103422 | 0447428 | wild rice |
| Onamia | OT1P6 | 1.1 | 20 | 5103371 | 0447456 | wild rice |
| Onamia | OT1P7 | 1.2 | 20 | 5103296 | 0447495 | wild rice |
| Onamia | OT1P8 | 1.2 | 10 | 5103230 | 0447530 | wild rice |
| Onamia | OT1P9 | 1.2 | 2 | 5103134 | 0447577 | wild rice |
| Onamia | OT1P10 | 1.2 | 0 | 5103012 | 0447645 | |
| Onamia | OT1P11 | 1.5 | 0 | 5102943 | 0447690 | |
| Onamia | OT1P12 | 1.4 | 0 | 5102881 | 0447732 | |
| Onamia | OT1P13 | 1.4 | 0 | 5102803 | 0447769 | |
| Onamia | OC1P1 | 1.4 | 0 | 5103163 | 0447828 | |
| Onamia | OT2P1 | 0.9 | 0 | 5102164 | 0447677 | |
| Onamia | OT2P2 | 1.0 | 0 | 5104949 | 0447218 | |
| Onamia | OT2P3 | 0.7 | 100 | 5103601 | 0446904 | |
| Black Bass | BB1P1 | 7.0 | 0 | 5108404 | 0445625 | control |

## Collection of Paleo Lake Sediments

The McAndrews Core. Paleo lake sediments from Lake Ogechie were supplied and sub-sampled by John McAndrews, Professor Emeritus, University of Toronto, Canada. In 1968, McAndrews lifted a 1,185 cm Livingstone piston core from the north end of Lake Ogechie. He returned in 1969 and lifted a core that spanned 1000 cm to 1,700 cm. In a report prepared for the Minnesota Department of Transportation, McAndrews (2000), recounted pollen grains and radiocarbon dated three levels to reconstruct a 10,000 year vegetation and environmental change history for the Lake Ogechie area. Based on grass pollen relative abundance and grass pollen grain size analysis, he concluded that wild rice was probably present in Lake Ogechie for the past 3000 years. For this thesis study, McAndrews supplied sub-samples from the 10, 30, 70, 90, 110, 150, 200, 250, 300, 350, 370, 400, 450, 500, 550, 600, 650 and 700 cm levels. This range encompasses the most likely possible span of wild rice occurrence for Lake Ogechie. All of these samples were processed and counted for wild rice and all other grass silica short cell phytoliths.

~~SCSU Vibracore~~. As part of a Lake Ogechie wild rice reintroduction feasibility study being conducted by principal investigator Richard Rothaus at Saint Cloud State University (SCSU), a transect of 5 long cores from south to north were lifted from Lake Ogechie in April of 2006. Core extraction was facilitated by using micro-vibrations to drive a 20 foot, 3 inch diameter aluminum tube into lake sediment (Smith and Clausner, 1993). Initial core description and lithology for all five cores

was completed by Joe Boyce and Eduard Reinhardt, McMaster University, Hamilton, Ontario, Canada. The first core, OGI-1, a 389 cm core, was lifted from the south end of Lake Ogechie. Sub-sampling was conducted at McMaster University and three to five cubic centimeter wet samples were mailed to SCSU and processed for phytoliths at the 1, 5, 10, 15, 20, 25, 30, 35, 40, 45, 50, 55, 70, 85, 100, 115, 130, 145, 160, 175, 190, 200, 220, 240, 260, 280, 300, 320, 340 and 360 cm levels.

### Extraction of Phytoliths from Modern and Paleo Lake Sediments

For this study, phytolith extraction from modern and paleo lake sediments generally follows a wet oxidation technique commonly employed by phytolith analysts (Zhao and Pearsall, 1998; Pearsall, 2000; Piperno, 2006). However, modifications were developed over a year-long trial and error period, resulting in a procedure that is optimized for extraction of wild rice phytoliths from shallow depth, highly organic lake sediments.

The amount of sample processed for phytoliths varied slightly between the modern sediments, McAndrews' core sediments and SCSU's Vibracore sediments. For the modern sediments, 1 gram of dry lake sediment was processed for each transect collection point, and 1 ml of exotic diatom spike (310,663 +/- 19,916 diatoms) was added to each sample after processing. During storage at the University of Toronto, McAndrews' Lake Ogechie core had completely dried-out. Since shrinkage and compaction had occurred, wet volumetric sampling was not possible. Therefore, for the McAndrews' core, 0.1 gram of dry sediment was processed for each sample

level, and 0.1 ml of exotic diatom spike (31,066 +/- 1,992 diatoms) was added to each sample. For the SCSU Lake Ogechie vibracore (OGI-1), 1 cubic centimeter of wet sediment was processed for each sample level and 0.2 ml of exotic diatom spike (62,132 +/- 3,984 diatoms) was added to each sample. All modern and paleo samples were then subjected to the same phytolith extraction protocol outlined next (Figure 15).

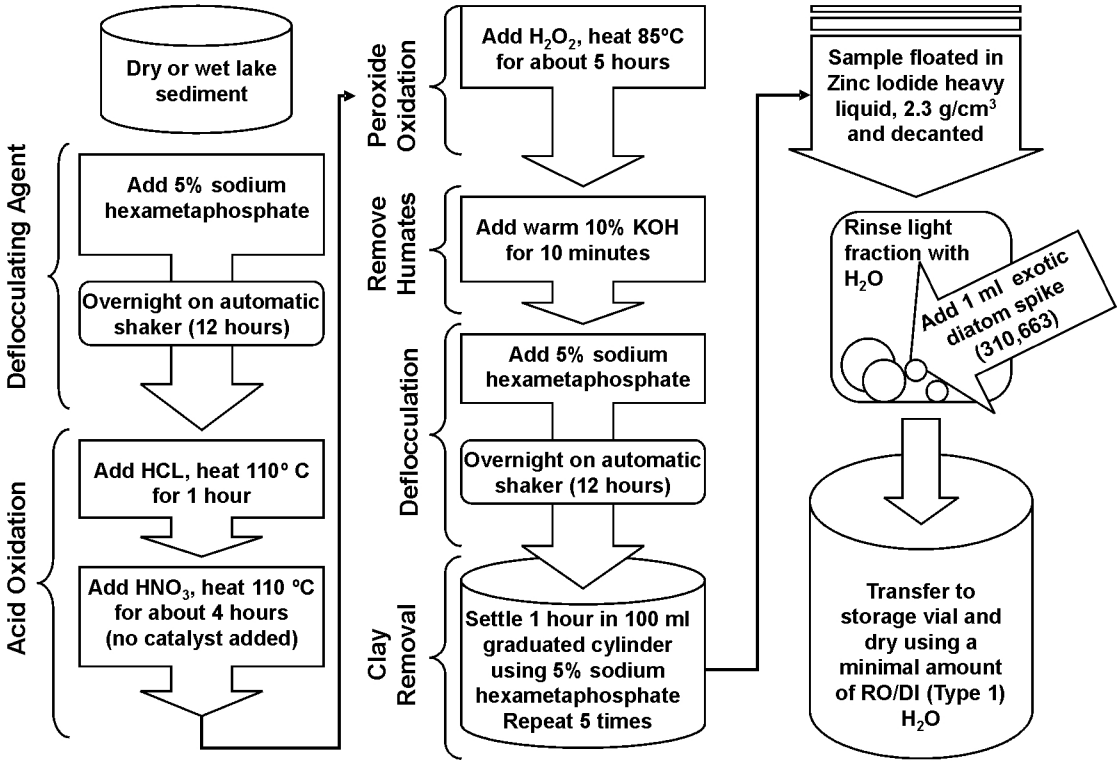


Figure 15

Flowchart for Phytolith Extraction from Modern and Paleo Lake Sediments
(Detailed steps can be found in Appendix B)

Samples were first disaggregated overnight on an automatic shaker in 5% sodium hexametaphsphate, rinsed in distilled water and transferred to 200 ml beakers.

Samples were then heated without a watch glass at 110º C for 1 hour in 20 ml 36% hydrochloric acid (HCl) to remove carbonates. To break down and remove organics, 69% nitric acid ($HNO_3$) was then added directly to each beaker and returned to heat for 2.5 hours with watch glasses and 1.5 hours without watch glasses to evaporate-off excess liquid. To completely remove all remaining organics, samples were then rinsed with distilled water (centrifuge and decant cycles), and returned to beakers with 35% hydrogen peroxide ($H_2O_2$) and heated for 4.5 hours with watch glasses and 1.5 hours without watch glasses at 85º C. Samples were then removed from heat, centrifuged, decanted and rinsed with distilled water. Rinsing was repeated several times to remove all $H_2O_2$. Next, to remove humates unoxidized by acid or peroxide, 20 ml warm 10% potassium hydroxide (KOH) was added to each sample. Samples were then rinsed with distilled water once, rinsed with 10% HCl once and then rinsed twice more with distilled water. These rinses remove all potentially destructive KOH and return sample material from highly basic to acidic conditions. Samples were then returned to an overnight shake with 5% sodium hexametaphosphate and then subjected to 4 or 5 rounds of 1 hour, 10 cm, gravity settling to remove clays, some diatoms and other small particles (Lentfer and others, 1999; Lentfer and Boyd, 2003). Samples were then rinsed several times with distilled water and floated in zinc iodide ($ZnI_2$) heavy liquid set to 2.3 $g/cm^3$ to separate the light phytolith fraction from the heavier mineral fraction. Samples were then thoroughly rinsed with distilled water. Next, a known quantity of exotic diatom spike was added to each sample and samples were rinsed and decanted again, but with reverse osmosis deionized water (RO/DI Type 1

water). After the final decant, only a small fraction of water will remain with the phytolith sample. Each sample was then transferred from its centrifuge tube to a 1-dram glass vial and dried in a drying oven for 4 or 5 days at 50º C. Phytolith samples were then prepared for light microscopy. A very detailed step-by-step extraction procedure is provided in Appendix B.

## Observation and Classification of Extracted Phytoliths

Slide preparation. A very small amount of immersion oil (Cargill, low viscocity, Type-A, refractive index 1.515) was first dropped onto a microscope slide. A small amount of dry phytolith extract was then removed from the glass storage vial using a small metal spatula, dabbed onto the microscope slide with the oil drop, and thoroughly mixed. A square cover slip was then gently lowered onto the oil/phytolith drop. Addition of too much oil will cause some oil and phytoliths to migrate outside of the cover slip boundary. A very small micro-drop of clear nail polish was dabbed onto two opposite corners of the cover slip, anchoring it to the microscope slide (Figure 16).

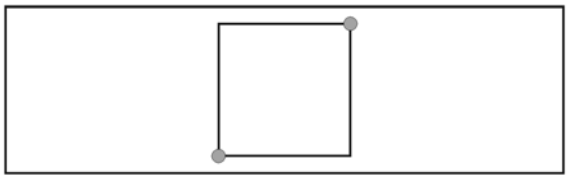

Figure 16

Microscope Slide Mounting Diagram
Illustration of nail polish applied to two opposing corners of the cover slip.

Anchoring the cover slip in this manner allows for the slow controlled rotation of phytoliths by gentle application of pressure to the cover slip with a fine-point probe. When pressure is removed, phytoliths will return to their original position and orientation. This allows for accurate phytolith quantification along slide transects. After mounting, slides are typically set aside for a few hours to allow phytoliths to settle to the same plane of focus. When finished counting, cover slips were completely lined (sealed) with nail polish.

Light microscopy. Initial comparative phytolith observations were made under 1000X oil immersion magnification and 400X magnification using a Leica DM LB light microscope. Still image micrographs were captured using a Nikon CoolPix 990 with a phototube mount. Video of phytoliths in rotation were captured using Motic Images 2000 version 1.3 software. Final comparative phytolith observations and all modern and paleo sediment extracted phytoliths were made under 400X magnification using a Leica DM 3000 with integrated still and video capture via Leica Imaging Software Suite version 2.5. Micrographs for each sample were saved in jpg format and videos, when captured, were saved in avi format.

Phytolith descriptions and classification. Wild rice (*Zizania*) and rice cut grass (*Leersia*) phytoliths were first observed, then photographed (still and video) and sketched in detail. The sketches (line drawings) are in 2-D and 3-D perspective. Wild rice and *Leersia* phytoliths were classified by anatomical origin and a morphotype numeric designation. Individual plant-parts (leaf, culm, inflorescence, etc.) and entire

plants were dry ashed and observed, resulting in plant-part specific and whole plant morphotype assemblages of taxonomically important grass silica short cells. Other taxa from the comparative collection were photographed (some with video), but since no other wild rice confuser phytoliths were observed outside of *Leersia*, grass silica short cell morphotype assemblages and line drawings for other comparative taxa were not acquired.

Phytoliths extracted from modern and paleo lake sediments were classified using ICPN nomenclature (Madella and others, 2005), or when known, anatomical origin naming conventions from the phytolith literature and this study. Since this thesis is focused primarily on wild rice phytoliths, only grass silica short cells and a few grass silica long cell types were counted. Phytoliths from *Equisetum* and the Cyperaceae are the only exception to this rule and were counted in the modern sediment studies. Although present in modern and paleo lake sediments, elongate and blocky phytoliths from arboreal taxa were not counted.

### ~~Dry Weight to Wet Volume Conversion~~

In order to make direct phytolith abundance comparisons between McAndrews' core from the north end of Lake Ogechie and the SCSU vibracore from the south end of Lake Ogechie, the dry weight ($W_d$) sub-samples from the McAndrews core were converted to a wet volume ($V_t$). In paleolimnology, starting with a known volume of sediment is preferred because concentration (phytoliths per $cm^3$) and annual influx (phytoliths per $cm^2$ per year) can be determined. A conversion from the known, $W_d$ to the unknown $V_t$ for the McAndrews samples is possible through an inverse

relationship that exists between dry bulk density (BD) and the percent organic matter (OM) of lake sediments (Avnimelech, 2001). Dry bulk density (measured in $g/cm^3$) for sediments was determined by the weight of the sample dry ($W_d$) / total sample volume ($V_t$), and can be written as: $BD = W_d / V_t$. Percent organic matter (OM) was calculated by loss-on-ignition (Dean, 1974; Heiri and others, 2001). To determine the relationship between BD and OM for Lake Ogechie, a linear regression correlation was calculated for the SCSU vibracore sediments (Figure 17 and Table 5). The resulting equation is: $\text{Log}_e (BD) = -0.296 - 3.719 \cdot (OM)$ with an $R^2$ of 0.80, which can be rewritten as: $W_d / V_t = e^{(-0.296-3.719 \cdot OM)}$. Since percent organic matter (OM) and dry weight ($W_d$) is known for each sample from the McAndrews core, the original wet volume ($V_t$) was solved for (Table 6). If the outlier at 2.1 $g/cm^3$ is removed from the regression, the $R^2$ would increase to 0.86; however, this outlier was not removed and remains in the final regression equation.

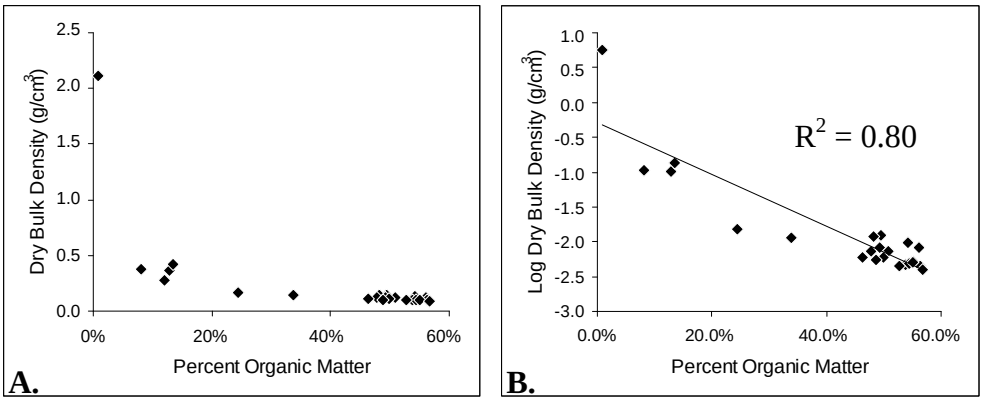


Figure 17

Bulk Density vs. Organic Matter Scatterplot and Regression
A. Scatterplot of BD vs. OM for Lake Ogechie Vibracore sediments. B. Regression scatterplot of $\text{Log}_e$ BD vs. OM with the equation: $\text{Log}_e (BD) = -0.296 - 3.719 \cdot (OM)$

Table 5

Bulk Density & % Organic Matter Determined for Lake Ogechie Vibracore ($V_t$ = 1 $cm^3$)

| Depth | BD (g/cm3) | OM (%) | Depth | BD (g/cm3) | OM (%) | Depth | BD (g/cm3) | OM (%) |
|---|---|---|---|---|---|---|---|---|
| 1 | 0.1483 | 0.4949 | 40 | 0.1028 | 0.5506 | 180 | 0.1040 | 0.4875 |
| 5 | 0.1453 | 0.4811 | 45 | 0.0978 | 0.5450 | 200 | 0.1431 | 0.3382 |
| 10 | 0.1188 | 0.4781 | 50 | 0.0951 | 0.5626 | 240 | 0.1624 | 0.2438 |
| 15 | 0.1254 | 0.4920 | 55 | 0.1014 | 0.5513 | 260 | 0.3803 | 0.0813 |
| 20 | 0.1327 | 0.5418 | 80 | 0.0911 | 0.5675 | 280 | 0.2750 | 0.1193 |
| 25 | 0.1233 | 0.5604 | 105 | 0.0951 | 0.5268 | 320 | 0.3702 | 0.1278 |
| 30 | 0.1179 | 0.5081 | 130 | 0.1075 | 0.4995 | 360 | 0.4174 | 0.1344 |
| 35 | 0.0973 | 0.5375 | 155 | 0.1082 | 0.4630 | 380 | 2.1099 | 0.0087 |

Table 6

Wet Volume ($V_t$) for McAndrews Core Calculated from Vibracore Regression Eq.

| Depth | OM (%) | $V_t$ ($cm^3$) | Depth | OM (%) | $V_t$ ($cm^3$) | Depth | OM (%) | $V_t$ ($cm^3$) |
|---|---|---|---|---|---|---|---|---|
| 10 | 50.0 | 0.9393 | 150 | 50.0 | 0.8800 | 400 | 37.5 | 0.6104 |
| 30 | 54.0 | 1.0323 | 200 | 47.5 | 0.8410 | 450 | 32.5 | 0.5540 |
| 70 | 48.0 | 0.6536 | 250 | 42.5 | 0.7153 | 500 | 30.0 | 0.5189 |
| 90 | 45.0 | 0.7966 | 300 | 34.0 | 0.5534 | 550 | 31.0 | 0.5335 |
| 110 | 45.5 | 0.3876 | 350 | 31.0 | 0.5223 | 600 | 22.5 | 0.4085 |
| 130 | 50.0 | 0.5955 | 370 | 35.0 | 0.5791 | 650 | 21.0 | 0.3842 |
| | | | | | | 700 | 18.0 | 0.3712 |

Phytolith Slide Counts

For modern lake sediment samples, all grass silica short cell phytoliths were counted until a total of 500 exotic diatom spike phytoliths were counted. These samples had 310,663 +/- 19,916 diatoms added to each 1 gram dry sediment processed sample.

For the McAndrews core sediments, all grass silica short cell phytoliths were counted until a total of 100 exotic diatom spike phytoliths were counted. These samples had 31,066 +/- 1,992 diatoms added to each 0.1 gram dry sediment sample.

For the SCSU vibracore only wild rice phytoliths were counted. Counts with over 30 wild rice phytoliths were stopped at an exotic diatom count of 200. Samples with less than 30 wild rice phytoliths were stopped at an exotic diatom count of 400. These samples had 62,132 +/- 3,984 diatoms added to each 1.0 cubic centimeter wet sediment processed sample.

Calculation of Phytolith Concentration

An estimate of the total number of phytoliths in a known weight ($W_d$) or volume ($V_t$) of lake sediment sample was calculated by the addition of a known quantity of the previously calibrated diatom spike ($S_1$) using the following equation:

phytolith concentration ($P_c$) = phytoliths counted ($P_1$) · spike added ($S_1$) / spike counted ($S_2$)

For modern sediments, $P_c$ is expressed as phytoliths per gram dry sediment ($P_c/W_d$). For paleo lake sediments, $P_c$ is expressed as phytoliths per $cm^3$ of lake sediment ($P_c/V_t$). Phytolith concentration was calculated for each modern sediment collection point and for each paleo lake sediment level processed for phytoliths.

Calculation of Annual Phytolith Influx
(Accumulation Rates)

Although many, if not the majority, of paleolimnological studies use relative counting methods, absolute quantification was deemed necessary here to accurately interpret periodic oscillations in wild rice abundance. With relative counting, percents of relative abundance are calculated from the total sum of target items. When one item increases in abundance, all others are relatively reduced in abundance, whether or

not they *actually* are reduced in number. Changes in lake margin vegetation could therefore change the relative abundance of wild rice without wild rice abundance actually changing.

Calculating an absolute quantity wild rice phytoliths per weight or volume of lake sediment (phytolith concentration) is really only part of the story. Since lake sedimentation rates often change, the amount of time that it takes for a known weight or volume of sediment with a given quantity of wild rice phytoliths to accumulate also changes. By calculating the sedimentation rate, phytolith concentration can then be expressed as the number of wild rice phytoliths per area of lake sediment per year, otherwise known as phytolith accumulation rates or influx rates.

In order to calculate phytolith influx ($P_i$) for paleo lake sediments, sedimentation rates must be known. Sedimentation rates are calculated by dating as least three (preferably more) levels from a lake core. Usually levels with distinct changes in lithology or phytolith/pollen assemblages are sent in for $^{14}C$ radiocarbon dating. An age model (years BP) and sedimentation rates (centimeters per year) are then calculated for all lake core levels based on linear interpolation.

The SCSU vibracore was sub-sampled for lead ($^{210}Pb$) and $^{14}C$ radiocarbon dates; however, results have not been returned. Only the McAndrews core had dates (4 radiocarbon dates), so sedimentation rates (SR) were calculated. Annual phytolith influx ($P_i$) expressed as phytoliths per $cm^2$ per year, were then calculated using the following equation:

$$P_{i\ (cm^{2}\text{-}1 yr^{-1})} = SR_{(cm\ yr^{-1})} \cdot P_{c\ (cm^{3}\text{-}1)}$$

where SR equals sedimentation rate, expressed as centimeters per year and $P_c$ equals phytolith concentration, expressed as phytoliths per $cm^3$.

Phytoliths concentration and absolute abundance values, as well as comparisons with corresponding pollen data were stratigraphically graphed and displayed using C2 version 1.4.3 (Juggins, 2006).

## Conclusion

With the majority of phytolith studies taking place within a terrestrial context, this thesis developed useful methodologies optimized for the extraction, concentration and quantification of the phytolith fraction from highly organic lake sediments.

With the help of Dr. Matthew Julius, Department of Biology, St. Cloud State University, a novel method of phytolith quantification was established by using extinct diatoms from a Japanese Pleistocene diatomite deposit as an exotic spike to calculate absolute abundance of phytoliths. Since fossil diatoms and phytoliths are both comprised of biogenic opal silica, the diatom spike can be subjected to phytolith extraction steps without degradation or dissolution. However, since centric diatoms do not follow Stokes' law of gravity settling, the spike needs to be added after clay removal settling steps. Since clay sized particles, including native diatoms, were necessarily removed by gravity settling, the diatom spike was added *after* gravity settling. If gravity settling is not necessary, this technique may allow researchers to better assess recovery and loss of phytoliths during extraction treatments by addition of the diatom spike during initial extraction steps.

Also, the use of a Battarbee evaporation tray to quantify absolute abundance of phytoliths is a novel approach in phytolith analysis. Although a standard technique in limnology, application of this technique is not mentioned in the phytolith literature and may prove useful for other phytolith researchers.

Perhaps the most crucial outcome of this methodological phase of study was the development of a lake sediment phytolith extraction method. Modifications to standard wet oxidation techniques (Pearsall, 2000; Piperno, 2006) were developed over a year-long trial and error period, resulting in a procedure that is optimized for extraction of wild rice phytoliths from highly organic lake sediments (Appendix B). Although the extraction protocol takes about 5 days to process a set of sediment samples, it is possible that certain steps may be reduced or eliminated without a noticeable reduction in total phytolith extract.

# Chapter III

# COMPARATIVE PHYTOLITH ANALYSIS

## INTRODUCTION

This chapter presents the results of the comparative phytolith analysis for wild rice and other common species from the study area. The Results section is divided into three subtopics: 1) Lake Margin Phytolith Producers and Morphotypes; 2) *Leersia* Phytolith Morphotypes; and 3) Wild Rice Phytolith Morphotypes. The goal of this chapter is to identify any potential wild rice confuser morphotypes from non-wild rice phytolith producing taxa. In the Diagnostic *Zizania* Morphotype Determination section, final determination of locally diagnostic wild rice phytolith morphotypes is made. These locally diagnostic morphotypes are then used in chapters 4 and 5 for modern and paleo lake sediment analysis and interpretation. All of the findings are summarized in the Conclusion section.

## METHODOLOGY

The data presented in this chapter are the result of the phytolith extraction from plant material method described in Chapter 2. Specific methods and considerations unique to each subtopic are briefly summarized within the subsection.

It should be noted that only grass silica short cell phytoliths and a few grass silica long cell phytolith morphotypes were described, classified and counted. Counting of Equisetaceae and Cyperaceae phytoliths are the only exception to this rule. Because of their ubiquity within the Poaceae and the requirement for detailed morphometric analysis for possible species separation (Pearsall, 1995; Zhao, 1998), a comprehensive study of bulliform cells was not undertaken.

Wild rice and many other phytolith bearing plants produce a multitude of lightly silicified epidermal cells (cast phytoliths); however, upon observation of lake sediments prior to comparative collection analysis, very few of these lightly silicified phytoliths were observed. In an aqueous environment, lightly silicified epidermal cells, and even lightly silicified short cells, may be especially vulnerable to dissolution. Differential preservation of wild rice morphotypes likely was the cause of a low correlation of wild rice zone phytolith assemblages for the Davidson (2003) wild rice study. Thus, to save time, the majority of comparative phytolith descriptions and designation of wild rice morphotypes are limited to grass silica short cell phytoliths.

~~On Descriptive Terminology~~

Many of the terms and nomenclature used to describe and classify phytoliths herein are derived from the International Code for Phytolith Nomenclature 1.0 (Madella and others, 2005). The descriptors top, side, base and end are adapted from Mulholland and Rapp (1992). Some specific examples of terms commonly used in this study are illustrated in Figure 18.

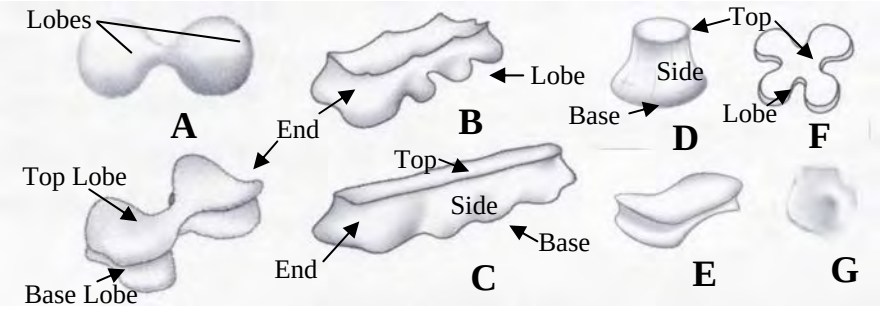


Figure 18

Schematic Drawings of Common Poaceae Phytolith Types (Madella and others, 2005) A) bilobates in top and oblique views; B) trapeziform polylobate in oblique view; C) trapeziform sinuate in oblique view; D) rondel in side view; E) saddle in oblique view F) cross in top view; G) papillae in top view.

The broadest face of a phytolith, when present, is referred to as the base, and the opposite face, by default, is the top. When viewed *in situ*, typically, the phytolith base is anatomically the top face and protrudes slightly from the epidermis. When disarticulated from the epidermis, this "top" face typically settles face-down on the microscope slide. In general, the broadest face (base) of a phytolith settles base-down.

On Plant Anatomy Terminology

In describing source material for phytoliths in this study, some basic plant anatomical terms are explained here (see Figures 4 & 5 for *Zizania* illustrations). In grasses, the main stem is referred to as the culm. The leaf is divided into two primary parts: the leaf sheath and the leaf blade. The leaf sheath originates from a node and runs parallel to the culm until it turns away from the culm, at which point, it is referred to as the leaf blade. The flowering part of a plant is referred to as the inflorescence.

For the grasses, the inflorescence is divided into many different specialized structures but is summarized here into only two main parts: the rachis (braches) and the spikelet (flowering and seed producing structures). The spikelet can be either male (staminate) or female (pistillate), and can be further subdivided into glumes, lemmas, paleas and awns (see Figures 4 & 5 for illustrations).

## RESULTS

### Lake Margin Phytolith Producers and Morphotypes

Although a total of 37 different trees, shrubs, forbs and aquatic plant species from the study area or similar locations were examined for production of possible wild rice confuser phytoliths (Appendix A), only Poaceae, Equisetaceae and Cyperaceae taxa found near the lake margin are discussed here. These are plants observed by myself and also observed during a Lake Ogechie plant community study conducted by Arriagada (2006). Arriagada classified the plant community surrounding Lake Ogechie as emergent marsh with two subtypes: 1) a mixed emergent marsh dominated mainly by *Carex comosa* and *Carex stricta*; and 2) a cattail marsh dominated by *Typha angustifolia* (Table 7). I observed a few additional common grass species not listed in the Arriagada study (Table 8). At least one species from each genus in Table 7 and all taxa in Table 8 were analyzed for phytolith production. All taxa in Table 8 are represented by phytolith micrograph Figures 19 through 24.

Table 7

Dominant Taxa and Associated Poaceae and Cyperaceae Taxa for Lake Ogechie Plant Communities (Arriagada, 2006)

EMERGENT MARSH DOMINANT SPECIES

| Scientific | Common | Scientific | Common |
|---|---|---|---|
| *Carex comosa* | Bottlebrush sedge | *Phalaris arundinacea* | Reed canary grass |
| *Carex stricta* | Hummock sedge | *Phragmites australis* | Giant Reed |
| *Calamagrostis canadensis* | Canada bluejoint | *Typha angustifolia* | Narrow-leaved cattail |

EMERGENT AND CATTAIL MARSH ASSOCIATED POACEAE AND CYPERACEAE SPECIES

| Scientific | Common | Scientific | Common |
|---|---|---|---|
| *Carex lacustris* | Lake sedge | *Leersia oryzoides* | Rice cut grass |
| *Carex sterilis* | Sterile sedge | *Glyceria grandis* | Tall manna grass |
| *Poa palustris* | Waterfowl meadow grass | *Schoenoplectus acutus* | Hard stem bulrush |
| *Scirpus americanus* | Three-square bulrush | *Scirpus validus* | Soft stem bulrush |

SUBMERSED PLANT COMMUNITY DOMINANT SPECIES

| Scientific | Common | Scientific | Common |
|---|---|---|---|
| *Ceratophyllum demersum* | Coontail | *Potamogeton pusillus* | Lesser Pondweed |
| *Potamogeton amplifolius* | Large-leaved pondweed | *Vallisneria amaricana* | Wild celery |
| *Potamogeton natans* | Floating-leaf pondweed | *Myriophyllum verticillatum* | Water milfoil |
| *Potamogeton pectinatus* | Sago pondweed | *Nuphar lutea* | Yellow water-lily |
| *Potamogeton illinoensis* | Illinois pondweed | *Nymphaea odorata* | White water-lily |

Table 8

Grass Species Commonly Found Near Study Area Wild Rice Stands

| Scientific | Common | Subfamily | Tribe |
|---|---|---|---|
| *Calamagrostis canadensis* | Canada bluejoint | Pooideae | Aveneae |
| *Calamagrostis inexpansa* | Slim bluejoint | Pooideae | Aveneae |
| *Glyceria canadensis** | Rattlesnake manna grass | Pooideae | Meliceae |
| *Glyceria grandis* | Tall manna grass | Pooideae | Meliceae |
| *Leersia oryzoides* | Rice cut grass | Erhartoideae | Oryzeae |
| *Muhlenbergia glomerata* | Spike Muhly | Chloridoideae | Eragrostideae |
| *Phalaris arundinacea* | Reed canary grass | Pooideae | Aveneae |
| *Phragmites australis* | Giant reed | Arundinoideae | Arundineae |
| *Poa palustris* | Waterfowl meadow grass | Pooideae | Poeae |

*collected from Big Rice Lake, St. Louis Co., MN.

What follows next are phytolith micrographs for the dominant grass species commonly found near wild rice stands and lake margins for study area lakes (Figures 18 through 23). Since many of the plants were divided into anatomical plant parts (e.g. leaf, culm, inflorescence), general anatomical origin of many of the phytolith morphotypes was established and is reflected in the caption description. Although not empirically calculated, the morphotypes depicted represent the most abundant forms observed for each plant-part analyzed. Extra examination emphasis was placed on morphotypes with features similar to those observed in wild rice phytoliths. Phytolith micrographs for wild rice follow the common grass species treatment.

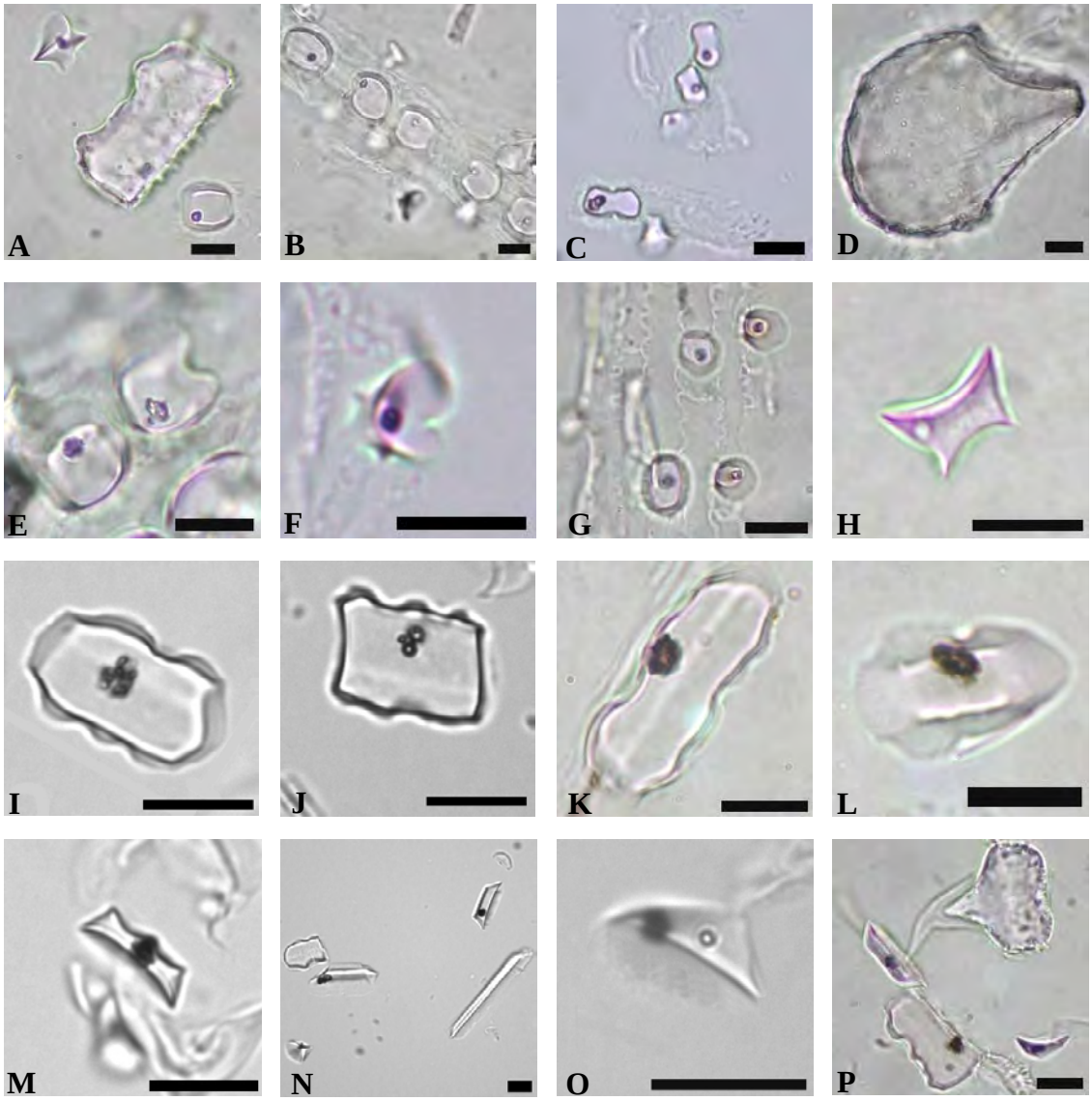


Figure 19

*Phragmites australis* (A-H) and *Phalaris arundinacea* (I-P) Phytolith Micrographs Scale bar = 10 µm: A) disarticulated oblique view leaf concave rondel, leaf blocky bulliform and leaf concave rondel in top view; B) sequence of leaf concave rondels *in situ*, top view; C) inflorescence bilobates, top and side view; D) leaf cuneiform bulliform; E) leaf rondels, top view; F) inflorescence rondel, base/oblique view; G) culm rondels, top view *in situ*; H) leaf rondel, side view; I – L ) leaf/culm trapeziform sinuates, top view; M) inflorescence elongated rondel, side view; N) leaf/culm trapeziform sinuates, side and top view; O) inflorescence conical rondel, side view; P) trichome in side view and trapeziform sinuates in side and top view.

*Phragmites australis* (Figure 19 A-H) short cell phytoliths from culm, leaf and stem material are dominated by rondels with concave base, top and sides. My rondel typological designation differs from common definition in the literature, which typically classifies the morphotypes in Figure 19 A-B and E-H as saddles. Specific examples include: “wide saddles” by Brown (1984); “saddle-topped short trapezoids” by Ollendorf and others (1988); and “plateaued saddles” by Piperno (2006); also called bidolabriform-patelliform by Bombin (1984). In fixed mounting media, these phytoliths in top or base view can appear as classic Chloridoideae saddles; however, full rotation reveals the tall, more trapezoid rondel-like appearance of the morphotype. To avoid confusion with Chloridoideae species, I have dropped “saddle” from the descriptor for *Phragmites* phytoliths. Since four or more faces are typically concave, I use concave rondel as the descriptor for this morphotype. These phytoliths have been described as distinctive by Piperno (2006) and may be diagnostic to the genus.

*Phalaris arundinacea* (Figure 19 I-P) short cell phytoliths from the inflorescence are lightly silicified conical rondels and extremely numerous in number (Figure 19 O). These phytoliths were also observed on the culm, but tended to have a keeled top. These lightly silicified phytoliths may be prone to dissolution in lake sediments. Short cell phytoliths from leaf and culm material are dominated by trapeziform elongate sinuates of varying length and number of undulations. These phytoliths are often described as short wavy and long wavy phytoliths, and the plant has been analyzed by many researchers (Brown, 1984; Hodson and others, 1985; Piperno and Pearsall, 1998; Mulholland, 1989; Fredlund and Tieszen, 1994).

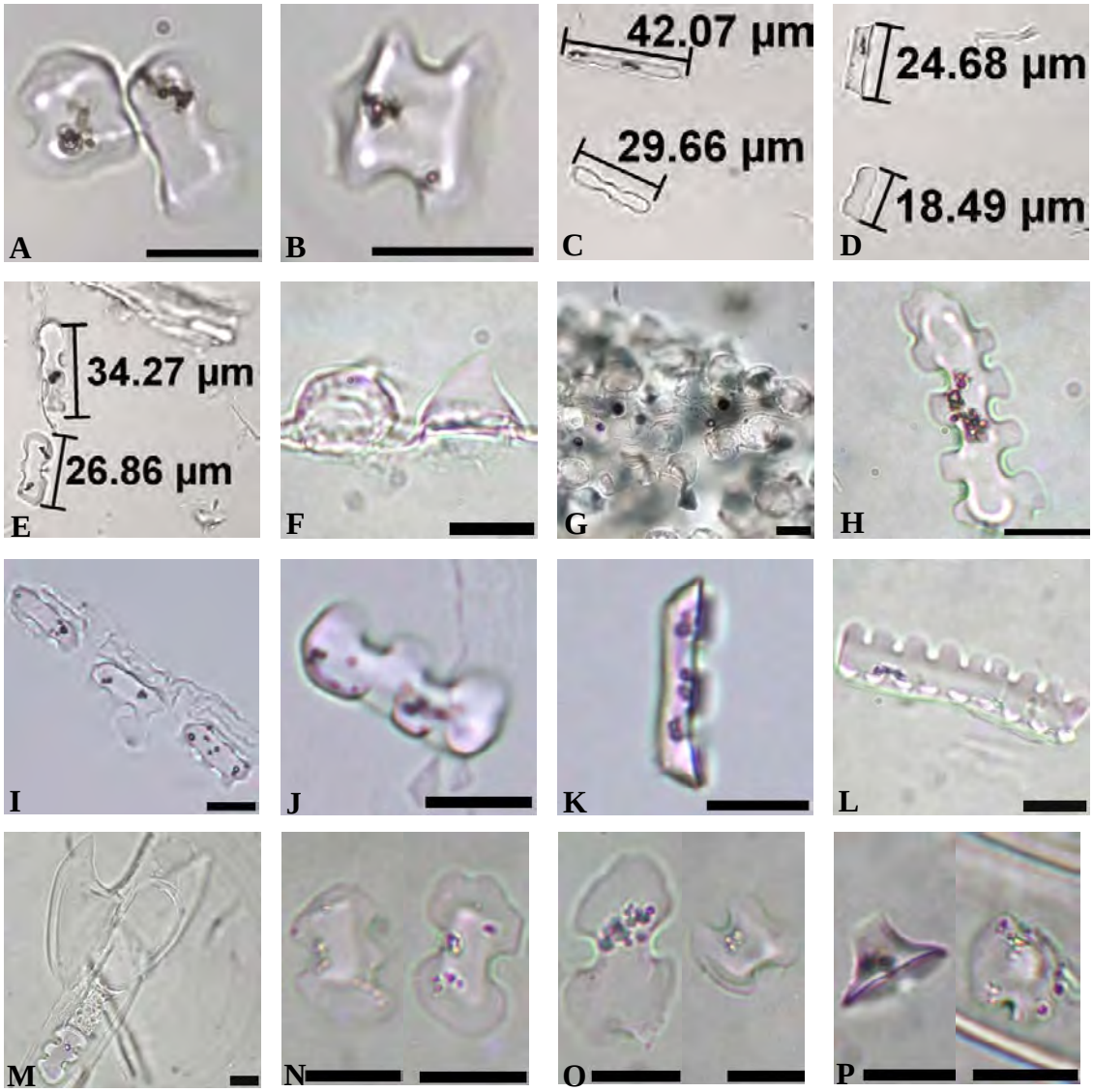


Figure 20

*Calamagrostis* and *Glyceria* Phytolith Micrographs

*Calamagrostis inexpansa* (A-E), *C. canadensis* (F-H), *Glyceria grandis* (I-K) and *G. canadensis* (L-P); Scale bar = 10 µm: A) leaf trapeziform bilobates, top view; B) leaf cross, top view; C-E) leaf/culm trapeziform sinuates and polylobates in top and side view; F-G) inflorescence papillae in side and top view; H) leaf trapeziform polylobate in top view; I) inflorescence trapeziform polylobates *in situ*; J-K) leaf trapeziforms in base and side views; L) leaf trapeziform polylobate, base view; M) leaf trichomes and trapeziform polylobate *in situ*; N) inflorescence bilobates in top view; O) inflorescence bilobates in top view; P) culm rondel in side view and papillae *in situ*.

*Calamagrostis inexpansa* and *C. canadensis* (Figure 20 A-H) silica short cell phytoliths from leaf and culm material are dominated by trapeziform elongates with crenate margins (Figure 20 C-E & H). Inflorescence short cells are dominated by conical rondels (Figure 20 F-G) but also produce a moderate amount of trapeziform bilobates (Figure 20 A) that occasionally approach a 4-lobed cross designation (Figure 20 B). Plants from the genus have been analyzed by some phytolith researchers including Brown (1984), Piperno and Pearsall (1998) and Blinnikov (2005). Blackman (1971) has a detailed account of phytolith production for *Calamagrostis inexpansa*.

*Glyceria grandis* and *G. canadensis* (Figure 20 I-P) silica short cell phytolith assemblages are very similar to that observed for *Calamagrostis*; however, length of body and number of crenate lobes may be slightly higher for *Glyceria*. A conical rondel with 2 opposing clefts on the base, and a similar phytolith, possibly a papillae cell, were occasionally observed (Figure 20 P). Although the *Glyceria* morphotypes in Figure 20 N-O, and *Calamagrostis* morphotypes in Figure 20 A are commonly classified as bilobates, they are clearly very different from the "classic" Panicoideae and Erhartoideae bilobates and should perhaps be given a more appropriate 3-D and/or Pooideae specific descriptor (see Lu and Liu, 2003a, 2003b, for a comprehensive account of bilobate production across the Poaceae). It appears that accounts of *Glyceri*a phytolith production are somewhat underrepresented in the literature, with Bombin's 1984 Ph.D. dissertation as the only North American publication that I found with specific *Glyceria* phytolith analysis and illustrations.

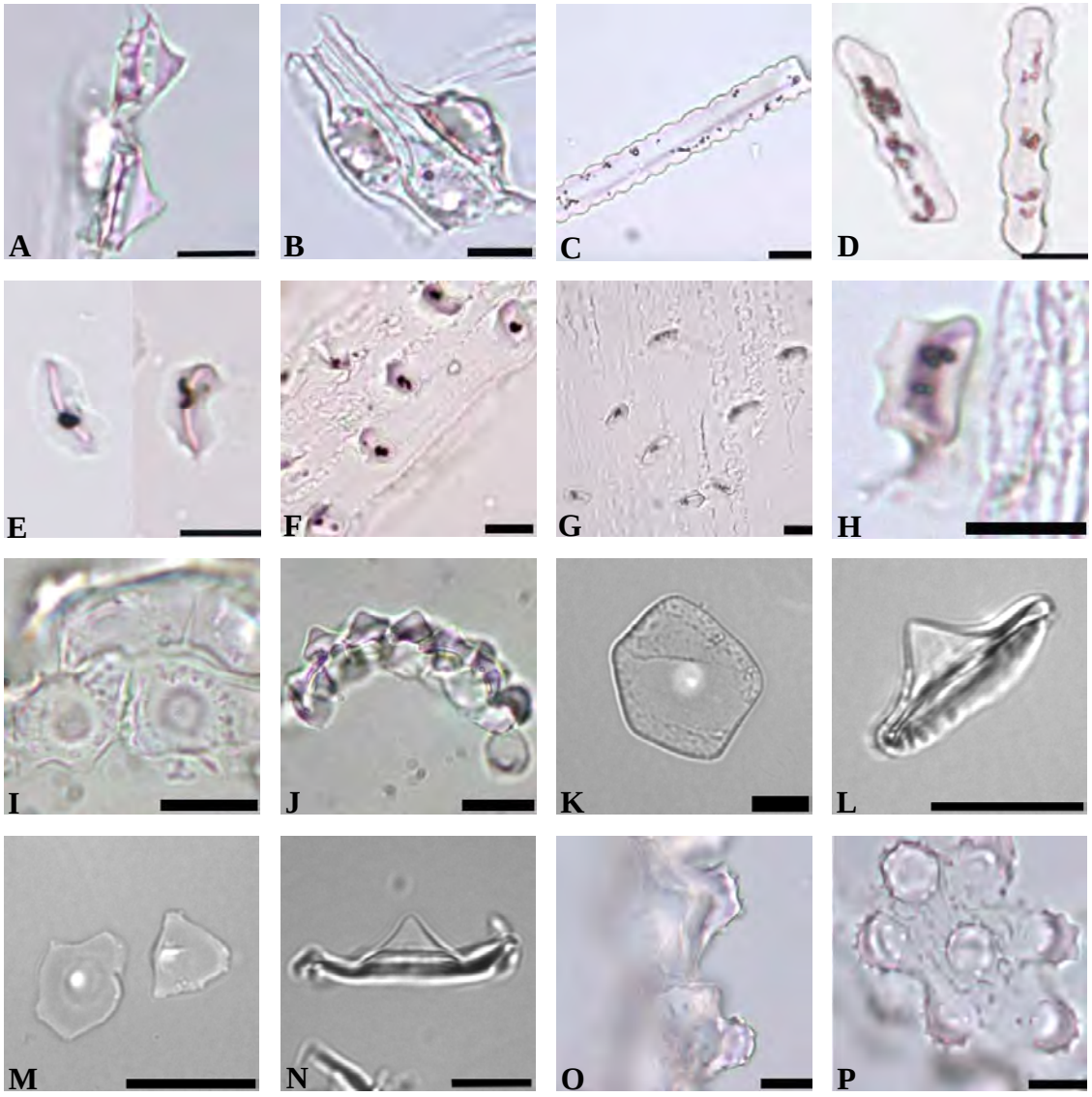


Figure 21

*Poa*, *Dulichium* and *Carex* Phytolith Micrographs

*Poa palustris* (A-H), *Dulichium arundinaceum* (I-J), *Carex sterilis* (K-L), *C. lacustris* (M-N), and *Equisetum pratense* (O-P); Scale bar = 10 µm: A-B) inflorescence papillae in side and top views; C-D) leaf elongate trapeziform sinuates; E) culm keeled reniform rondels; F) culm keeled reniform rondels *in situ*; G) culm keeled reniform rondels *in situ*; H) culm keeled reniform rondel in side view; I-N) polygonal Cyperaceae cone cells in side and top views; O-P) semi-globular echinate cystoliths.

*Poa palustris* (Figure 21 A-H) silica short cell phytoliths are typical for what is commonly observed for the Pooideae, with leaf trapeziform elongate sinuates (Figure 21 C-D), lightly silicified inflorescence papillae (Figure 21 A-B) and culm conical rondels (Figure 21 E-H) predominating. The genus has been widely examined by phytolith analysts, but accounts specific to *Poa palustris* are lacking. Of interest here, are the slightly indented keeled culm rondels (Figure 21 E-H) which are a bit more robust than the inflorescence rondels and will be compared with *Zizania* inflorescence rondels later in diagnostic morphotype determination section at the end of this chapter.

Although they are non-Poaceae genera, *Dulichium arundinaceum* (Cyperaceae), *Carex spp*. (Cyperaceae) and *Equisetum* (Equisetaceae) were collected and analyzed for phytolith production. These taxa are abundant near wild rice stands, and in the case of *Dulichium*, can be found within wild rice stands occurring in shallow water. They do not produce any potential wild rice confuser phytolith morphotypes, but can be encountered during lake sediment phytolith analysis. It is interesting to note that in 2-D, disarticulated semi-globular echinate cystoliths from *Equisetum* (Figure 21 O-P) can appear identical to globular echinate spherules, which are widely reported as diagnostic for the Arecaceae (Palmae). Disarticulated *Equisetum* cystoliths often settle with the hollow opening facing the microscope slide, thus hiding their full 3-D morphology. Members of the Cyperaceae have been investigated by several phytolith researchers (e.g., Mehra and Sharma, 1965; Schuyler, 1971; Ollendorf and others, 1987).

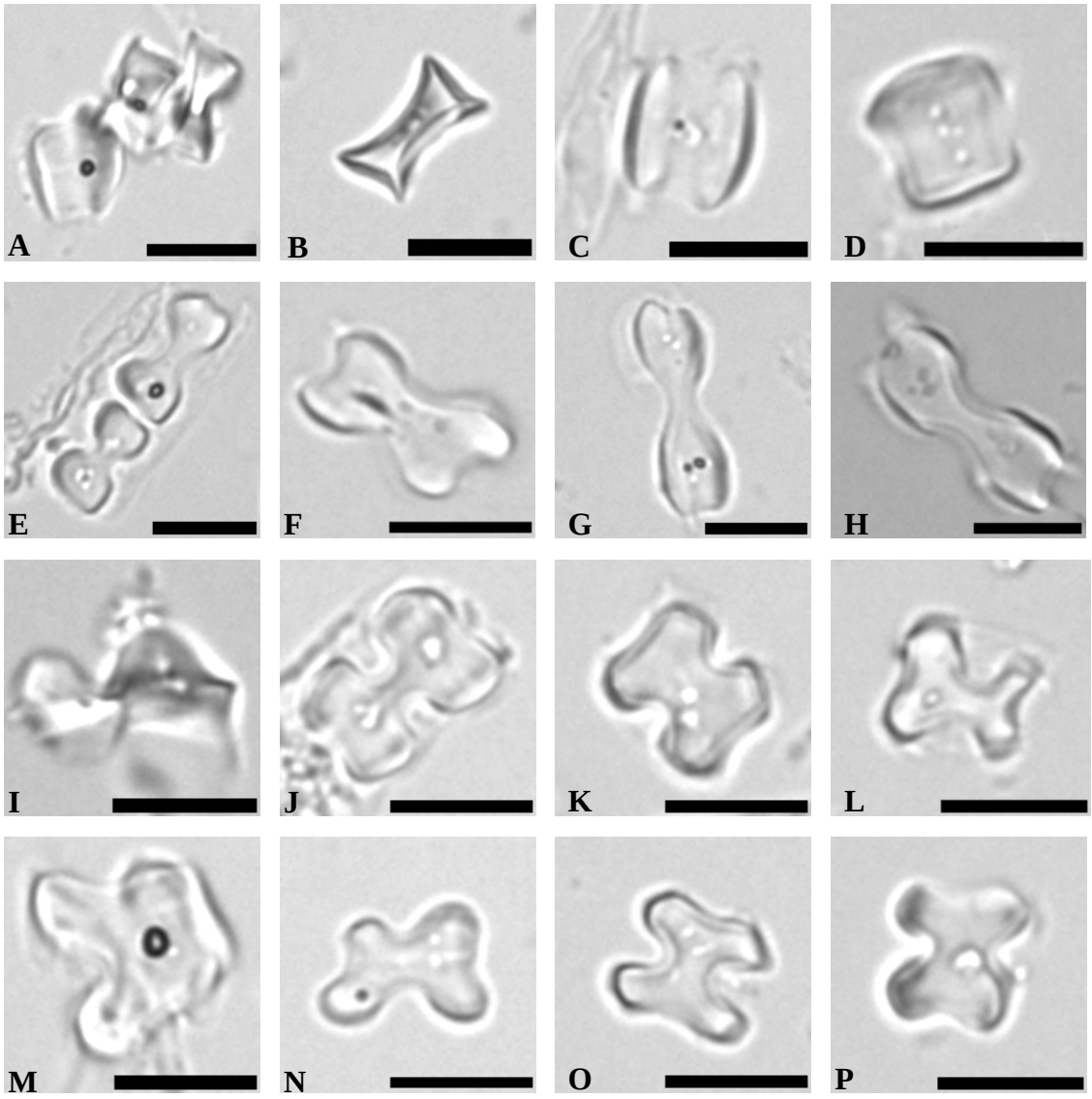


Figure 22

*Muhlenbergia glomerata* Phytolith Micrographs
Scale bar = 10 µm: A-D) tabular saddle morphotypes in top and side views; E) bilobate morphotypes *in situ*; F) bilobate morphotypes *in situ*; G-H) bilobate morphotypes; I) bilobate in oblique view; J-K) bilobate/cross morphotypes; L-P) cross morphotypes.

*Muhlenbergia glomerata* (Figure 22 A-P) silica short cell phytoliths show a wide variety of morphologies that include saddles, bilobates (some Erhartoideae-like)

and Panicoide-like crosses. The genus is primarily found in the Western Hemisphere, with *M. glomerata* primarily found in northern and northeastern North America. Of particular interest is the occurrence of square (equal length and width) tabular saddles found in abundance throughout the plant. Saddle phytoliths are typically associated with dry habitat Chloridoideae species (Twiss and others, 1969; Fredlund and Tieszen, 1994), and their presence in soil samples are often interpreted as such. Caution must be taken when the presence of significant amounts of square dimension tabular saddles recovered from lake sediments are used to make broad ecological interpretations.

*Leersia oryzoides* Phytolith Morphotypes

With its *Zizania* co-tribal association, *Leersia oryzoides* (rice cut grass) phytoliths deserve extra scrutiny. Phytoliths were extracted from the entire dry-ashed fraction of each individual plant-part (leaf, culm, and inflorescence). Each sample was sonicated to disarticulate silica short cell phytoliths from lightly silicified epidermal sheets, thus allowing for uniform and accurate calculation of morphotype assemblage. Light microscope micrographs, line drawings and type-designations are presented here for the predominant short cell phytolith morphotypes (Tables 9-12 & Figures 23-27).

Table 9

*Leersia oryzoides* Plant-Part & Total Silica Phytolith Extraction Weights

| Plant-Part | Dry Wt. (g) | % of Total Plant Dry Wt. (g) | Phytolith Extract (g) | % of Dry Weight[a] | % of Total Plant Phytolith Extract |
|---|---|---|---|---|---|
| Inflorescence* | 0.2913 | 22.4 | 0.0067 | 2.3 | 8.2 |
| Leaf & Sheath | 0.5772 | 44.4 | 0.0552 | 9.6 | 67.5 |
| Culm | 0.4308 | 33.2 | 0.0199 | 4.6 | 24.3 |

* Inflorescence = rachis and spikelets

[a] Total silicification of *Leersia* plant by dry weight = 6.3%

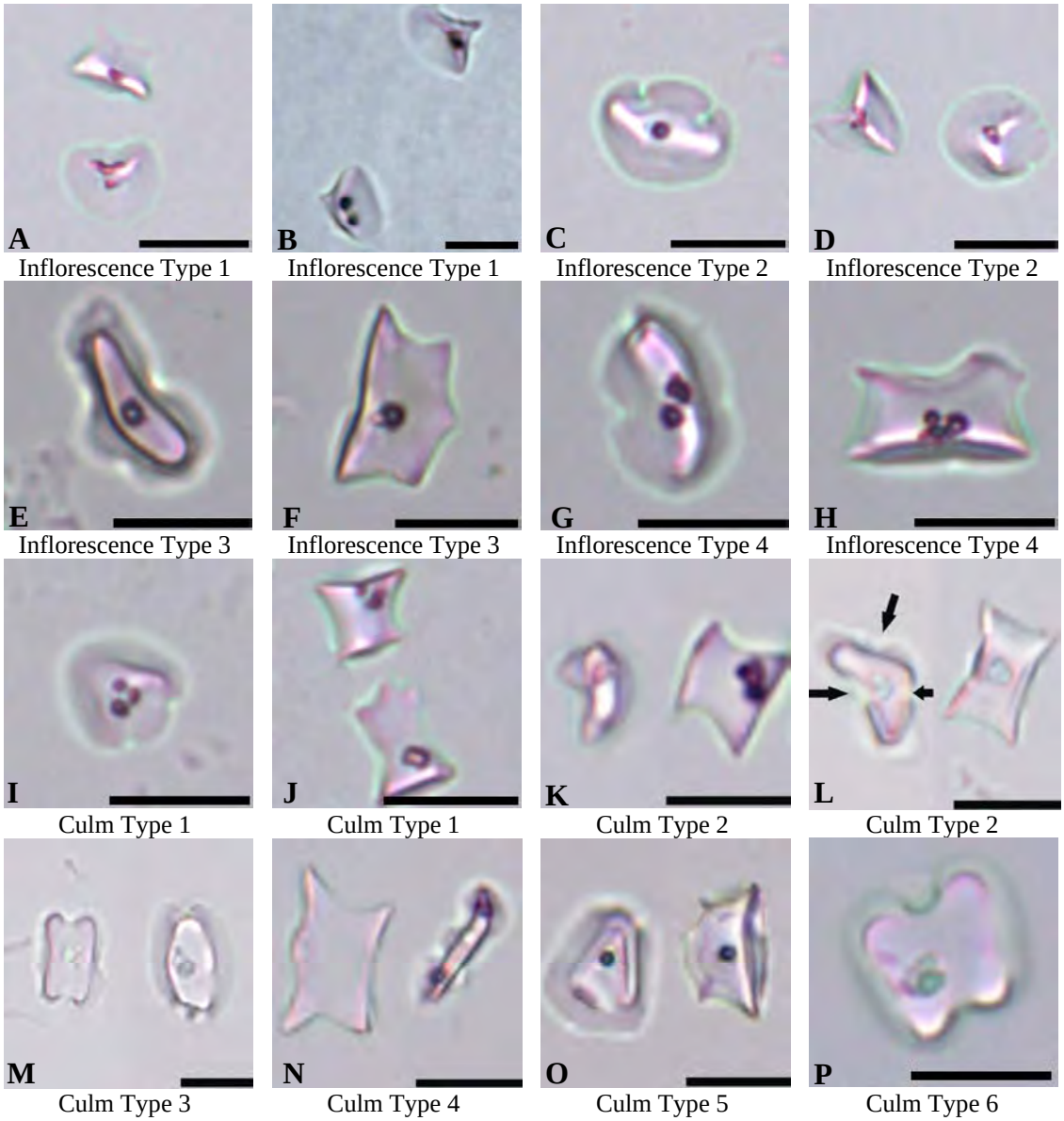


Figure 23

*Leersia oryzoides* Inflorescence and Culm Phytolith Micrographs
Scale bar = 10 µm: A-B) inflorescence reniform rondels in top, side and oblique view; C-D) inflorescence 2-cleft rondels in top and side views; E-F) inflorescence elongate 3-cleft trapeziform in top and side view; G-H) inflorescence elongate 2-cleft rondel in top and side view; I-J) culm 2-cleft rondels in top and side views; K) culm reniform rondel in top and side view; L) culm reniform 3-cleft rondel in top and side view; M) culm long-axis bifid trapeziform morphotypes in top view; N) culm elongate 3-cleft trapeziform in side and top view; O) culm cuneiform rondel in top and side view; P) culm cross in top view.

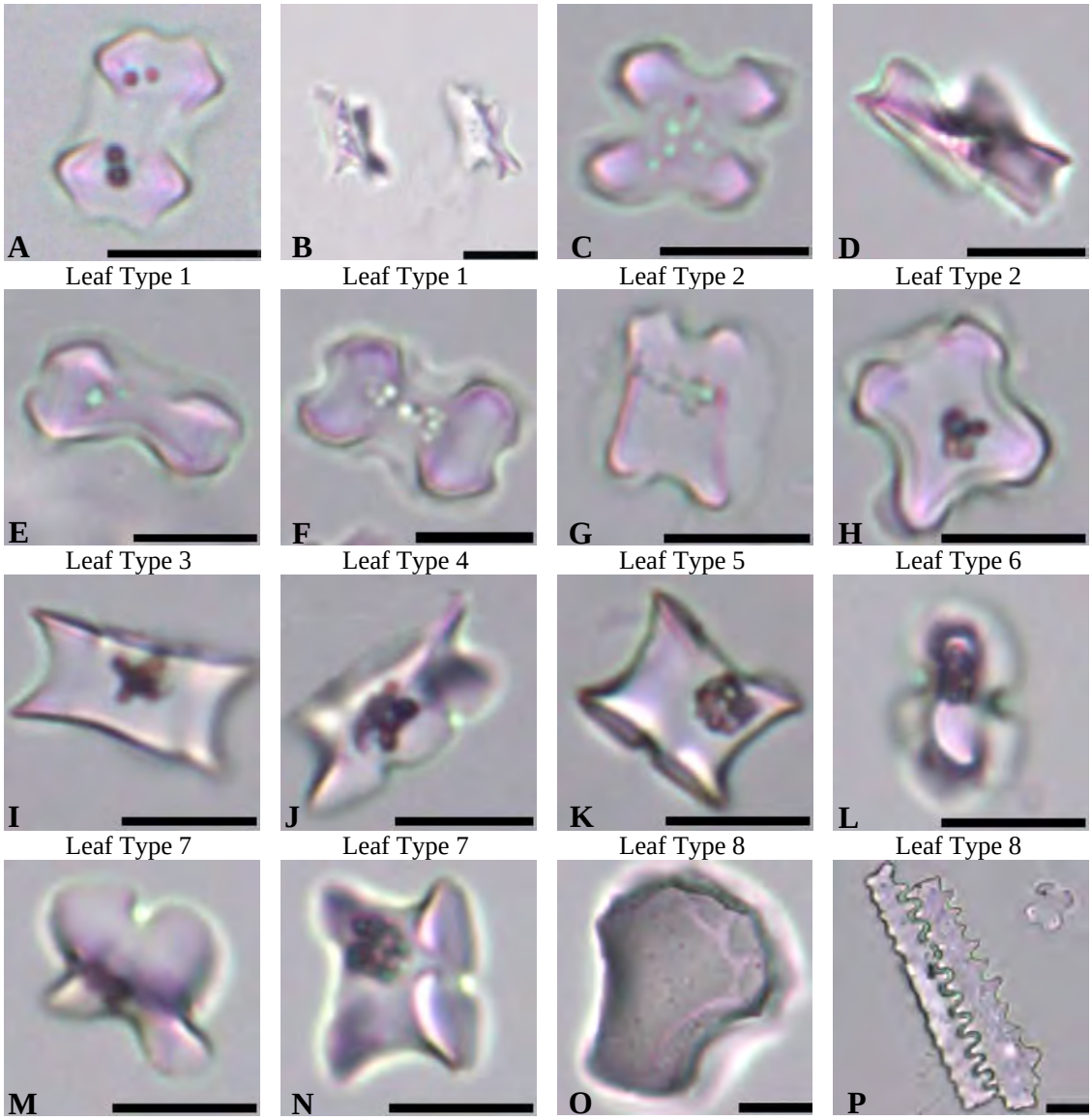


Figure 24

*Leersia oryzoides* Leaf Phytolith Micrographs

Scale bar = 10 µm: A) acute-lobed bilobate in top view; B) acute lobe margin bilobate in oblique view; C) acute-lobed cross in top view; D) acute-lobed cross in oblique view; E) acute-lobe and obtuse-lobe bilobate; F) obtuse-lobed bilobate; G) elongate cross; H) obtuse-lobed cross; I) elongate 3-cleft trapeziform in side view; J) elongate 3-cleft trapeziform in oblique view; K) bifid trapeziform (rondel?) in side view; L) bifid trapeziform in top view; M-N) bifid trapeziform in oblique views; O) cuneiform bulliform; P) tuberculate long cells.

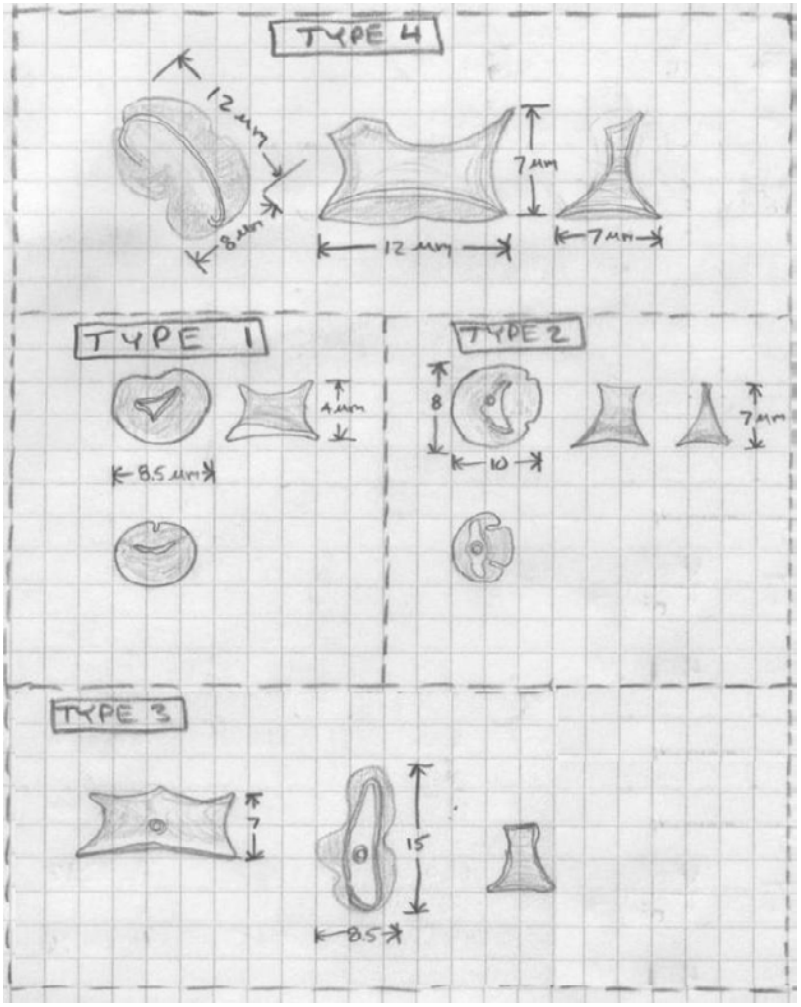


Figure 25

*Leersia oryzoides* Inflorescence Short Cell Phytolith Morphotype Line Drawings

Table 10

*Leersia oryzoides* Inflorescence Short Cell Percent Morphotype Assemblage

| *Leersia* Morphotype[a] | ICPN* Nomenclature | % Morphotype[b] |
|---|---|---|
| Inflorescence Type 1 | 1-cleft rondel | 69.6 |
| Inflorescence Type 2 | 2-cleft rondel | 29.4 |
| Inflorescence Type 3 | Elongate 3-cleft trapeziform | 0.6 |
| Inflorescence Type 4 | Elongate 2-cleft rondel | 0.4 |

[a] Inflorescence = spikelets and rachis; [b] n=500

*ICPN=International Code for Phytolith Nomenclature

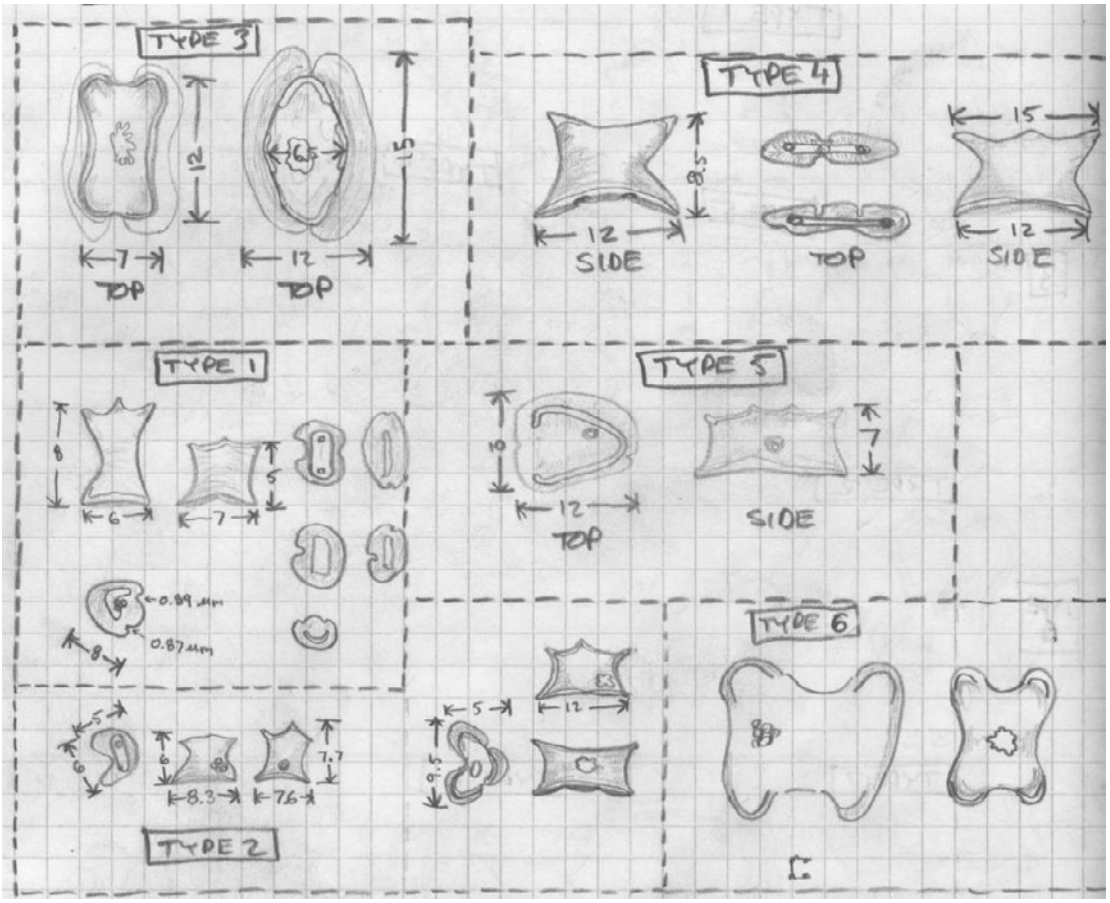


Figure 26

*Leersia oryzoides* Culm Short Cell Phytolith Morphotype Line Drawings

Table 11

*Leersia oryzoides* Culm Short Cell Percent Morphotype Assemblage

| *Leersia* Morphotype | ICPN* Nomenclature | % Morphotype[a] |
|---|---|---|
| Culm Type 1 | 1 & 2 cleft rondel | 86.6 |
| Culm Type 2 | Reniform 1 & 3-cleft rondel | 1.8 |
| Culm Type 3 | Long axis bifid trapeziform | 2.4 |
| Culm Type 4 | Elongate 2 & 3-cleft trapeziform | 5.6 |
| Culm Type 5 | Cuneiform rondel | 2.2 |
| Culm Type 6 | Cross | 1.4 |

[a] n=500; *ICPN=International Code for Phytolith Nomenclature

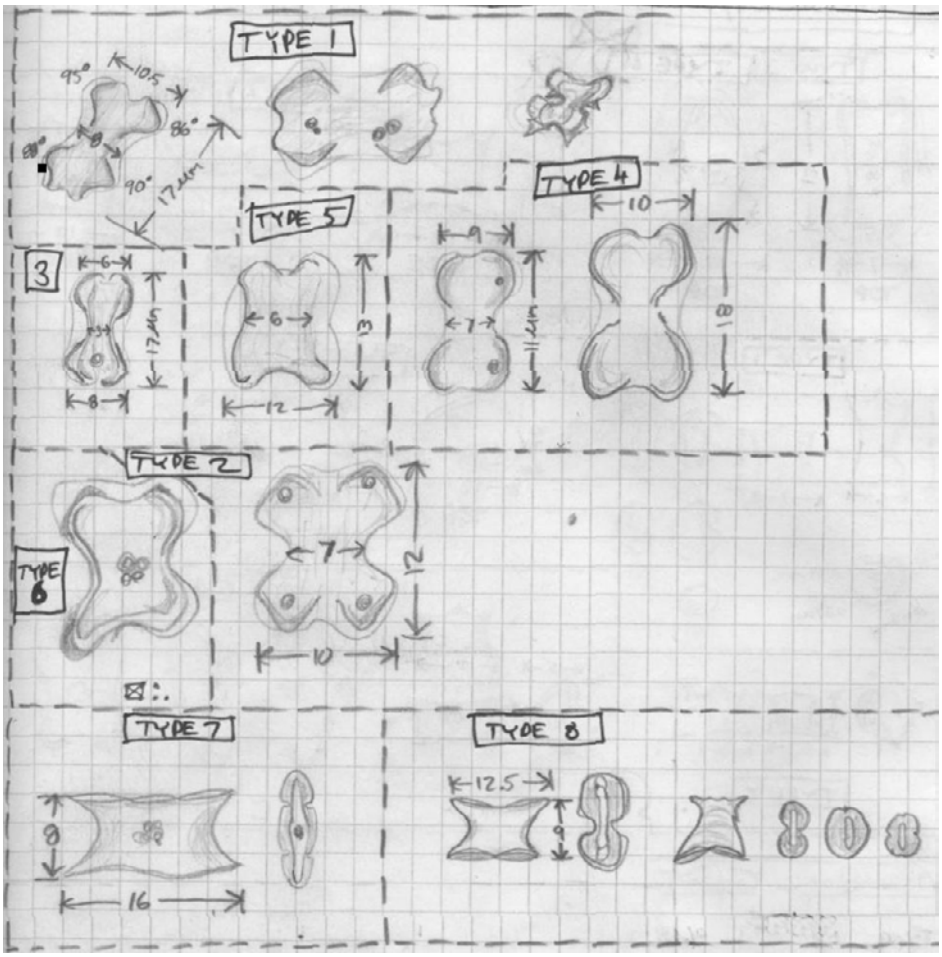


Figure 27

*Leersia oryzoides* Leaf & Sheath Short Cell Phytolith Morphotype Line Drawings

Table 12

*Leersia oryzoides* Leaf & Sheath Short Cell Percent Morphotype Assemblage

| *Leersia* Morphotype | ICPN* Nomenclature | % Morphotype[a] |
|---|---|---|
| Leaf & Sheath Type 1 | Acute-lobed bilobate | 57.3 |
| Leaf & Sheath Type 2 | Acute-lobed cross | 23.4 |
| Leaf & Sheath Type 3 | Acute-lobe and obtuse-lobe bilobate | 5.4 |
| Leaf & Sheath Type 4 | Obtuse-lobed bilobate | 5.4 |
| Leaf & Sheath Type 5 | Elongate cross | 0.6 |
| Leaf & Sheath Type 6 | Obtuse-lobed Cross | 2.5 |
| Leaf & Sheath Type 7 | elongate 3-cleft trapeziform | 0.2 |
| Leaf & Sheath Type 8 | bifid trapeziform (rondel?) | 5.2 |

[a] n=520; *ICPN=International Code for Phytolith Nomenclature

*Leersia oryzoides*, with a 6.3% of dry weight phytolith extraction, is rather heavily silicified. Much of that weight is in the form of lightly silicified epidermal long cells and sheets of silica passively deposited as a result of evapotranspiration (ET). The high percentage silicification in the leaves is likely a direct result of ET. Where leaf and culm silica short cells have greater separation, spikelet lemmas and paleas are densely packed with 1 and 2-cleft (*Leersia* Inflorescence Type 1 and 2) rondels (Figure 23 A-D). Direct comparisons with wild rice phytolith morphotypes are made in the diagnostic morphotype determination section at the end of this chapter.

*Zizania palustris* Phytolith Morphotypes

*Zizania palustris* var. *palustris* (Northern wild rice) phytoliths were extracted from the entire dry-ashed fraction of each individual plant-part (leaf, sheath, culm, pistillate spikelet, and rachis). All of these parts came from the same plant. In addition, one entire wild rice plant (2 culms and 4 tillers) was dry-ashed and a known quantity of exotic diatom spike added to calculate absolute abundance of short cell phytolith morphotypes. Wild rice leaf, sheath and culm material at the immature floating leaf stage was also examined, with entire fractions of each plant-part processed. Each sample was sonicated to disarticulate silica short cell phytoliths from lightly silicified epidermal sheets, thus allowing for uniform and accurate calculation of morphotype assemblage. Light microscope micrographs, line drawings and type-designations are presented here for the predominant short cell phytolith morphotypes (Tables 13-21 & Figures 28-38).

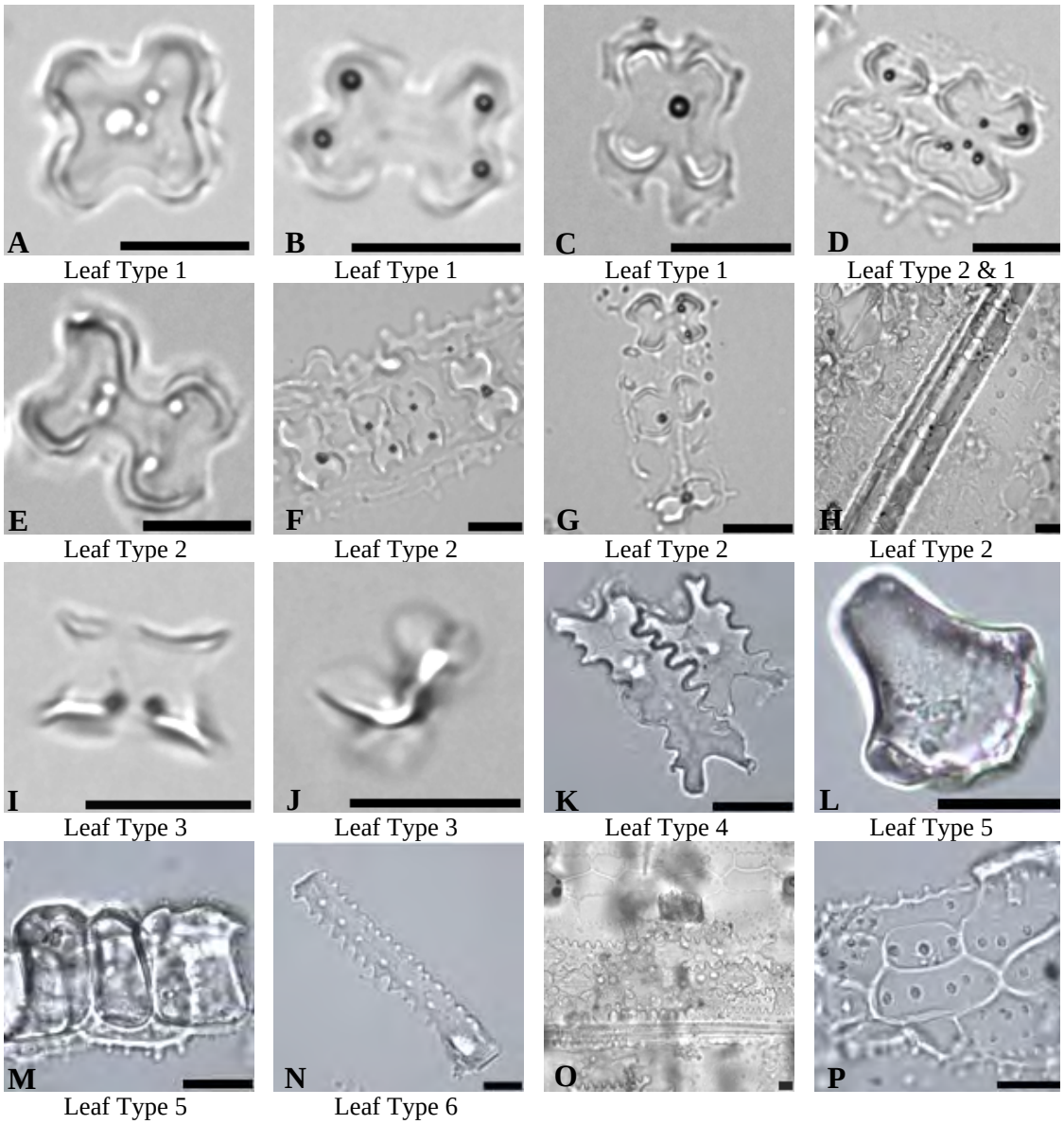


Figure 28

*Zizania palustris* var. *palustris* Leaf Phytolith Micrographs
Scale bar = 10 µm: A-C) disarticulated obtuse-lobed cross morphotypes; D) bilobate (left) and cross (right) *in situ*; E) obtuse-lobed bilobate; F-G) bilobate sequences *in situ*; H) bilobate and cross sequence *in situ*; I) bifid trapeziform in side view; J) bifid trapeziform in base/oblique view; K) interstomatal ground cells; L) cuneiform bulliform cell; M) blocky bulliform cells; N) elongate tuberculate long cell; O) silicified epidermal sheet *in situ*; P) lightly silicified long cells with rounded projections *in situ*.

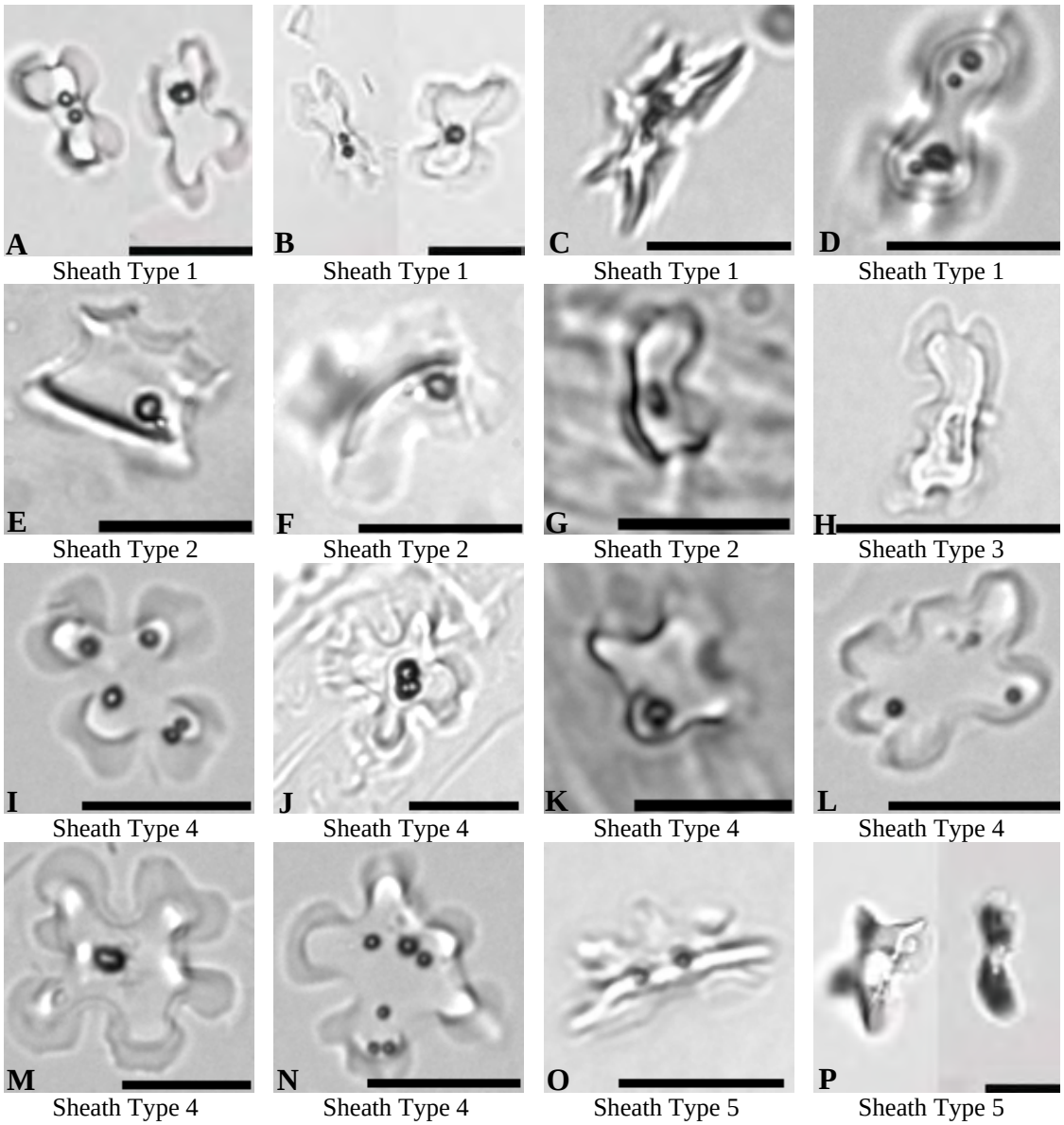


Figure 29

*Zizania palustris* var. *palustris* Sheath Phytolith Micrographs
Scale bar = 10 µm: A-B) concave-end bilobates with enlarged base lobes; C) concave-end bilobate in side view; D) bulbous-end bilobate with enlarged base lobes; E-G) reniform rondel with central sinus in side, oblique and top view; H) polylobate with enlarged, cleft, base lobes; I-K) 4-lobed cross with base lobes slightly to deeply cleft; L-N) 5 and 6-lobed crosses with base lobes slightly to deeply cleft; O) narrow elongate trapeziform in side view; P) narrow elongate trapeziform in oblique and bottom view.

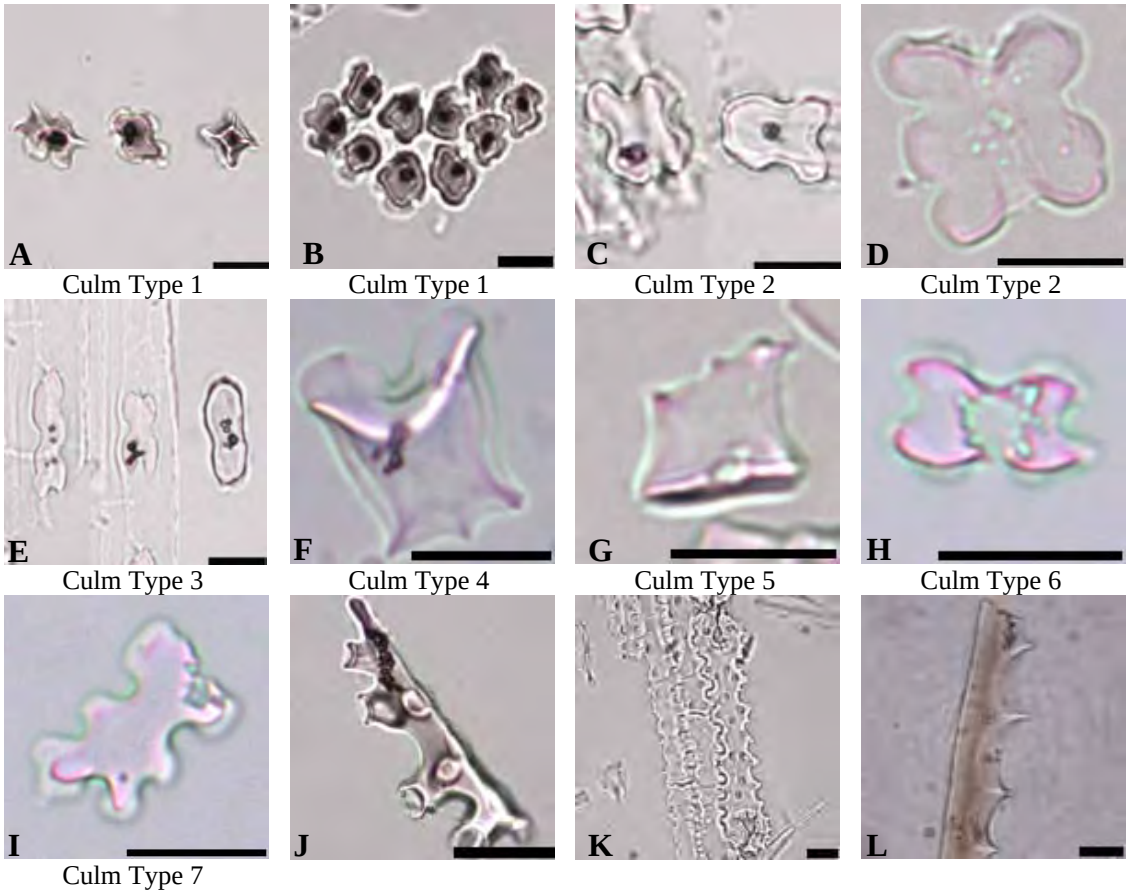


Figure 30

*Zizania palustris* var. *palustris* Culm Phytolith Micrographs
Scale bar = 10 µm: A) trapeziform cross with slightly cleft basal lobes in oblique, top and side view, and B) *in situ*; C-D) elongate 3,4 and 5-lobed crosses with equal top and base dimensions; E) bilobates and elongate polylobate with typically concave and sometimes bulbous ends; F) reniform rondel with central sinus in oblique view; G) narrow trapeziform in side view, base (not in view) with prominent central sinus (see Figure 34, Type 5); H) bilobate with concave ends and scooped top lobes; I) 6-lobed polylobate with some basal lobes slightly cleft; J) silicified xylem element; K) silicified epidermal long cells *in situ*; L) tracheid xylem element with one wavy and one straight margin.

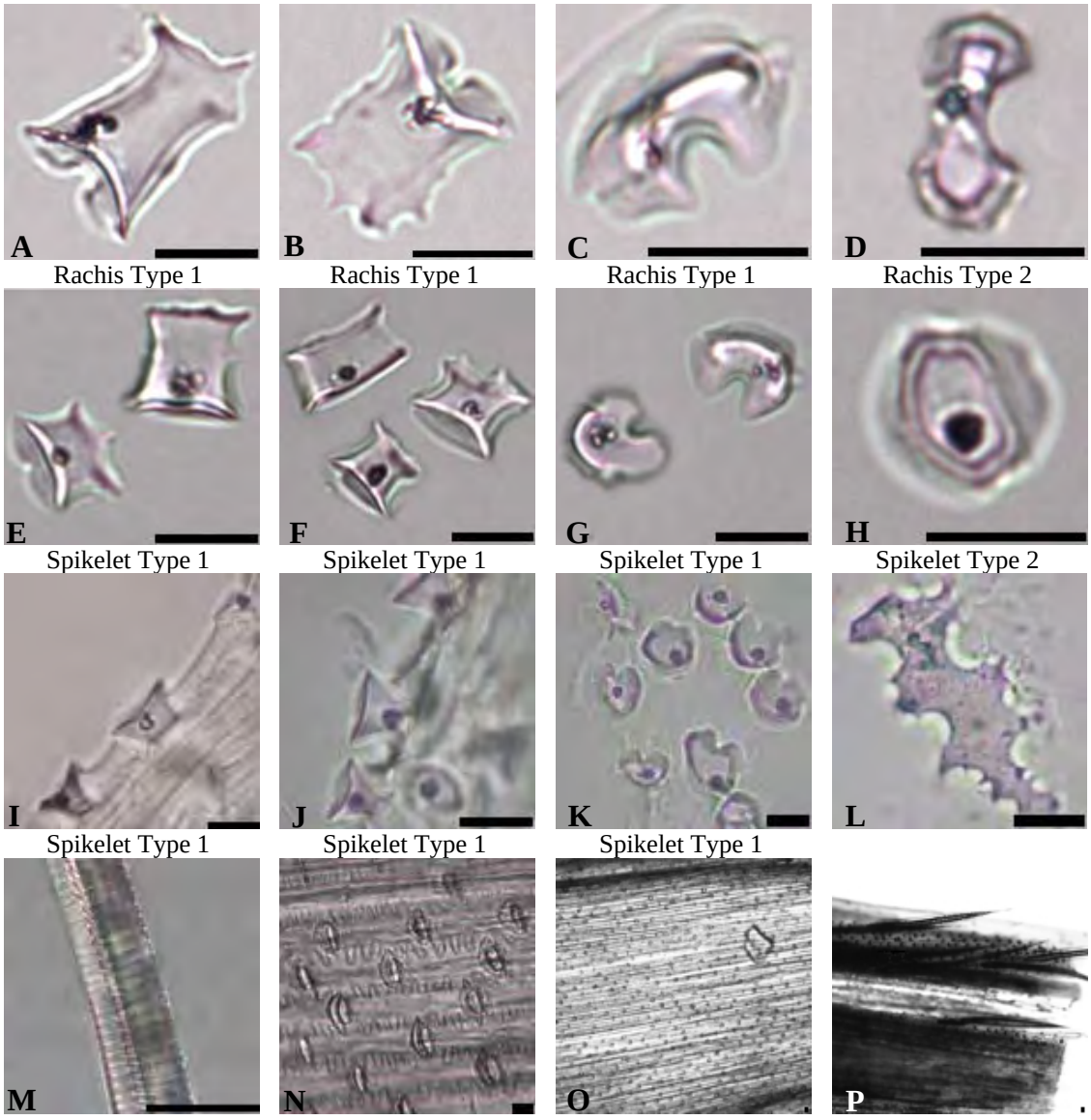


Figure 31

*Zizania palustris* var. *palustris* Pistillate Inflorescence Phytolith Micrographs Scale bar = 10 µm: A-C) rachis reniform rondels with large central sinus in side and top view; D) rachis rondel with two opposing sinuses in top view; E-F) spikelet reniform rondels with central sinus in side view; G) spikelet reniform rondels in top (right) and base (left) view; H) spikelet rondel with 2 or 3 minor clefts in top view; I – J) spikelet reniform rondels *in situ* side view (note that the widest face (base) is anatomically the top); K) spikelet reniform rondels *in situ* on lemma; L) dendriform phytolith from lemma; M) xylem element from awn; N) reniform rondels *in situ* on lemma (400X); O-P) reniform rondels *in situ* on lemma appear as dark dots (100X, note silicified hair cells).

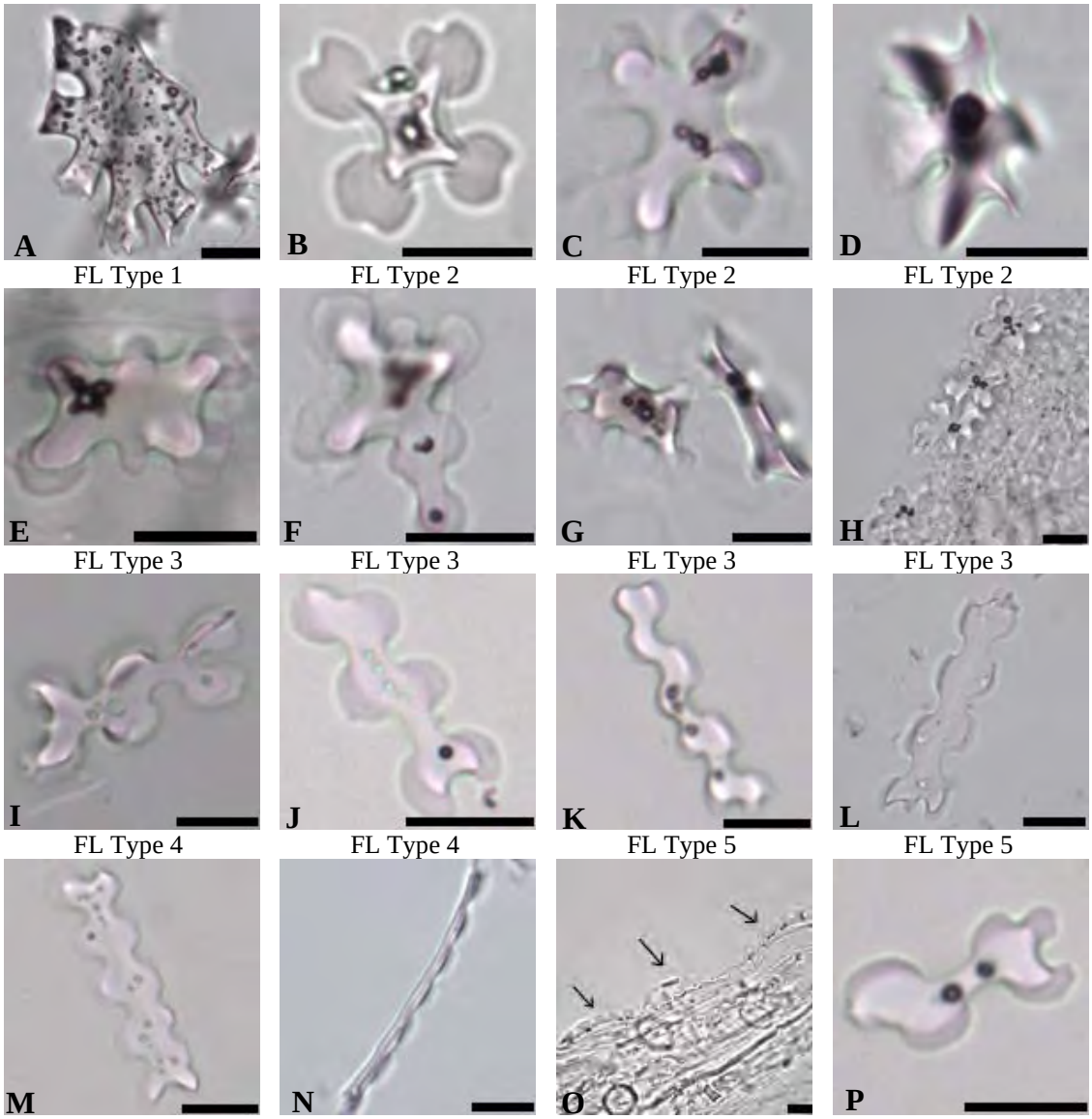


Figure 32

*Zizania palustris* var. *palustris* Floating Leaf Stage Phytolith Micrographs
The entire plant was dry-ashed; scale bar = 10 µm: A) silicified xylem element; B-C) cross morphotypes with ampliate cleft basal lobes; D) cross in oblique view; E-G) extra-lobed cross morphotypes in top and oblique view with ampliate basal lobes; H) extra-lobed cross morphotypes *in situ* where leaf separated along vein; I-J) 3-lobed (6 basal lobed) polylobate with ampliate basal lobes; K-M) elongate (>3 lobes) polylobates; N) elongate polylobate in side view; O) elongate polylobate *in situ*; P) bilobate with ampliate basal lobes and concave ends.

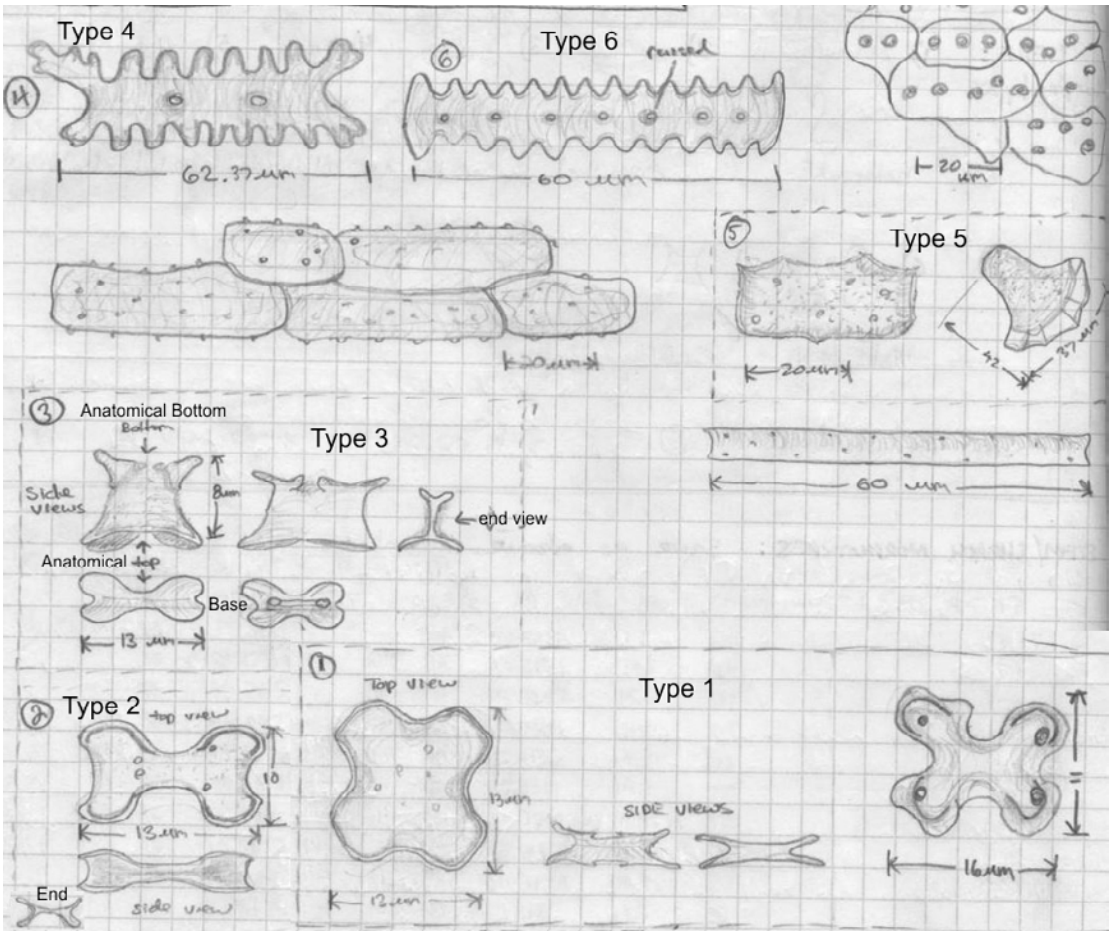


Figure 33

*Zizania palustris* var. *palustris* Leaf Short Cell Phytolith Morphotype Line Drawings

Table 13

*Zizania palustris* var. *palustris* Leaf Short Cell Percent Morphotype Assemblage

| *Zizania* Morphotype | ICPN* Nomenclature | % Morphotype[a] |
|---|---|---|
| Leaf Type 1 | Cross | 15.1 |
| Leaf Type 2 | Bilobate | 22.3 |
| Leaf Type 3 | Trapeziform | 19.6 |
| Leaf Type 4 | Interstomatal Ground Cell | 12.1 |
| Leaf Type 5 | Blocky and cuneiform bulliform | 22.7 |
| Leaf Type 6 | Elongate tuberculate long cell | 8.2 |

[a] n=515; *ICPN=International Code for Phytolith Nomenclature

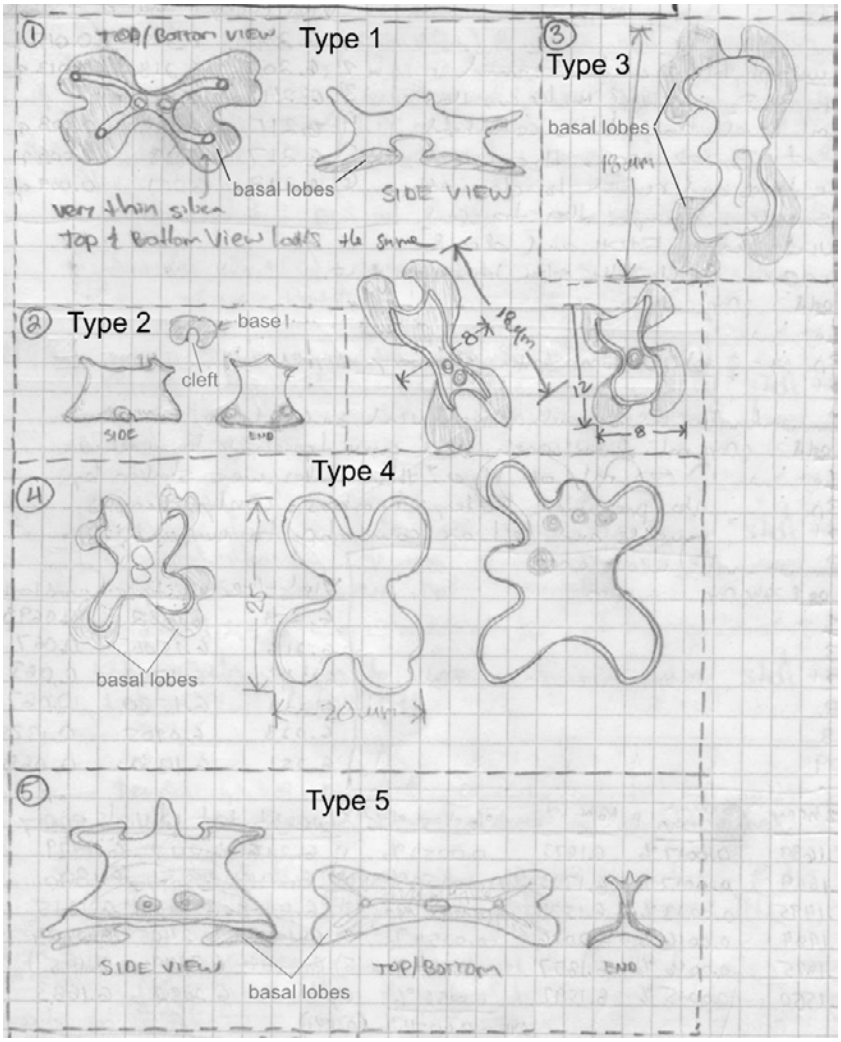


Figure 34

*Zizania palustris* var *palustris* Sheath Short Cell Phytolith Morphotype Line Drawings

Table 14

*Zizania palustris* var. *palustris* Sheath Short Cell Percent Morphotype Assemblage

| *Zizania* Morphotype | ICPN* Nomenclature | % Morphotype[a] |
|---|---|---|
| Sheath Type 1 | Bilobate with ampliate basal lobes | 28.5 |
| Sheath Type 2 | Reniform rondel with basal sinus | 5.3 |
| Sheath Type 3 | Polylobate with ampliate basal lobes | 3.4 |
| Sheath Type 4 | Cross with 4-6 ampliate basal lobes | 7.2 |
| Sheath Type 5 | Trapeziform with bilobate base | 55.6 |

[a] n=207; *ICPN=International Code for Phytolith Nomenclature

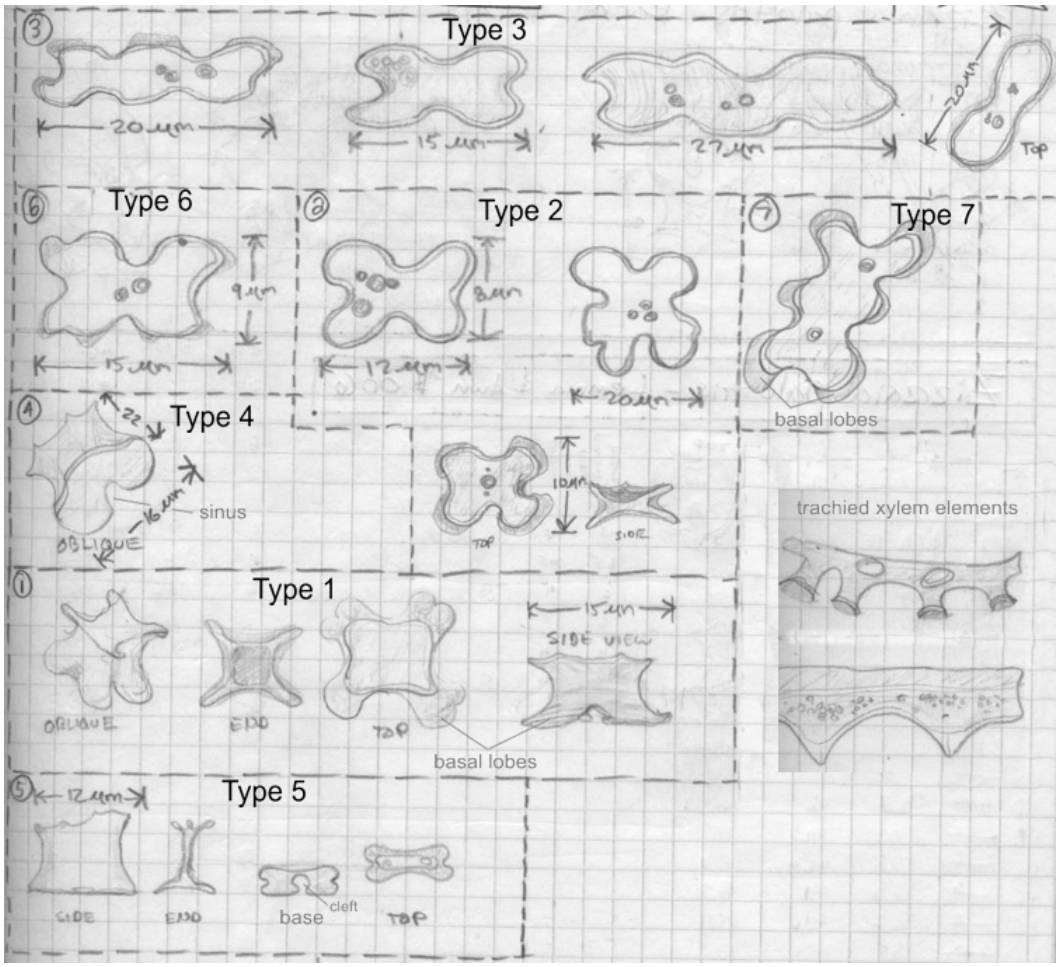


Figure 35

*Zizania palustris* var. *palustris* Culm Short Cell Phytolith Morphotype Line Drawings

Table 15

*Zizania palustris* var. *palustris* Culm Short Cell Percent Morphotype Assemblage

| *Zizania* Morphotype | ICPN* Nomenclature | % Morphotype[a] |
|---|---|---|
| Culm Type 1 | Cross with ampliate basal lobes | 36.3 |
| Culm Type 2 | Cross without ampliate basal lobes | 12.6 |
| Culm Type 3 | Polylobates & bilobates | 11.6 |
| Culm Type 4 | Reniform rondel with basal sinus | 6.9 |
| Culm Type 5 | Trapeziform with 1-cleft base | 26.1 |
| Culm Type 6 | Bilobate with cleft lobes | 5.1 |
| Culm Type 7 | Polylobate with 6 ampliate basal lobes | 1.4 |

[a] n=215; *ICPN=International Code for Phytolith Nomenclature

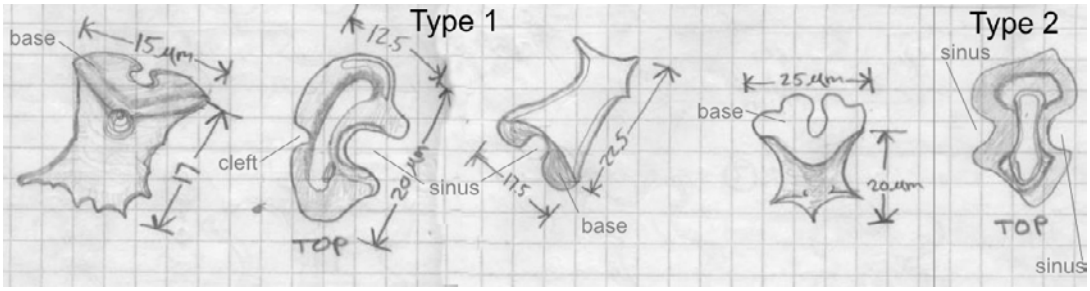


Figure 36

*Zizania palustris* var *palustris* Rachis Short Cell Phytolith Morphotype Line Drawings

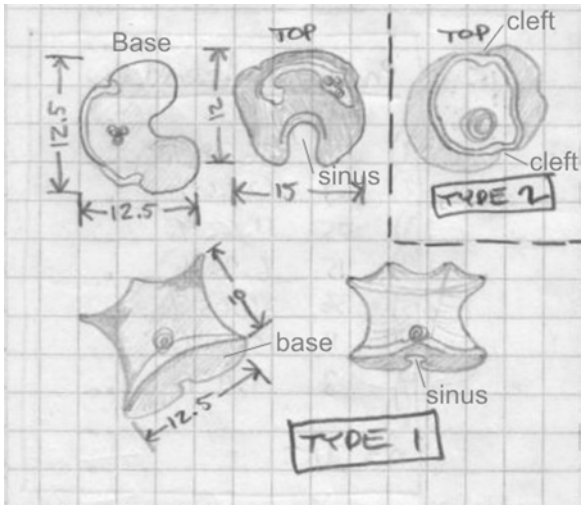


Figure 37

*Zizania palustris* var *palustris* Spikelet Short Cell Phytolith Line Drawings

Table 16

*Zizania palustris* var *palustris* Inflor. Short Cell Percent Morphotype Assemblage

| *Zizania* Inflorescence Morphotype | ICPN* Nomenclature | % Morphotype |
|---|---|---|
| Rachis Type 1 = Inflorescence Type 1[a] | Reniform rondel with basal sinus | 95.0 |
| Rachis Type 2 = Inflorescence Type 3 | Rondel w/opposing basal sinuses | 5.0 (n=500) |
| | | |
| Spikelet Type 1 = Inflorescence Type 1[a] | Reniform rondel with basal sinus | 60.0 |
| Spikelet Type 2 = Inflorescence Type 2 | Rondel with 2-3 basal clefts | 30.0 (n=500) |

*ICPN=International Code for Phytolith Nomenclature

[a] Rachis Type 1 and Spikelet Type 1 are equivalent and reclassified here as Inflorescence Type 1

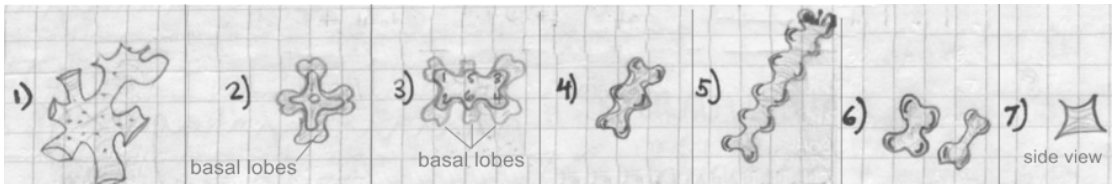


Figure 38

*Zizania palustris* var. *palustris* Floating Leaf Stage (FL) Short Cell Phytolith Morphotype Line Drawings

Table 17

*Zizania palustris* var. *palustris* Floating Leaf Stage (FL) Leaf Short Cell Percent Morphotype Assemblage

| *Zizania* FL Morphotype | ICPN* Nomenclature | % Morphotype[a] |
|---|---|---|
| FL Type 1 | Xylem element | 2.7 |
| FL Type 2 | Cross with ampliate basal lobes | 10.3 |
| FL Type 3 | Polylobate with >4 ampliate basal lobes | 13.4 |
| FL Type 4 | Polylobate without basal lobes | 14.6 |
| FL Type 5 | Elongate polylobate without basal lobes | 51.0 |
| FL Type 6 | Bilobate | 6.4 |
| FL Type 7 | Trapeziform | 1.6 |

[a] n=561; *ICPN=International Code for Phytolith Nomenclature

Table 18

*Zizania palustris* var. *palustris* Floating Leaf Stage (FL) Culm & Sheath Short Cell Percent Morphotype Assemblage

| *Zizania* FL Morphotype | ICPN* Nomenclature | % Morphotype[a] |
|---|---|---|
| FL Type 1 | Xylem element | 1.6 |
| FL Type 2 | Cross with ampliate basal lobes | 11.2 |
| FL Type 3 | Polylobate with >4 ampliate basal lobes | 19.4 |
| FL Type 4 | Polylobate without basal lobes | 6.0 |
| FL Type 5 | Elongate polylobate without basal lobes | 59.3 |
| FL Type 6 | Bilobate | 2.4 |
| FL Type 7 | Trapeziform | 0.0 |

[a] n=617; *ICPN=International Code for Phytolith Nomenclature

Table 19

Short Cell Morphotype Assemblage for Entire *Z. palustris* var. *palustris* Plant

| *Zizania* Morphotype | ICPN* Nomenclature | % Morphotype[a] |
|---|---|---|
| Leaf Type 1 | Cross | 6.0 |
| Leaf Type 2 | Bilobate | 2.2 |
| Leaf Type 3 | Trapeziform | 0.4 |
| Leaf Type 4 | Interstomatal Ground Cell | 0.0 |
| Leaf Type 5 | Blocky and cuneiform bulliform | 0.0 |
| Leaf Type 6 | Elongate tuberculate long cell | 0.2 |
| | | *Leaf Type Total: 8.8* |
| Sheath Type 1 | Bilobate with ampliate basal lobes | 9.8 |
| Sheath Type 2[b] | Reniform rondel with basal sinus | 1.8 |
| Sheath Type 3 | Polylobate with ampliate basal lobes | 0.6 |
| Sheath Type 4 | Cross with 4-6 ampliate basal lobes | 7.2 |
| Sheath Type 5 | Trapeziform with bilobate base | 8.2 |
| | | *Sheath Type Total: 27.6* |
| Culm Type 1 | Cross with ampliate basal lobes | 6.0 |
| Culm Type 2 | Cross without ampliate basal lobes | 3.6 |
| Culm Type 3 | Polylobates & bilobates | 3.2 |
| Culm Type 4[b] | Reniform rondel with basal sinus | 0.8 |
| Culm Type 5 | Trapeziform with 1-cleft base | 6.2 |
| Culm Type 6 | Bilobate with cleft lobes | 1.8 |
| Culm Type 7 | Polylobate with 6 ampliate basal lobes | 3.4 |
| | | *Culm Type Total: 25.0* |
| Inflorescence Type 1[c] | Reniform rondel with basal sinus | 29.0 |
| Inflorescence Type 2 | Rondel with 2-3 basal clefts | 8.8 |
| Inflorescence Type 3 | Rondel with opposing basal sinuses | 0.0 |
| | | *Inflorescence Type Total: 37.8* |
| Other (FL Type 5)[d] | Elongate polylobate without basal lobes | 0.8 |

[a] n=500; ICPN=International Code for Phytolith Nomenclature
[b] These morphotypes are equivalent
[c] Combines the analogous reniform rondel morphotypes from rachis and spikelet
[d] Likely from floating leaf material still attached to lower culm

Table 20

*Zizania palustris* var. *palustris* Plant-Part Silica Phytolith Extraction Weights[a]

| Plant-Part | Dry Weight (g) | Phytolith Extract (g) | % of Dry Weight |
|---|---|---|---|
| Inflorescence[b] | 0.1910 | 0.0070 | 3.7 |
| Leaf | 0.1170 | 0.0162 | 13.8 |
| Sheath | 0.2360 | 0.0221 | 9.4 |
| Culm | 0.4190 | 0.0188 | 4.5 |

[a] Entire plant was not dry-ashed. Sub-samples for analysis taken from plant-parts.
[b] Inflorescence = rachis and spikelets

Table 21

*Zizania palustris* var. *palustris* Entire Plant Silica Phytolith Extraction Weights

| Sample # | Entire Plant Components | Dry Weight(g) | Phytolith Extract (g) | % of Dry Weight |
|---|---|---|---|---|
| 173 | 2 main culms & 4 tillers [a] | 13.2000 | 0.7370 | 5.6 |
| 174 | 1 culm (no tillers present) [b] | 6.5430 | 0.2091 | 3.2 |
| 143 | floating leaf stage culm [c] | 0.5924 | 0.0219 | 3.7 |
| 145 | floating leaf stage culm [c] | 0.5174 | 0.0149 | 2.9 |
| 147 | floating leaf stage culm [c] | 0.5166 | 0.0159 | 3.1 |

[a] Plant from Lake Ogechie, Mille Lacs Co., MN with 368 pistillate spikelets, no staminate remaining
[b] Plant from Little Indian Sioux River, St. Louis Co., MN. Spikelets not counted (estimate around 175)
[c] Plants from Lake Ogechie, Mille Lacs Co., MN. Collected during the floating leaf stage (07-12-2006)

*Zizania* plant-part type designation was determined primarily by pre-counting scans used to estimate abundance and distinctiveness of form. Degree of silicification and resistance to dissolution was also considered. The *Zizania* plant-part types in Table 19 are the wild rice morphotypes most likely to be encountered in modern and paleo lake sediment studies. Not all of the *Zizania* plant-part types illustrated here were used in modern and paleo lake sediment analysis. Final determination of locally diagnostic types is discussed in the final section of this chapter.

An estimate of the absolute abundance of *Zizania palustris* var. *palustris* silica short cell morphotypes identified in Table 19 were calculated by the addition of an exotic spike to a 0.0036 sub-sample taken from sample #173. Using aliquot methodology, it was calculated that the 13.2 gram dry weight sample contained 59,812,668 of the designated wild rice type morphotypes listed in Table 19 (spike added: 930,462; spike counted 1000; phytoliths counted, 314). Averaging this total

out for the 2 culms and 4 tillers, approximately 9,968,778 short cell phytoliths are found in each culm or tiller.

Like its Oryzeae cohort *Leersia* with around 6.3% silicification, mature *Zizania* examined here ranges from 3.2 to 5.6% silicification overall and is considered highly silicified. *Zizania* leaves are highly silicified at 13.8%, but when compared to culms, sheath and even inflorescence material, do not contribute as many short cell morphotypes overall (Table 19). Although contributing just a fraction of the dry weight and phytolith extract weight overall, the inflorescence contributes the highest number of silica short cell morphotypes. This is likely due to the high concentration of reniform rondels densely arrayed over the entire spikelet surface (Figure 31 N-P). These Inflorescence Type 1 rondels, with the distinctive deep sinus, are found almost exclusively on the inflorescence spikelet (Figure 31 A-C, E-G), with only 5.2% occurrence in sheath material (Sheath Type 2) and 6.9% occurrence in culm material (Culm Type 4). When total plant contributions are considered, occurrence outside of the inflorescence drops to 1.8% for sheath material and 0.8% for culm material (Table 19). Overall, inflorescence rondels contribute an impressive 37% of the total silica short cell morphotype contribution.

One other potentially important localized within-plant morphotype variation is the occurrence of 5 and 6-lobed crosses. These “extra” lobed crosses are only found in sheath and culm material, not in leaf material and have the potential to be diagnostic regionally or even at the continent level. Although crosses are technically quadra-lobes with mirror or double mirror-symmetry, I classify these extra-lobed

morphotypes as crosses (e.g. Figure 25 L-M). It is clear that cross-forming silica cells are responsible for producing these extra lobe variations. Occasionally, a sheath or culm quadra-lobed cross will have one or more lobes with a deep sinus or cleft, that could be described as an additional lobe. Davidson (2003), in her examination of *Zizania aquatica* leaf material, noted the presence of "a small indent" on cross lobes. These are likely analogous to the 1-cleft ampliate basal lobes I observed on leaf, sheath and culm crosses (Figures 33-35). She did not mention the occurrence of an additional lobe extending off of the central cross body. Although no mention of an extra-lobed cross was found in the literature review of grass phytolith classification manuscripts, phytolith researchers need to be consulted to fully resolve the distinctiveness of the form.

It should be noted that I am using the term ampliate to describe the very common occurrence in wild rice for bilobates, polylobates and crosses to have enlarged basal lobes (e.g. Sheath Type 1, 3, 4; Culm Type 1). These basal lobes are anatomically the top of the phytolith, but are typically the widest face and often settle base-down in slide mounts.

~~*Zizania* Floating Leaf Stage Phytoliths~~

Since wild rice leaves from the floating leaf stage senesce their leaves when aerial leaves develop, floating leaves were examined for phytolith production. In addition, sheath, culm and root material were examined for phytolith production as well. Several distinct floating leaf stage (FL) forms (FL 2, 3, 4 & 5) not found in mature *Zizania* material were observed, with the FL Type 1 xylem element the only

non-silica short cell counted in the assemblage calculation (Figure 38). Interestingly, the FL sheath/culm assemblage is statistically identical to the FL leaf morphotype assemblage; however, few of these forms are recovered from the mature plant. In fact, in excluding xylem elements from the count, only FL Type 5 was observed in the entire mature plant assemblage at 0.8% (Figures 32 & 38). With floating leaf senescence, FL morphotype recovery from modern and paleo lake sediments is likely and is discussed in chapters 4 and 5.

## DIAGNOSTIC *ZIZANIA* MORPHOTYPE DETERMINATION

After close examination of nine wetland grass taxa (Table 8) and 28 other dominant trees, shrubs and forbs from the study area (Appendix A), only 5 out of 28 designated wild rice phytolith morphotypes were determined to be unreliable local indicators of wild rice. A few potential confuser phytoliths were also identified, but with thorough observation through 3-D rotation, they pose no barrier to correct *Zizania* or non-*Zizania* designation.

### Unreliable *Zizania* Phytolith Morphotypes

Of the five unreliable *Zizania* phytolith morphotypes identified, two are epidermal long cells (Leaf Type 4, Leaf Type 6), one is a cuneiform bulliform (Leaf Type 5), and two are silica short cells (Inflorescence Types 2 & 3). *Zizania* Leaf Type 4 is an interstomatal ground cell, *Zizania* Leaf Type 6 is an elongate tuberculate long cell and *Zizania* Leaf Type 5 is a bulliform cell from vascular tissue (Figure 28).

With *Zizania* Leaf Type 4 common in leaf epidermis throughout the Poaceae and *Zizania* Leaf Types 5 & 6 found in other Oryzeae (Pearsall and others, 1995), 3-D visual inspection alone cannot unequivocally assign a *Zizania* origin; however, the use of morphometric and discriminate function analysis may be able to find long and bulliform cell characteristics unique to *Zizania*. This type of analysis was successfully used by Pearsall and others (1995) and Zhao and others (1998) to distinguish wild *Oryza* double-peaked epidermal glume cells from domesticated *Oryza* glume cells; however, they were unsuccessful in unequivocally distinguishing *Leersia* bulliforms from *Oryza* bulliforms. According to Pearsall and others (1995) the *Zizania* Leaf Types 5, 6 (Figure 28 L & N) and the lightly silicified long cells with rounded projections (Figure 28 P) that I observed are apparently diagnostic to the Oryzeae. In a separate *Oryza* study, Wang and others (1998) demonstrated the usefulness of computer aided image analysis to statistically describe cross and bilobate metric variation within and between different *Oryza* species.

While the aforementioned studies show the potential for successful discrimination of some long cell forms, the preponderance of other highly diagnostic useful forms rendered this type of analysis unnecessary for *Zizania* Leaf Types 4, 5, and 6 wild rice morphotypes.

*Zizania* Inflorescence Type 2 (Figure 31), while not observed in any of the lake margin grass species (Table 8), could potentially be confused with *Phragmites* rondels (Figure 19 E) and *Leersia* Inflorescence Types 1, 2, and 4 in top views (Figure 23). It was also felt that other Poaceae not examined by myself, but observed in the literature,

may produce a similar type of rondel. *Zizania* Inflorescence Type 2 is not reniform in outline and lacks the large sinus as in Type 1 (Figures 31 & 37). It does have 2 opposing, and sometimes 3, small clefts visible along the basal margin in top view and comprises about 30% of the total rondel assemblage from *Zizania* spikelets (Table 16). In the entire *Zizania* plant morphotype assemblage study, Inflorescence Type 2 comprised 8.8% of the total morphotype assemblage (Table 19). In an effort to remain conservative and unambiguous as possible, *Zizania* Inflorescence Type 2 was not tallied as wild rice; however, further examination of *Zizania* and other Poaceae may ultimately return this type to the locally diagnostic wild rice phytolith category.

*Zizania* Inflorescence Type 3, a rondel with two opposing sinuses, is produced in low numbers (5.0%) in rachis epidermal tissue (Figure 31 D and Figure 36). In general typological terms, it was felt that this form shares a close affinity with some *Leersia* Leaf and Sheath Type 8 morphotypes (Figure 27). The preponderance of other highly diagnostic useful forms rendered inclusion of this low occurrence confuser unnecessary.

~~Potential *Zizania* phytolith confusers~~

Although the majority of *Phragmites* rondels are easily distinguished from *Zizania* rondels, an undetermined proportion has a single sinus in the base that can appear similar to that observed on *Zizania* Inflorescence Type 1 rondels, especially in some oblique base views (Figure 19 E). However, careful comparison of top face features and rotation will reveal clear distinctions between *Phragmites* and *Zizania* rondels.

*Poa palustris* culms produce a reniform rondel that has a slight resemblance to *Zizania* Inflorescence Type 1 rondels; however, the *Poa palustris* rondel indentation is too shallow and wide to be classified as a sinus (Figure 21 E-H). Also, these reniform *Poa palustris* rondels are shorter in height than *Zizania* rondels. Miguel Bombin (1984, figure 12) has a good SEM image for *Poa alpigena* in base view (currently classified as *Poa pratensis* subsp. *alpigena*) exhibiting a sinus indistinguishable from that observed for *Zizania* in base view. He provides no further information on this species, but full rotation would likely reveal non-*Zizania* characteristics in top and side view. Other *Poa* species, especially wetland species, merit further investigation for reniform single-sinus rondel production and abundance.

*Leerisa oryzoidies*, with its co-tribe Oryzeae affiliation, produces many similar phytolith morphotypes; however, clear distinctions can be made between potential wild rice confusers using 2-D and 3-D based visual observation.

*Leersia* vs. *Zizania* Inflorescence Phytoliths

Although both species produce an abundance of rondels, *Leersia* and *Zizania* inflorescence phytoliths are distinct. *Leersia* inflorescence rondels are typically reniform (Figure 39 A) or circular in outline (Figure 39 B-D), exhibit 0 to 3 small clefts and are generally smaller than *Zizania* rondels in all dimensions. *Zizania* inflorescence rondels are either reniform with a single deep sinus (Figure 39 G) or are circular in outline with 2 or 3 small clefts (Figure 39 H).

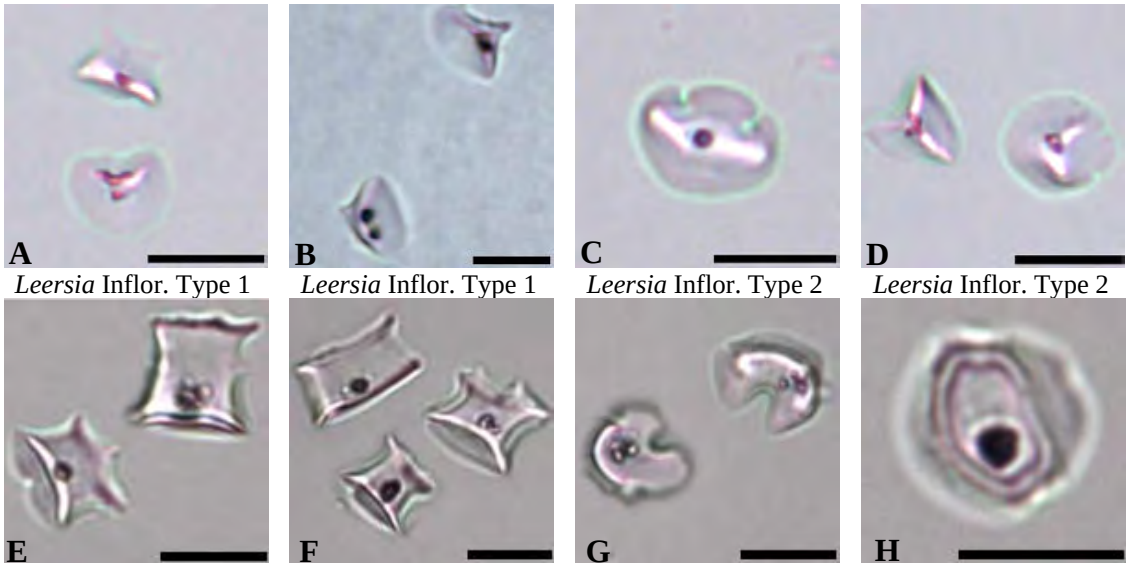


*Leersia* Inflor. Type 1 | *Leersia* Inflor. Type 1 | *Leersia* Inflor. Type 2 | *Leersia* Inflor. Type 2

*Zizania* Inflor. Type 1 | *Zizania* Inflor. Type 1 | *Zizania* Inflor. Type 1 | *Zizania* Inflor. Type 2

Figure 39

A Comparison of some *Leersia* (A-D) and *Zizania* (E-G) Inflorescence Phytoliths

<u>*Leersia* vs. *Zizania* Culm phytoliths</u>

Interestingly, the *Leersia* and *Zizania* culm phytolith assemblages show very little affinity. In fact, the *Leersia* culm phytolith assemblage is dominated (86.6%) by *Leersia* Culm Type 1 (Figure 40 A & B), which is analogous to *Leersia* inflorescence Type 2. The only potential wild rice confuser is *Leersia* Culm Type 2 (Figure 40 C & D) which is a reniform rondel with 1 to 3 clefts; however, this morphotype comprises only 1.8% of the *Leersia* culm phytolith assemblage. The *Zizania* culm phytolith assemblage (Figures 30 & 35) is dominated by cross and trapeziform morphotypes not represented in *Leersia*.

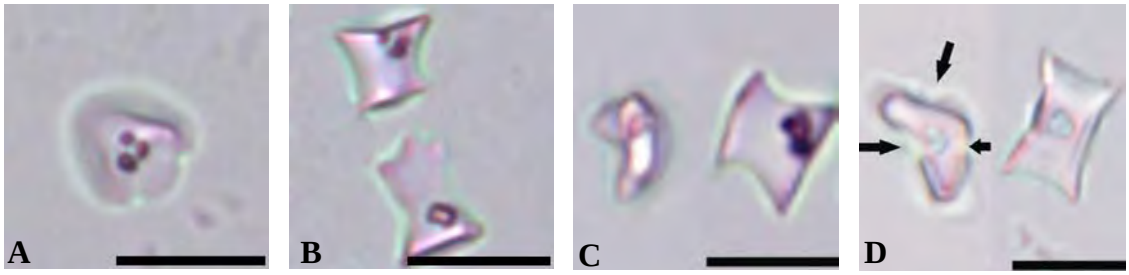


Culm Type 1 Culm Type 1 Culm Type 2 Culm Type 2

Figure 40

Some *Leersia* Culm Rondel Phytoliths
(Culm Type 2 is possible wild rice rondel confuser)

*Leersia* vs. *Zizania* Leaf and Sheath Phytoliths

*Leersia* and *Zizania* leaf and sheath phytoliths share many general typological characteristics; however, a few very important distinctions are present. For cross typological classification I use a definition from Sue Mulholland (personal communication) which states that a cross has 3 or 4 lobes and that the length and width are approximately equidistant. For bilobate designation, I use the shaft-to-lobe width of less than 2/3 definition (Mulholland and Rapp, 1992).

The *Zizania* leaf and sheath phytolith assemblage is rich in morphotype diversity, with many of the major silica body typologies (cross, bilobate, rondel and trapeziform) present in moderate to high amounts (Figures 28, 29, 33, 34; Tables 13, 14). The *Leersia* leaf and sheath phytolith assemblage is dominated by bilobate and cross phytoliths with distinctly pointed lobes (Figures 24, 27, 41; Table 12). Clearly, the bilobate in Figure 41 A and the cross in Figure 41 C originate ontologically from the same basic silicification process, but with a slight modification that allows for a change from approximately 1:1.5 to 1:1 in the length to width ratio for the *Leersia*

Leaf Type 1 or 3 (bilobate) and *Leersia* Leaf Type 2 (cross) types respectively. Thus, a *Leersia* Leaf Type 2 (cross) occupies approximately 33% more area than a *Leersia* Leaf Type 1 or 3 (bilobate). It is likely that this same bilobate/cross ontological process is controlling some of the bilobate and cross production in *Zizania*, as evidenced by the *in situ* juxtaposition of a *Zizania* Leaf Type 2 (bilobate) and Zizania Leaf Type 1 (cross) in Figure 41 G.

An important distinction between *Leersia* and *Zizania* cross/bilobate morphotypes is found in the outline of the raised ridges that define the top face lobes. *Leersia* Leaf Type 1 and 3 morphotypes have pointed or acute top face lobes. *Zizania* Leaf Type 1 and 2 morphotypes have blunt or obtuse top face lobes. It is important that the determination of acuteness or obtuseness be made on the side of the lobe that is facing the long axis of the leaf blade (white arrows in Figure 41) and not the side facing the short axis or leaf margin of the leaf blade (black arrows in Figure 41).

There is one important morphotype exception to the general *Leersia*/acute lobe and *Zizania*/obtuse lobe rule, *Leersia* Leaf Type 4, which is a bilobate with blunt/rounded or obtuse lobes (Figure 41 D). This morphotype comprises 5.4% of the *Leersia* leaf and sheath assemblage and is visually very similar to *Zizania* Leaf Type 2 (Figure 41 H), which comprises 22% of the *Zizania* leaf assemblage.

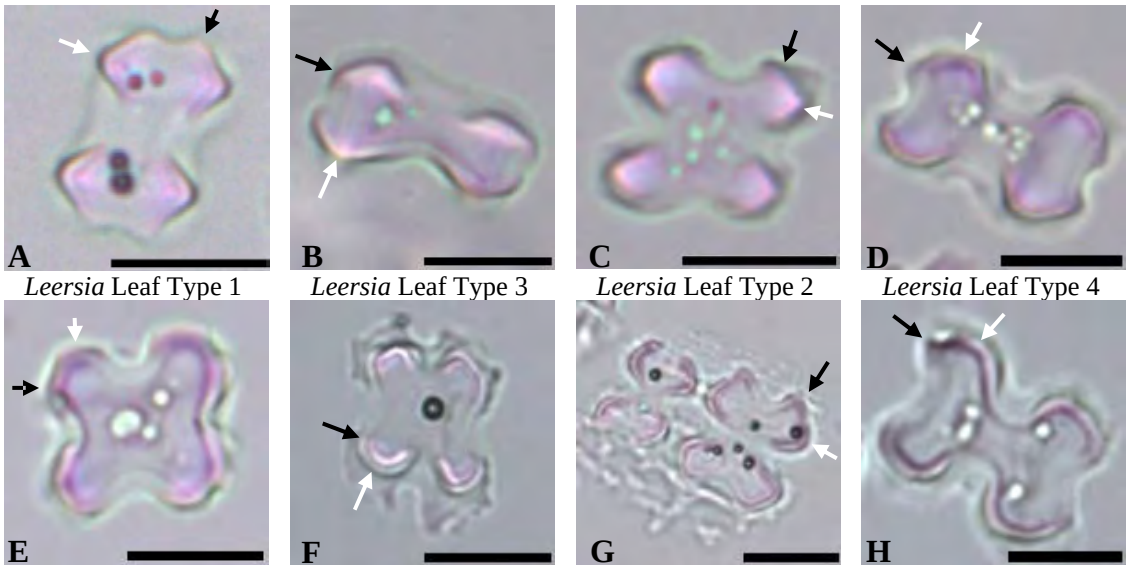


*Leersia* Leaf Type 1 | *Leersia* Leaf Type 3 | *Leersia* Leaf Type 2 | *Leersia* Leaf Type 4

*Zizania* Leaf Type 1 | *Zizania* Leaf Type 1 | *Zizania* Leaf Type 2 & 1 | *Zizania* Leaf Type 2

Figure 41

Comparison of *Leersia* Acute-Lobed and *Zizania* Obtuse-Lobed Morphotypes

If *Zizania* leaf and sheath material was dry-ashed together as in the case of *Leersia*, then the *Zizania* Leaf Type 2 contribution would drop significantly. When considered in the entire plant contribution assemblage, *Zizania* Leaf Type 2 only comprises 2.2% of the total morphotype assemblage (Table 19). Although not quantified and only anecdotal, it appears possible that lobe-to-shaft width ratios between *Leersia* Leaf Type 4 and *Zizania* Leaf Type 2 may be statistically significant.

There are occasional variations where acute and obtuse lobes are on the same silica body, but these morphotypes occur in very low frequencies. A few of these types are illustrated in Figure 41 B & F, where *Leersia* Leaf Type 3 (B) has two acute lobes and two obtuse lobes, the defining feature for this morphotype; and in *Zizania* Leaf Type 1, which occasionally has two lobes that are fairly acute and pointed (F).

# CONCLUSION

Although a few *Leersia* short cell silica bodies can be potential wild rice confusers, 2-D and 3-D rotation at 400X magnification is sufficient to discriminate between all wild rice and *Leersia* morphotypes except the obtuse-lobed bilobate found in both *Leersia* and *Zizania*. However, because of the very low contribution of this wild rice confuser to lake sediments, *Zizania* Leaf Type 2 is still considered to be locally diagnostic for wild rice. Further, after close examination of nine wetland grass taxa (Table 8) and 28 other dominant trees, shrubs and forbs from the study area (Appendix A), only 5 out of 28 designated wild rice phytolith morphotypes were determined to be unreliable and therefore non-diagnostic local indicators of wild rice. These five unreliable morphotypes are *Zizania* Leaf Types 4, 5, 6 and *Zizania* Inflorescence Types 2 and 3. All other morphotypes listed in Table 19 are considered locally diagnostic indicators of wild rice.

A few potential confuser phytoliths were also identified (*Poa palustris* reniform rondels and *Phragmites* rondels with a single sinus), but with thorough observation through 3-D rotation, these pose no barrier to correct *Zizania* or non-*Zizania* designation. Until additional grass taxa common to lake margins are examined across a wider geographic area, it is unknown as to whether these locally diagnostic morphotypes can be considered regionally or possibly even universally diagnostic. However, I do feel that these locally diagnostic morphotypes would at least hold for northern North America.

One other tribe Oryzeae species found in the southern United States, *Zizaniopsis miliacea* (giant cut grass) was not examined here and is a priority for future research. For wild rice studies in areas thought to be *Zizania* refugia during the last glacial maximum, Bambusoideae taxa of the American Tropics will have to be thoroughly investigated for *Zizania* phytolith morphotype confusers. The similarity between Oryzeae and Bambusoideae subfamilies is readily apparent (see Piperno and Pearsall, 1998, figure 57, wild rice-like reniform rondel). Most importantly, full and comprehensive resolution of phytolith production in all species and varieties of *Zizania* awaits completion.

Main Conclusion Points

1) Dominant study area grass species produce phytoliths distinct from *Zizania* phytoliths.

2) *Phragmites australis* and *Poa palustris* produce rondel phytoliths with some similarities to *Zizania*; however, these potential wild rice confusers occur in low numbers and can be identified based on 3-D morphology.

3) *Leerisa oryzoidies* produces a few *Zizania*-like phytolith morphotypes; however, these potential wild rice confusers can be identified based on 2-D and 3-D morphology.

4) *Zizania palustris* produces a wide variety of phytolith morphotypes, many of which are only found in certain parts of the plant (e.g. Inflorescence Type 1 from the spikelet).

5) *Zizania palustris* produces 23 locally diagnostic phytolith morphotypes that can be used to determine the presence and abundance of wild rice in modern and paleo lake sediments.

# Chapter IV

# PHYTOLITH DEPOSITION IN MODERN LAKE SEDIMENTS

## INTRODUCTION

Of the few phytolith studies that take place within the context of lacustrine sediments (e.g., Piperno, 1993b; Fearn, 1998; Zhao and Piperno, 2000; Carter, 2002; Piperno and Jones, 2003; Davidson, 2003; Wrenn and Tedford, 2004), an even fewer number have looked at local or extralocal modern phytolith deposition patterns and factors relating to taphonomy (the study of decaying organisms over time).

To assist with interpretation of a paleo estuarine core from Louisiana, Fearn (1998) studied modern phytolith deposition and morphotype assemblage patterns along a moisture gradient; however, this was conducted on a regional scale and was not specific to the estuary itself. Also from Louisiana, Wrenn and Tedford (2004) are undertaking a comprehensive analysis of phytolith production and taphonomy from Lake Catahoula lakebed, shoreline and surrounding forest plant taxa, thus allowing for better interpretation of their two lake cores; however, it is unclear whether they will be investigating phytolith deposition patterns across the lake.

Other than top-core samples, none of the aforementioned studies have looked systematically at modern sediment phytolith deposition patterns throughout the coring

lake. This type of analysis is somewhat rare for pollen analysis; however, a few studies have clearly demonstrated the existence of sediment focusing, redeposition, spatial patchiness, and the influence it can have on a number of phenomena, including pollen deposition and water chemistry (e.g., Janssen, 1966; for pollen transect diagram used to determine local, extralocal and regional pollen sources; Davis, 1973; Dowling and Rath, 1988; Blais and Kalff, 1995). Phytolith taphonomy and deposition, largely a decay-in-place mechanism in a terrestrial context, is undoubtedly subject to these same lacustrine depositional influences. Interpretations derived from lake sediment cores will need to take into consideration phytolith taphonomy and core location.

This chapter presents modern lake sediment phytolith assemblage results for transect samples collected across three wild rice lakes and one non-wild rice control lake from the study area. This chapter concludes with a discussion and summary on wild rice and non-wild rice phytolith deposition in modern lake sediments.

## METHODS AND RESULTS

The data presented in this chapter are the result of methodologies developed in Chapter 2 and detailed in Appendix B. Specific methods and considerations unique to each subtopic are briefly summarized within the subsection.

### Common Lake Sediment Phytoliths

In addition to *Zizania* phytolith morphotypes (Chapter 3, Table 19), all Poaceae silica short cell phytoliths encountered were categorized into ten general typological categories and counted (Table 22, Figure 42). Two epidermal long cell

types were counted: elongate tuberculate phytoliths, distinctive of the Oryzeae; and interstomatal guard cells, common in *Zizania* and other Poaceae leaves. In addition, globular echinates of the Equisetaceae, and Cyperaceae cone cells were tallied for Lake Ogechie sediments. Most of the Poaceae silica short cells encountered in modern lakes sediments could be traced to specific comparative collection grass taxa and will be discussed at the end of this chapter. Although observed in lake sediments, dicotyledonous phytoliths from trees, shrubs and forbs were not tallied. A few of the most common forms not tallied can be seen in Figure 43.

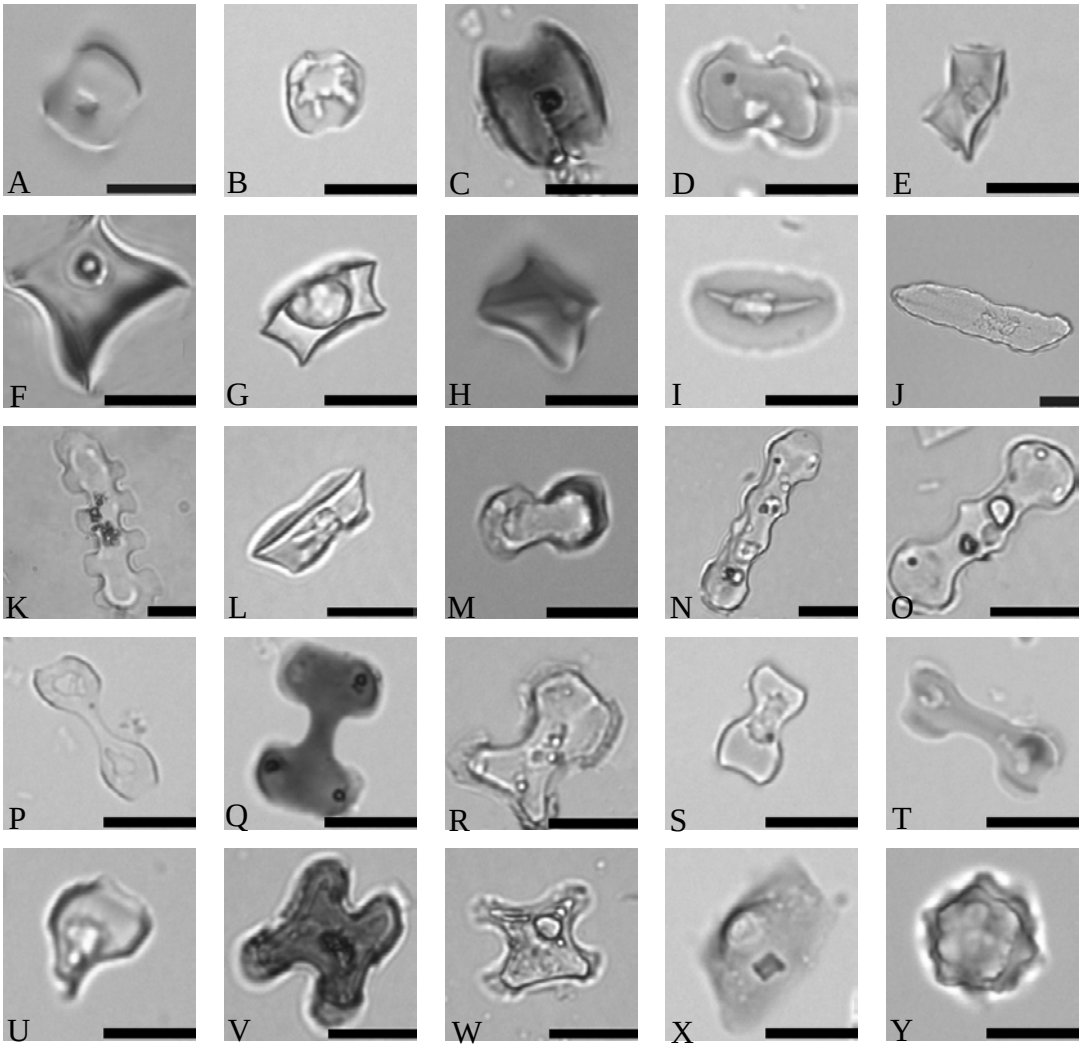


Figure 42

Common non-*Zizania* Lake Sediment Phytolith Micrographs
Scale bar = 10 µm: A-C) saddles, square tabular; D) saddle, elongate tabular; E) trapeziform with concave top (called collapsed saddle by Piperno and Pearsall, 1998); F) rondel, concave (*Phragmites*); G-H) Rondels; I) rondel, keeled top; J) trapeziform sinuate; K) trapeziform polylobate; L) Stipa-type, side view; M) Stipa-type, top view; N-O) polylobates, P-T) bilobates; U) broken bilobate; V-W) crosses; X) Cyperaceae cone cell; Y) Equisetaceae globular echinate spherules.

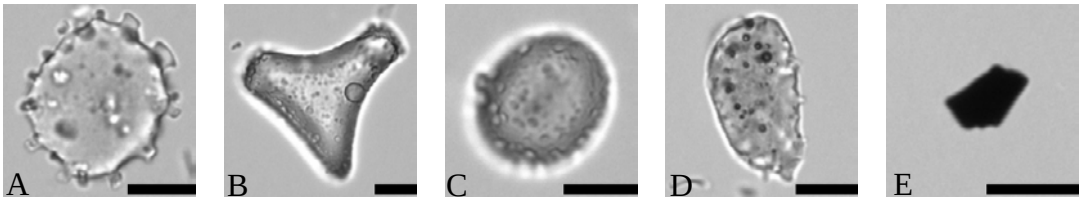


Figure 43

Common non-*Zizania* Phytoliths Not Counted but Observed in Lake Sediments Scale bar = 10 µm: A) globular pilate sphere; B) blocky scrobiculate polyhedron, possibly *Picea mariana* (Bozarth, 1993); C) scrobiculate spherule, possibly coniferous; D) trichome base cell; E) micro-charcoal particle.

Table 22

Non-*Zizania* Phytoliths Counted in Modern Lake Sediments

| Typological Category | Figure | Typological Category | Figure |
|---|---|---|---|
| Saddle | 20, 40 A-D | Polylobate | 40 N-O |
| Rondel: Concave (Phragmites) | 17, 40 F | Bilobate | 40 P-U |
| Rondel | 40 G-I | Cross | 40 V-W |
| Trapeziform Sinuate | 17, 19, 40 J | Elongate Tuberculate | 26 N |
| Trapeziform Polylobate | 18, 40 K | Interstomatal Guard Cell | 26 K |
| Trapeziform Bilobate (Stipa-type) | 40 L-M | Globular echinate | 19, 40 Y |
| Trapeziform Concave Top (collapsed saddle) | 40 E | Cyperaceae cone cell | 19, 40 X |

## Lake Onamia Modern Phytolith Abundance

A total of 17 modern sediment samples were collected from Lake Onamia (10/14/2005; Figure 44). Samples were collected and processed using the methods described in Chapter 2 and in detail in Appendix B. Not all samples collected were processed or counted and await future analysis; however, seven Lake Onamia samples were counted (Tables 23 & 24; see Table 4 for UTM's, water depth & rice density).

Table 23

Lake Onamia Modern Lake Sediments Collected and Analyzed

| Sample Collected | Phytoliths Extracted | Phytoliths Counted [1] | Sample Collected | Phytoliths Extracted | Phytoliths Counted[1] |
|---|---|---|---|---|---|
| OT1P01 | X | S | OT1P09 | | |
| OT1P02 | | | OT1P10 | X | S |
| OT1P03 | X | B | OT1P11 | | |
| OT1P04 | | | OT1P12 | | |
| OT1P05 | X | S | OT1P13 | X | S, B |
| OT1P06 | | | OC1P1 | X | S |
| OT1P07 | | | OT2P01 | X | |
| OT1P08 | X | S | OT2P02 | X | |
| | | | OT2P03 | X | |

[1] S = exotic diatom spike method; B = Battarbee evaporation tray method

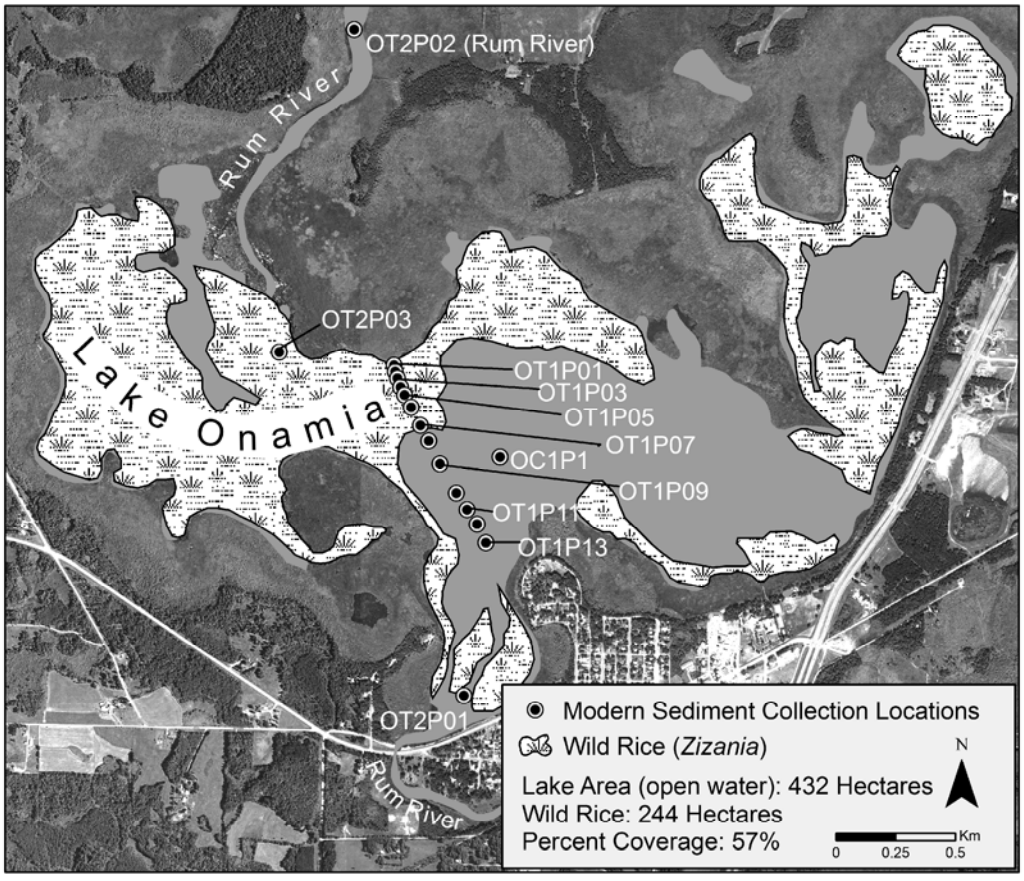


Figure 44

Map of Lake Onamia Modern Lake Sediment Collection Points

Table 24

Lake Onamia Modern Lake Sediment Phytolith Abundance per Gram Dry Sediment

| Lake Onamia Samples: | OT1P1 | OT1P5 | OT1P8 | OT1P10 | OT1P13 | OC1P1 |
|---|---|---|---|---|---|---|
| Percent Organic Matter (%) | 56.0 | 56.0 | 58.2 | 58.2 | 58.7 | 60.3 |
| | | | | | | |
| *Phytolith Morphotype* | | | | | | |
| Saddle (cf. *Muhlenbergia*) | 47,143 | 55,207 | 74,437 | 67,614 | 92,426 | 76,298 |
| Rondel: Concave (*Phragmites*) | 43,422 | 37,839 | 53,967 | 76,918 | 107,313 | 68,854 |
| Rondel | 26,673 | 30,395 | 39,079 | 49,004 | 62,651 | 75,678 |
| Trapeziform Sinuate | 23,572 | 40,940 | 29,775 | 34,737 | 58,309 | 44,662 |
| Trapeziform Polylobate | 4,342 | 5,583 | 6,203 | 1,861 | 3,722 | 4,962 |
| Trapeziform Bilobate (Stipa-type) | 2,481 | 1,241 | 1,861 | 3,722 | 3,102 | 3,102 |
| Trapeziform Concave [1] | - | - | - | - | - | - |
| Polylobate | 1,241 | 2,481 | 620 | 0 | 1,241 | 1,241 |
| Bilobate | 3,722 | 5,583 | 12,716 | 10,235 | 9,305 | 8,684 |
| Cross | 620 | 1,241 | 3,102 | 1,861 | 4,342 | 3,722 |
| Elongate Tuberculate | 3,722 | 3,722 | 1,241 | 0 | 1,241 | 0 |
| Interstomatal Guard Cell | 620 | 1,241 | 620 | 0 | 0 | 620 |
| Globular echinate (Equisetaceae) [2] | - | - | - | - | - | - |
| Cyperaceae cone cells [2] | - | - | - | - | - | - |
| *Zizania* Inflor. Type 1 (rondel) | 3,102 | 620 | 3,722 | 1,241 | 3,102 | 3,722 |
| *Zizania* Sheath Type 1 (bilobate) | 0 | 0 | 620 | 0 | 0 | 0 |
| *Zizania* Leaf Type 2 (bilobate) | 0 | 0 | 0 | 620 | 0 | 0 |
| *Zizania* Leaf Type 1 (cross) | 0 | 620 | 620 | 0 | 0 | 0 |
| *Zizania* Sheath Type 3 (polylobate) | 0 | 620 | 0 | 0 | 0 | 0 |
| | | | | | | |
| Total non-*Zizania* Short Cell Phyto. | 153,216 | 180,510 | 221,760 | 245,952 | 342,410 | 287,203 |
| Total non-*Zizania* Phytoliths | 157,558 | 185,472 | 223,621 | 245,952 | 343,651 | 287,823 |
| Total *Zizania* Phytoliths | 3,102 | 1,861 | 4,962 | 1,861 | 3,102 | 3,722 |

[1] Counted with saddle category and not tallied independently (collapsed saddles)
[2] Not counted for Lake Onamia samples

Estimates of absolute abundance for samples listed in Table 24 were quantified using the exotic diatom spike method and are expressed here in terms of phytoliths per gram of dry sediment. Replicate samples from OC1P1 and OT1P3 were quantified using the Battarbee evaporation tray method; thus, OC1P1 was quantified using both methods (see Table 29 for a side-by-side comparison). Wild rice phytoliths from the inflorescence were the most abundant *Zizania* morphotype recovered and occur in

approximately equal abundance across the basin, although some spatial patchiness is apparent.

## Shakopee Lake Modern Phytolith Abundance

A total of 12 modern sediment samples were collected from Lake Onamia (10/27/2005; Figure 45). Samples were collected and processed using the methods described in Chapter 2 and in detail in Appendix B. Not all samples collected were processed and counted and await future analysis (Table 25); however, a total of seven Lake Onamia samples were counted (see Table 4 for water depth, UTM's and wild rice density).

Table 25

Shakopee Lake Modern Lake Sediments Collected and Analyzed

| Sample Collected | Phytoliths Extracted | Phytoliths Counted [1] | Sample Collected | Phytoliths Extracted | Phytoliths Counted[1] |
|---|---|---|---|---|---|
| ST1P1 | | | ST1P7 | | |
| ST1P2 | | | ST2P1 | X [2, 3] | S [2] |
| ST1P3 | X [2, 3] | S [2] | ST2P2 | X [2, 3] | S [2] |
| ST1P4 | | | ST2P3 | X [2, 3] | S [2] |
| ST1P5 | | | ST2P4 | X [2, 3] | S [2] |
| ST1P6 | | | ST2P5 | X [2, 3] | |

[1] S = exotic diatom spike method; B = Battarbee evaporation tray method
[2] samples gravity-settled for 1 hour; [3] samples gravity-settled for 1.5 hours

Estimates of absolute abundance for samples listed in Table 26 were quantified using the exotic diatom spike method and are expressed in terms of phytoliths per gram of dry sediment. These samples were processed using a gravity-settling time of 1 hour. A replicate set of six samples were processed identically, except gravity-

settling was increased to a time of 1.75 hours. These samples were not counted and await future analysis. The idea was to evaluate whether increasing settling time would increase the abundance of taxonomically important Poaceae silica short cells. Desirable settling-times are based on Stokes' law, which describes settling times for various diameter spheres in liquid solutions. Since phytoliths are typically not spherical, it is unknown how closely they follow Stokes' law: particles around 7μm in diameter and larger will settle 10 cm in a 5% calgon solution in 1 hour; particles of 5 μm diameter and larger will settle in 1.75 hours (Lentfer and others, 2003). Since most of the Poaceae and *Zizania* phytoliths counted in this study are at least 10 μm in diameter, no significant change in abundance is expected; however, absolute determination awaits future analysis.

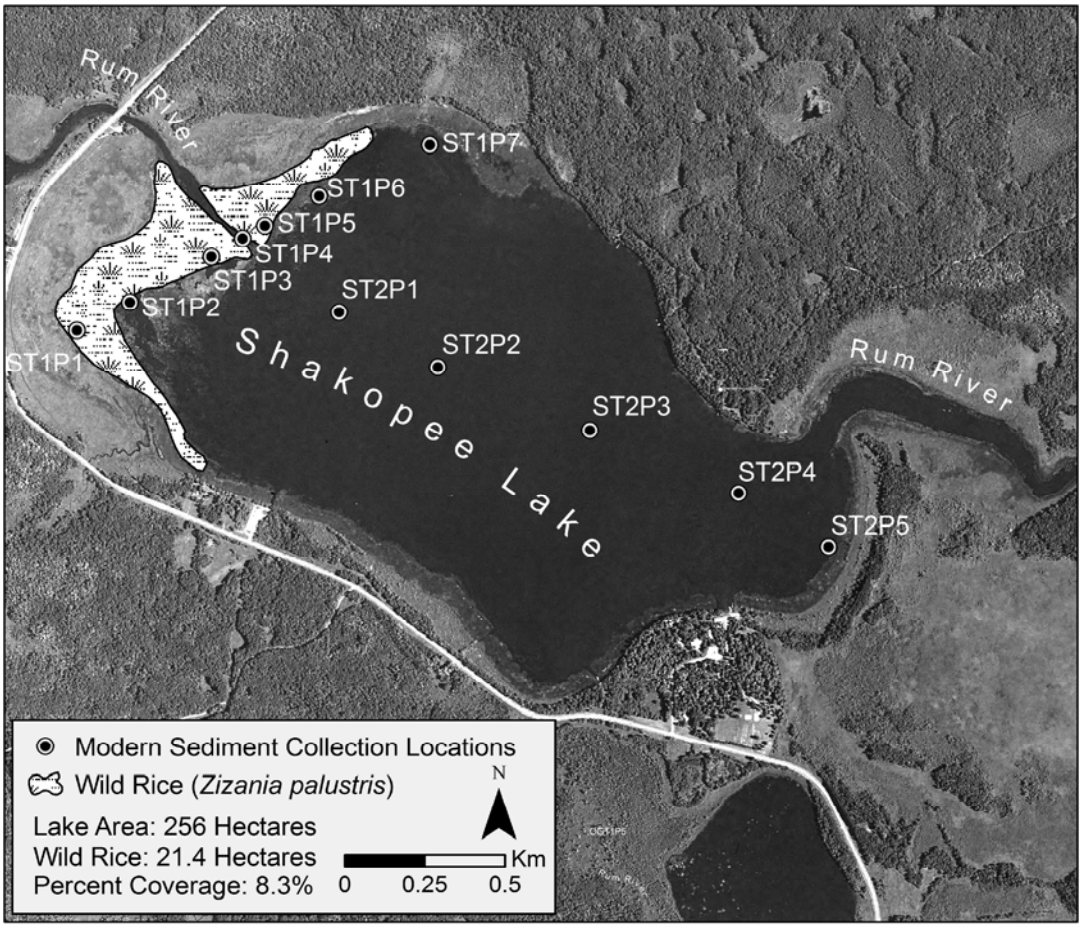


Figure 45

Map of Shakopee Lake Modern Lake Sediment Collection Points

Table 26

Shakopee Lake Modern Lake Sediment Phytolith Abundance per Gram Dry Sediment

| Shakopee Lake Samples: | ST1P3 | ST2P1 | ST2P2 | ST2P3 | ST2P4 |
|---|---|---|---|---|---|
| Percent Organic Matter (%) | 51.0 | 47.4 | 43.7 | 43.3 | 22.4 |
| | | | | | |
| *Phytolith Morphotype* | | | | | |
| Saddle ( cf. *Muhlenbergia*) | 63,271 | 51,486 | 30,395 | 40,940 | 14,887 |
| Rondel: Concave (*Phragmites*) | 47,764 | 74,437 | 66,373 | 55,828 | 19,229 |
| Rondel | 34,117 | 37,839 | 24,812 | 32,256 | 13,026 |
| Trapeziform Sinuate | 26,053 | 29,154 | 27,914 | 16,748 | 13,026 |
| Trapeziform Polylobate | 3,722 | 7,444 | 3,722 | 6,823 | 620 |
| Trapeziform Bilobate (Stipa-type) | 8,684 | 6,203 | 3,102 | 3,722 | 1,241 |
| Trapeziform Concave (collapsed saddle) [1] | - | - | - | - | - |
| Polylobate | 620 | 1,241 | 1,861 | 620 | 0 |
| Bilobate | 22,331 | 3,102 | 4,652 | 4,652 | 2,791 |
| Cross | 620 | 1,551 | 0 | 310 | 0 |
| Elongate Tuberculate | 620 | 2,481 | 3,102 | 0 | 620 |
| Interstomatal Guard Cell | 0 | 620 | 0 | 0 | 620 |
| Globular echinate (Equisetaceae) [2] | - | - | - | - | - |
| Cyperaceae cone cells [2] | - | - | - | - | - |
| *Zizania* Inflorescence Type 1 (rondel) | 14,267 | 9,305 | 3,102 | 3,102 | 620 |
| *Zizania* Sheath Type 1 (bilobate) | 1,085 | 0 | 0 | 0 | 0 |
| *Zizania* Sheath Type 3 (polylobate) | 0 | 0 | 0 | 310 | 0 |
| *Zizania* Sheath Type 4 (cross) | 0 | 0 | 0 | 310 | 0 |
| *Zizania* Culm Type 3 (polylobate) | 0 | 0 | 0 | 0 | 310 |
| *Zizania* Culm Type 4 (cross) | 620 | 930 | 0 | 0 | 0 |
| *Zizania* Leaf Type 1 (cross) | 310 | 310 | 310 | 310 | 0 |
| *Zizania* Leaf Type 2 (bilobate) | 1,085 | 1,241 | 930 | 310 | 310 |
| | | | | | |
| Total non-*Zizania* Short Cell Phytoliths | 194,777 | 212,455 | 161,900 | 161,280 | 64,822 |
| Total non-*Zizania* Phytoliths | 195,397 | 215,557 | 165,002 | 161,280 | 66,063 |
| Total *Zizania* Phytoliths | 17,679 | 11,786 | 4,342 | 4,342 | 1,241 |

[1] Counted with saddle category and not tallied independently
[2] Not counted for Shakopee Lake samples

The relatively simple bathymetry and large zone of accumulation (area of undisturbed lake sediment) for Shakopee Lake allows for clear-cut interpretations from phytolith abundance values. Also, with approximately 75% of the shoreline forested, the origin of Poaceae phytolith influx to the lake is limited to one dominant area adjacent to the wild rice stand. Although these results will be discussed and summarized in the discussion section of this chapter, a few important results are

highlighted here: 1) Poaceae phytolith abundance is well correlated with percent organic matter of lake sediment and 2) *Zizania* Inflorescence Type 1 rondels show a clear gradient of decreasing abundance as distance from the wild rice stand increases.

## Lake Ogechie Modern Phytolith Abundance

A total of six modern sediment samples were collected from Lake Ogechie. All of the samples except ML1 were processed and counted for phytoliths (Tables 27 & 28, Figure 46; see Table 4 for water depth, UTM's and wild rice density for each sample point).

Table 27

Shakopee Lake Modern Lake Sediments Collected and Analyzed

| Sample Collected | Phytoliths Extracted | Phytoliths Counted [1] | Sample Collected | Phytoliths Extracted | Phytoliths Counted[1] |
|---|---|---|---|---|---|
| ML1 | | | OGT1P3 | X | S, B |
| OGT1P1 | X | S | OGT1P4 | X | S, B |
| OGT1P2 | X | S | OGT1P5 | X | S |

[1] S = exotic diatom spike method; B = Battarbee evaporation tray method
[2] samples gravity-settled for 1 hour; [3] samples gravity-settled for 1.5 hours

Sample ML1 was collected from the inlet from Lake Mille Lacs and was not processed for phytoliths. ML1 is mostly sandy glacial till and is only 1.45 % organic matter. If processed, this sample may provide information on the level of phytolith influx from Lake Mille Lacs, but time constraints and likely insignificance of influx deemed this analysis a low priority. Replicate samples for OGT1P3 and OGT1P4 were quantified using the Battarbee evaporation tray method, resulting in a side-by-side comparison of the exotic spike and Battarbee evaporation tray method (Table 29).

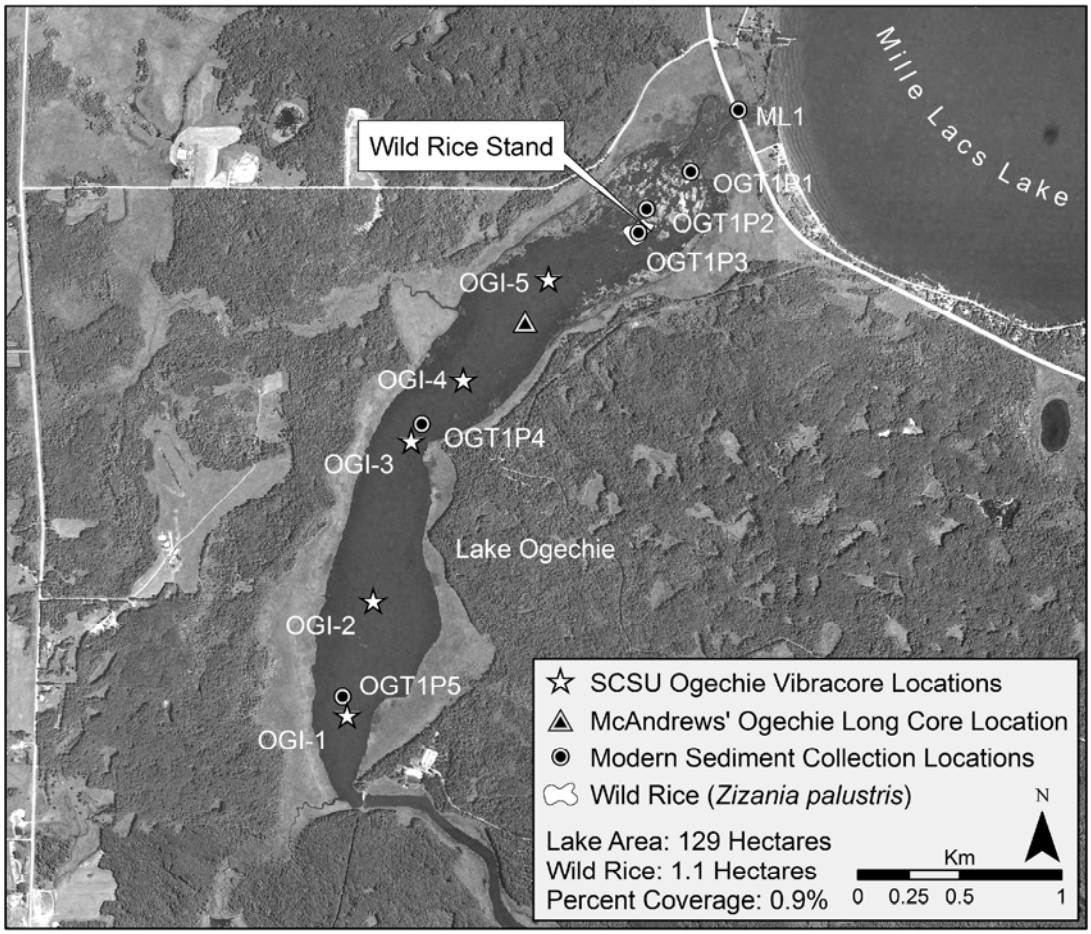


Figure 46

Map of Lake Ogechie Modern and Paleo Lake Sediment Collection Points

The long, narrow shape of Lake Ogechie is the result of a subglacial channel formed by meltwater that eroded the area. These channels are called tunnel valleys and they serve to drain water from the interior of a glacier to the margin (Anderson, 1998). Water flows into the north end of Ogechie from the Mille Lacs inlet and out the south end near OGI-1. Sand sized sediments are entering the north end of Ogechie from Mille Lacs. Percent organic matter increases from 36% near the inlet to 55%

near the south end. A small, sparse stand of wild rice grows on the north end, near the inlet from Mille Lacs. This population is perhaps sustained by the continual disturbance of sediment influx from Mille Lacs, thus reducing competition from annual aquatic perennials and providing at least a minimal amount of nutrients available for plant up-take.

Table 28

Lake Ogechie Modern Lake Sediment Phytolith Abundance per Gram Dry Sediment

| Lake Ogechie Samples: | OGT1P1 | OGT1P2 | OGT1P3 | OGT1P4 | OGT1P5 |
|---|---|---|---|---|---|
| Percent Organic Matter (%) | 36.3 | 37.5 | 39.8 | 51.2 | 55.3 |
| | | | | | |
| *Phytolith Morphotypes* | | | | | |
| Saddle (cf. *Muhlenbergia*) | 89,324 | 55,828 | 108,554 | 63,892 | 67,614 |
| Rondel: Concave (*Phragmites*) | 78,159 | 68,234 | 109,795 | 76,918 | 83,742 |
| Rondel | 60,790 | 61,410 | 68,854 | 40,940 | 78,159 |
| Trapeziform Sinuate | 71,956 | 45,903 | 67,614 | 33,497 | 40,320 |
| Trapeziform Polylobate | 17,369 | 9,925 | 4,342 | 3,102 | 4,342 |
| Trapeziform Bilobate (Stipa-type) | 1,861 | 4,342 | 2,481 | 4,342 | 2,481 |
| Trapeziform Concave (collapsed saddle) | 2,481 | 6,203 | 4,342 | 12,406 | 7,444 |
| Polylobate | 620 | 0 | 0 | 620 | 0 |
| Bilobate | 10,545 | 8,994 | 12,406 | 9,925 | 11,166 |
| Cross | 1,241 | 3,722 | 3,102 | 2,481 | 3,722 |
| Elongate Tuberculate | 2,481 | 0 | 0 | 1,241 | 1,861 |
| Interstomatal Guard Cell | 0 | 0 | 0 | 0 | 0 |
| Globular echinate (Equisetaceae) | 1,241 | 1,861 | 620 | 620 | 620 |
| Cyperaceae cone cells | 0 | 0 | 1,861 | 620 | 3,102 |
| *Zizania* Inflorescence Type 1 (rondel) | 0 | 620 | 1,861 | 2,481 | 620 |
| *Zizania* Sheath Type 1 (bilobate) | 0 | 0 | 310 | 310 | 0 |
| | | | | | |
| Total non-*Zizania* Short Cell Phytoliths | 334,346 | 264,561 | 381,489 | 248,123 | 298,988 |
| Total non-*Zizania* Phytoliths | 336,827 | 264,561 | 381,489 | 249,364 | 300,849 |
| Total *Zizania* Phytoliths | 0 | 620 | 2,171 | 2,791 | 620 |

Estimates of absolute abundance for samples listed in Table 28 were quantified using the exotic diatom spike method and are expressed in terms of phytoliths per gram of dry sediment. There is some evidence that OGT1P3 numbers suffer from an

overabundance error due to agarose in the diatom spike not being completely oxidized and adhering to the side of the drying vial. This caused some spike diatoms also to adhere and be underrepresented in the dried phytolith fraction. Further evidence for an overabundance error with OGT1P3 is indicated with the side-by-side Battarbee method resulting in a 58.5% total phytolith difference (Table 29). Residue is also apparent on the inside wall of the vials for OGT1P1 and OGT1P2; however, OGT1P4 and OGT1P5 show very little evidence of agarose residue. There is 90.3% agreement between Battarbee and diatom spike derived abundance values for OGT1P4. In summary, OGT1P1, OGT1P2 and OGT1P3 have an apparent total phytolith overabundance error of possibly around 50% or more. Samples OGT1P4 and OGT1P5 appear to be accurate.

Overabundance errors for Lake Ogechie modern samples may limit some interpretations; however, the main result still holds; the scarcity of wild rice plants is reflected in very low *Zizania* phytolith abundance values. In fact, even within the stand, wild rice is almost undetectable. It is unknown how often wild rice appears at this location, but anecdotal evidence suggests that presence is very sporadic and sometimes non-existent. With the apparent overabundance error, the total *Zizania* phytolith abundance value for OGT1P3, which is a point within the struggling wild rice stand, may be approximately 50% lower; thus giving OGT1P4, 1500 meters down current, an apparently much larger *Zizania* phytolith value. This is not surprising, given the fact that a relatively strong current (2.1 km/h measured at the inlet; Maki, 1970) and prevailing winds off of Lake Mille Lacs would transfer some quantity of

*Zizania* plant material towards OGT1P4. Slow *in situ* decay of wild rice debris is also a factor, and compounded with intermittent presence, may result in a low modern sediment *Zizania* phytolith signal within the stand.

Table 29

Estimates of Absolute Phytolith Abundance Using Battarbee and Exotic Diatom Spike Methodology

| SAMPLE | Method | Confidence Interval (0.05)[3] | Saddle | Rondel | Trapeziform Sinuate | Trapeziform Polylobate | Trapeziform Bilobate | Polylobate | Bilobate | Cross | Phytoliths per Gram Dry Sediment[1] | Percent Difference[2] |
|---|---|---|---|---|---|---|---|---|---|---|---|---|
| *Lake Ogechie* | | | | | | | | | | | | |
| OGT1P3 | Battarbee | ± 5.7% | 36,783 | 95,636 | 30,764 | 20,063 | 12,038 | 669 | 10,032 | 4,013 | 209,997 | 58.5 %† |
| OGT1P3 | Spike | ± 6.4% | 112,896 | 180,510 | 67,614 | 4,342 | 2,481 | 0 | 12,716 | 3,102 | 383,661 | |
| OGT1P4 | Battarbee | ±18.1% | 42,052 | 114,140 | 36,044 | 12,682 | 6,675 | 4,672 | 8,677 | 2,670 | 227,612 | 9.7 % |
| OGT1P4 | Spike | ± 6.4% | 63,892 | 120,339 | 33,497 | 3,102 | 4,342 | 620 | 10235 | 2,481 | 250,913 | |
| *Lake Onamia* | | | | | | | | | | | | |
| OC1P1 | Battarbee | ± 3.0% | 58,411 | 164,154 | 32,227 | 8,057 | 11,078 | 4,028 | 11,078 | 10,071 | 299,103 | 2.8% |
| OC1P1 | Spike | ± 6.4% | 76,298 | 148,254 | 44,662 | 4,962 | 3,102 | 1,241 | 8,684 | 3,722 | 290,925 | |
| OT1P3 | Battarbee | ± 3.9% | 64,129 | 152,817 | 36,158 | 10,916 | 14,327 | 2,729 | 8,869 | 7,504 | 297,448 | |

[1] Totals for silica short cell morphotypes listed in this table.

[2] For phytoliths per gram dry sediment calculation.

[3] 95% confidence interval for Battarbee method based on microscope slide replicate transect count variance (n=3); exotic diatom spike variance. based on transect count variance during calibration (n=24).

† Result of an overabundance error for the exotic diatom spike sample.

Black Bass Lake Modern Phytolith Abundance

Black Bass Lake is a small, 13 hectare seepage lake with no inlet or outlet and serves as a non-wild rice lake control for the modern phytolith study (Table 30, Figure 9). This lake was also chosen by McAndrews (2000) as a non-wild rice lake control for his paleo lake sediment Poaceae pollen analysis for Lake Ogechie and Lake Onamia. One sample, BB1P1 was collected from the center of the lake (see Table 4 for lake depth and UTM's).

Table 30

Black Bass Modern Lake Sediment Phytolith Abundance per Gram Dry Sediment

| Lake Ogechie Samples: | BB1P1 |
|---|---|
| Percent Organic Matter (%) | 39.6 |
| | |
| *Phytolith Morphotypes* | |
| Saddle (cf. *Muhlenbergia*) | 94,907 |
| Rondel: Concave (*Phragmites*) | 111,655 |
| Rondel | 135,847 |
| Trapeziform Sinuate | 39,700 |
| Trapeziform Polylobate | 19,230 |
| Trapeziform Bilobate (Stipa-type) | 14,267 |
| Trapeziform Concave (collapsed saddle) | 4,342 |
| Polylobate | 0 |
| Bilobate | 12,406 |
| Cross | 2,481 |
| Elongate Tuberculate | 0 |
| Interstomatal Guard Cell | 0 |
| Globular echinate (Equisetaceae) | 620 |
| Cyperaceae cone cells | 620 |
| *Zizania* Inflorescence Type 1 (rondel) | 0 |
| *Zizania* Sheath Type 1 (bilobate) | 0 |
| | |
| Total non-*Zizania* Short Cell Phytoliths | 0 |
| Total non-*Zizania* Phytoliths | 0 |
| Total *Zizania* Phytoliths | 0 |

Estimates of absolute abundance for samples listed in Table 30 were quantified using the exotic diatom spike method and are expressed in terms of phytoliths per gram of dry sediment. Examination of the Lake Ogechie, Lake Onamia and Black Bass Lake pollen diagrams from McAndrews (2000) indicate that the sedimentation rate for Black Bass Lake is likely to be significantly less than that for Ogechie or Onamia. Thus, one gram of dry modern lake sediment from Black Bass Lake encompasses a longer time period of phytolith accumulation than that for the other study area lakes.

## Correlation between Percent Organic Matter and Total Grass Phytolith Abundance

An apparent correlation between percent organic matter and total non-*Zizania* grass phytoliths extracted from modern lake sediments was observed for Lake Ogechie, Lake Onamia and Shakopee Lake. A linear regression analysis was used to test the validity and strength of the relationship using SPSS version 12 (Figure 47).

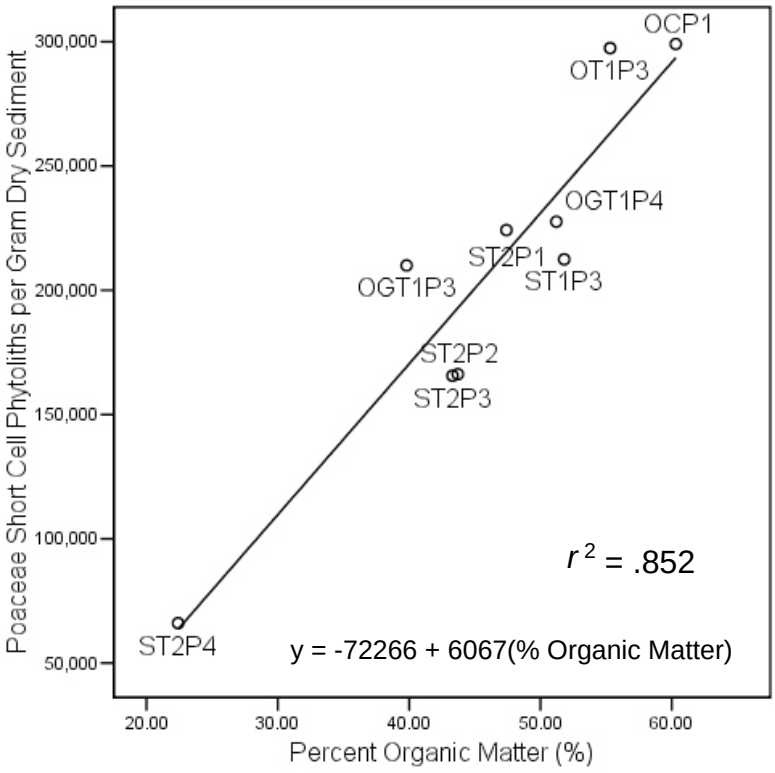


Figure 47

Linear Regression for % Organic Matter and Phytoliths per Gram Dry Sediment

Non-*Zizania* Poaceae short cell phytoliths per gram of dry sediment was the dependent variable and percent organic matter was the independent variable. The regression was run on eight data points (n = 8), from three lakes, and resulted in an equation with an adjusted $r^2$ of .852 and a $p$ value < 0.001, thus indicating a very strong correlation. The Lake Ogechie and Lake Onamia data points were taken from Battarbee derived abundance totals (Table 29) and Shakopee data points were taken from exotic diatom spike derived abundance totals (Table 26).

This strong relationship would seem to indicate that most of the organic matter is derived from terrestrial plant matter, with the balance from aquatic plants (mostly devoid of phytoliths) and phytoplankton. A measure of submerged aquatic vegetation and diatom abundance as a second and third variable would likely explain much of the unaccounted for variation. It also appears that disarticulated phytoliths are bound-up with partially decomposed organic matter and may remain in this condition for some extended period of time. Many of these shallow, highly productive wild rice lakes have oxygen deprived sediments with slow levels of oxidation and decomposition. The exact nature of the organic matter to phytolith abundance relationship is likely very lake specific and only lakes with fairly identical sedimentation rates, size and morphology could be described by the same equation. Other variables such as lake surface area and perimeter were analyzed along with percent organic matter in multiple variable regressions; however, no improvement of the model was achieved.

The decision to use only non-*Zizania* phytoliths in the regression analysis was based on a desire the analyze Poaceae influx from local sources without noise from the *Zizania* signal; although, with *Zizania* abundance values typically well below 9% of the total sum, the effect may have been fairly negligible.

A useful application of the model was employed to test the hypothesis that an overabundance error had occurred with some of the Lake Ogechie diatom spike derived phytolith abundance values. An overlay scatterplot using the previously described regression model and Lake Ogechie diatom spike derived data points was graphed with phytolith abundance on the y axis and percent organic matter on the x

axis (Figure 48). This graph dramatically illustrates the observed values that deviate in a positive direction from the predicted values of the model, apparently confirming an overabundance error for OGT1P1, OGT1P2 and OGT1P3.

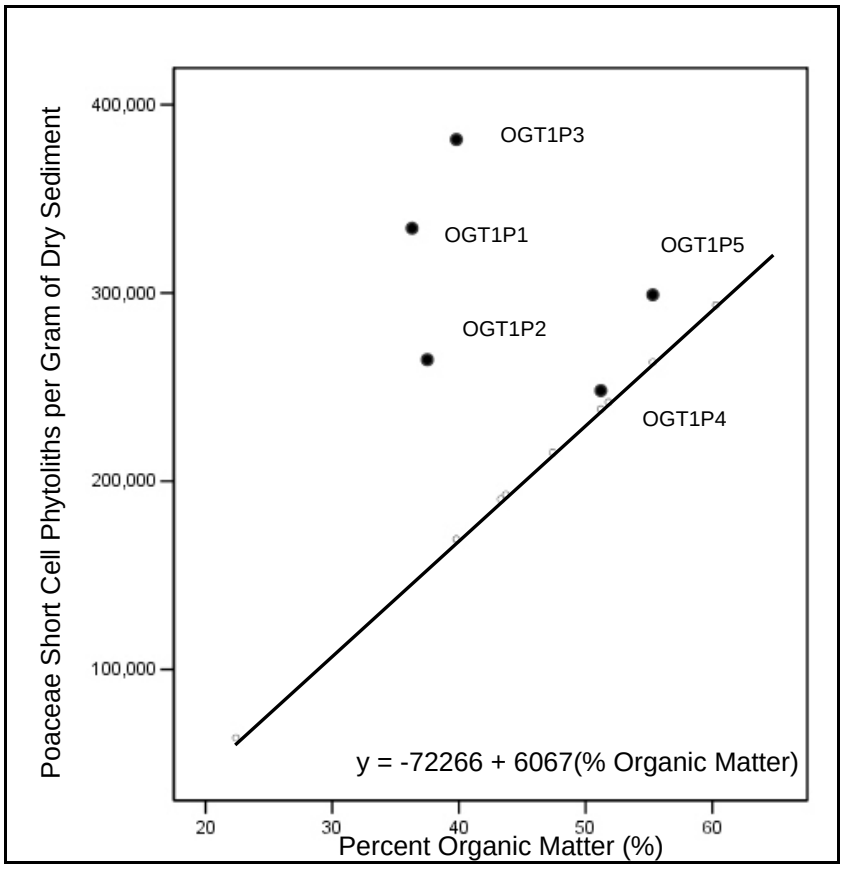


Figure 48

Overlay Scatterplot with Lake Ogechie Observed Values and Prediction Model (line)

# DISCUSSION

## Common Modern Sediment Phytoliths

Phytoliths from a wide variety of plant taxa are represented in silica extracts from modern lake sediments. Since this study is primarily concerned with the unambiguous detection of wild rice phytoliths, tree, shrub and other dicotyledonous phytoliths were briefly looked at in comparative studies (Appendix A), but not classified and quantified in modern lake sediments. Emphasis was placed on identifying, classifying and quantifying Poaceae silica short cell phytoliths from the local taxa most common to lake margins and adjacent areas in the study area so that extralocal and regionally derived phytoliths could be identified. This is important to establish so that local and possibly regionally diagnostic wild rice phytolith morphotypes could be designated.

The vast majority of Poaceae phytoliths appear to be derived from local sources, with very little evidence for inheritance from long distance vectors such as eolian and alluvial processes. This claim is supported by the fact that most Poaceae silica short cells encountered in study area modern lakes sediments can be traced to specific comparative collection grass taxa from the lake margin with some degree of certainty (Table 31). In fact, tabular saddles from *Muhlenbergia* and concave rondels from *Phragmites* are the most abundant of all grass phytolith morphotypes. Both of these species are found very close to the lake margin in high densities and are contributing phytoliths derived from light spikelet inflorescence material (Figure 49). *Phalaris arundinacea* is found in identical situations and is the likely source of the

majority of papillae and conical-type rondels, as well as trapeziform sinuates. These aforementioned morphotypes comprise the vast majority of what is counted in study area modern lake sediments. Saddles and rondels alone typically contribute around 70% of the total short cell morphotype assemblage.

Table 31

The Most Common Modern Lake Sediment Phytoliths and their Likely Plant Origin[1]

| Phytolith Morphotype | Likely Plant(s) of Local Origin |
|---|---|
| Saddle | *Muhlenbergia glomerata* |
| Rondel: Concave | *Phragmites australis* |
| Rondel | Many of the papillae, conical and keel tops can be linked to the inflorescence of *Calamagrostis*, *Glyceria* and *Phalaris*. |
| Trapeziform Sinuate | *Phalaris arundinacea* |
| Trapeziform Polylobate | *Calamagrostis* and *Glyceria* species |
| Trapeziform Bilobate | These "stipa-types" are relatively rare but could be derived from *Oryzopsis*. |
| Trapeziform Concave | These "collapsed saddles" may belong to *Muhlenbergia*, but this determination is quite uncertain. |
| Bilobate | A variety of panicoid morphotypes. If subcategorized, could be possibly traced to specific taxa such as *Andropogon* or *Schizachyrium.* |
| Cross | A variety of panicoid morphotypes. If subcategorized, could be possibly traced to specific taxa such as *Andropogon* or *Schizachyrium.* |

[1] Excluding *Zizania* phytoliths

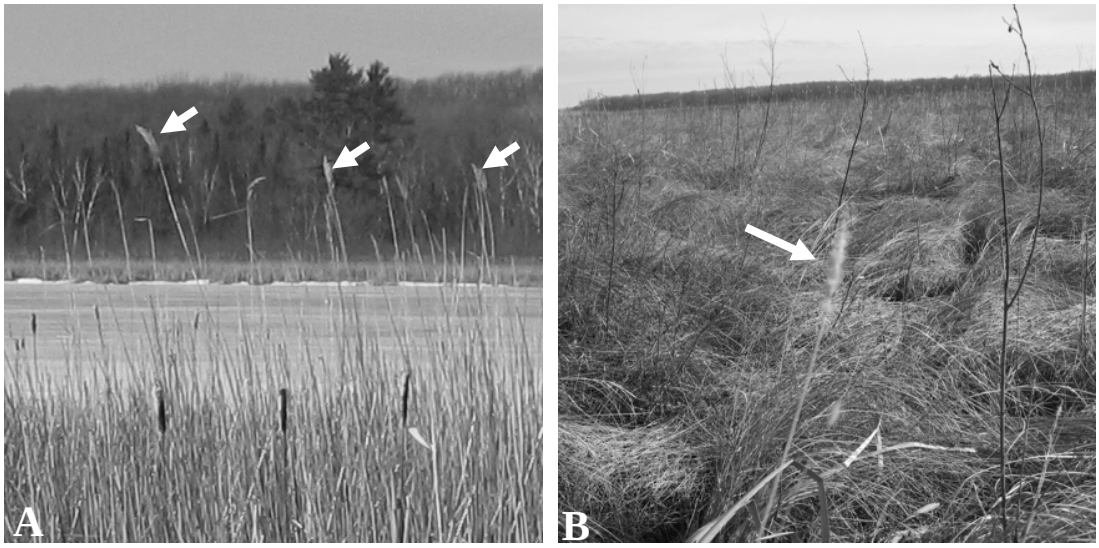


Figure 49

*Phragmites* and *Muhlenbergia* Growing Along the Lake Margin of Lake Ogechie A) *Phragmites australis* inflorescences elevated well above *Typha* and other Lake Ogechie vegetation. B) *Muhlenbergia glomerata* growing on a sedge mat just behind the area in A. Both pictures were taken in March with most plant lacking inflorescence material.

## *Zizania* Phytoliths in the Modern Record

With phytolith taphonomy typically considered to be largely decay-in-place, *Zizania* phytoliths were hypothesized to contribute a substantial fraction of the total short cell assemblage for wild rice lakes; however, phytolith laden inflorescence material from lake margin grass taxa is apparently easily transferred to lake sediments, thus reducing the overall *Zizania* contribution to a few percentage points (Figure 51). Nevertheless, a significant amount of *Zizania* phytoliths are present in modern lake sediments and their abundance is influenced by the density of wild rice and distance from the stand.

With *Zizania* being a highly silicified plant that produces a diverse suite of approximately 10 million short cell phytoliths per culm, the entire morphotype assemblage was expected to be encountered in modern sediment. This was not the case. Over 80% of the short cell *Zizania* phytoliths recovered from all three lakes were of *Zizania* Inflorescence Type 1 (rondel with sinus). This morphotype comprises 30% of the entire plant (Table 19), but is being overrepresented in modern sediment. This paradox can be explained however, by considering the slow decay rates of *Zizania* plant debris (Pastor and Walker, 2006) and the flocculent nature of the sediment water interface.

*Zizania* spikelets (lemmas and paleas) are papery thin, semi-translucent and designed to degrade quickly to release the seed. Despite being densely packed with rondel phytoliths, the inflorescence (spikelets and rachis), per unit dry weight, is the most lightly silicified part of the plant (Chapter 3, Table 20), thus allowing for rapid degradation and disarticulation of rondel phytoliths. Other parts of the plant are heavily silicified with sheets of epidermal silica and more resistant to decomposition and disarticulation of short cell phytoliths. There is some compelling evidence that delays in *Zizania* litter decay and microbial uptake of nitrogen cause an overall delay in nutrient cycling and availability to successive crops and may be responsible for the approximately four year population fluctuations in *Zizania* stands (Pastor and Walker, 2006).

The Hongve-type gravity corer used to collect modern sediment may also be partially responsible for mostly capturing disarticulated rondels (Figure 14). Highly

organic sediments from shallow lakes are notoriously difficult to sample. The flocculent nature of the sediment/water interface is highly prone to disturbance. For the study area lakes, this zone appears to be a half-meter or more in depth, thus making undisturbed access to the zone of accumulation very difficult. The idea behind the Hongve-collector is to gently lower it to the lake bottom and let the weight of the collector alone capture the top 2 to 4 centimeters. In actuality, I was most likely only compressing and sampling the flocculent mix zone and not the accumulation zone. Further, pieces of partially decomposed plant debris would have been too large to fit in the collector. Freeze-core methodology used to freeze loose sediments *in situ* would perhaps be a more appropriate method of modern sediment capture.

Despite these difficulties, the data indicates that phytolith deposition in modern lake sediments is spatially correlated with stand location and density of wild rice, and that lake morphology and bathymetry can have an effect on the exact nature of the depositional pattern (Figure 50). Lifting lake cores from areas close to wild rice stands will likely give a stronger phytolith signal than from areas further away. This is especially visible in Shakopee Lake data.

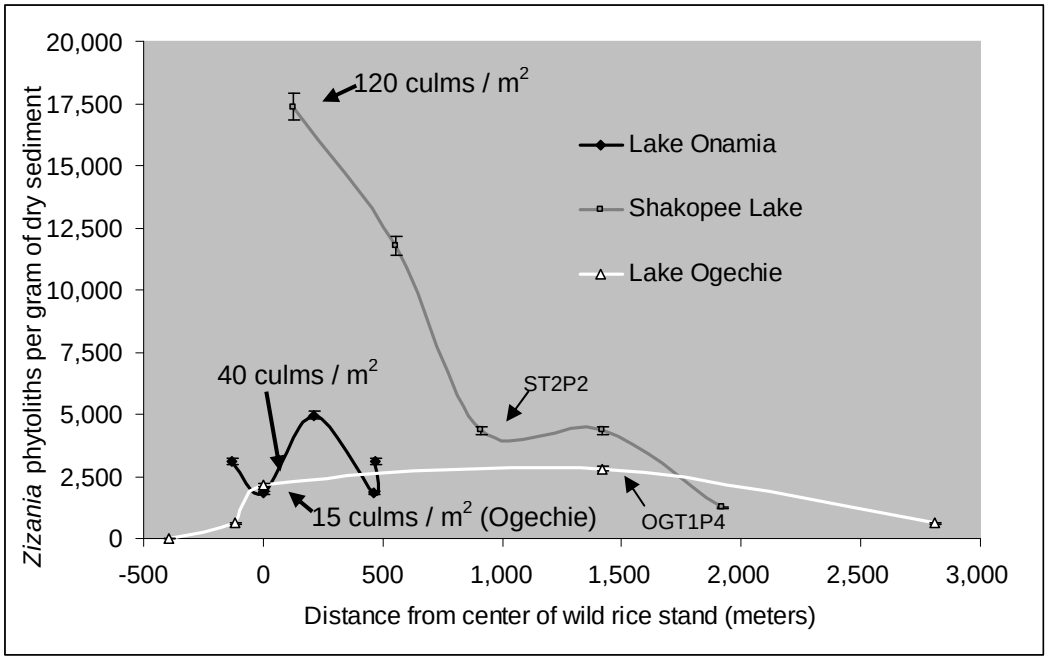


Figure 50

Overlay Scatterplot of *Zizania* Phytolith Abundance vs. Distance from Stand

It was hypothesized that since Lake Onamia had the most wild rice, it should also have had the highest abundance of wild rice phytoliths per gram of dry sediment. This may still be the case; however, data points processed and counted for Onamia were not located in the main wild rice producing basin (Figure 44). Instead, a deep water area with more intermittent wild rice presence and abundance was sampled, resulting in low abundance values (Figure 50). Also, the transect was too short and seemed to pick up a spatially patchy phytolith signal. Lake bottom sediments in Onamia are highly disturbed, especially during duck hunting season when motor boats use the wild rice stands as duck blinds. Since I collected lake sediments during duck hunting season, the variable phytolith signal is not surprising.

Shakopee Lake has a relatively small stand; however, the rice is very dense. Shakopee Lake is also the deepest lake, with ST2P2 collected near the lake center and at a water depth of 4.3 meters (Figure 45). With a more limited wetland zone around Shakopee Lake, *Zizania* phytoliths comprised a greater sum of the total Poaceae short cell count. With its bowl shaped bathymetry and a large undisturbed zone of accumulation, a decay-in-place taphonomy for Shakopee wild rice phytoliths is clearly demonstrated.

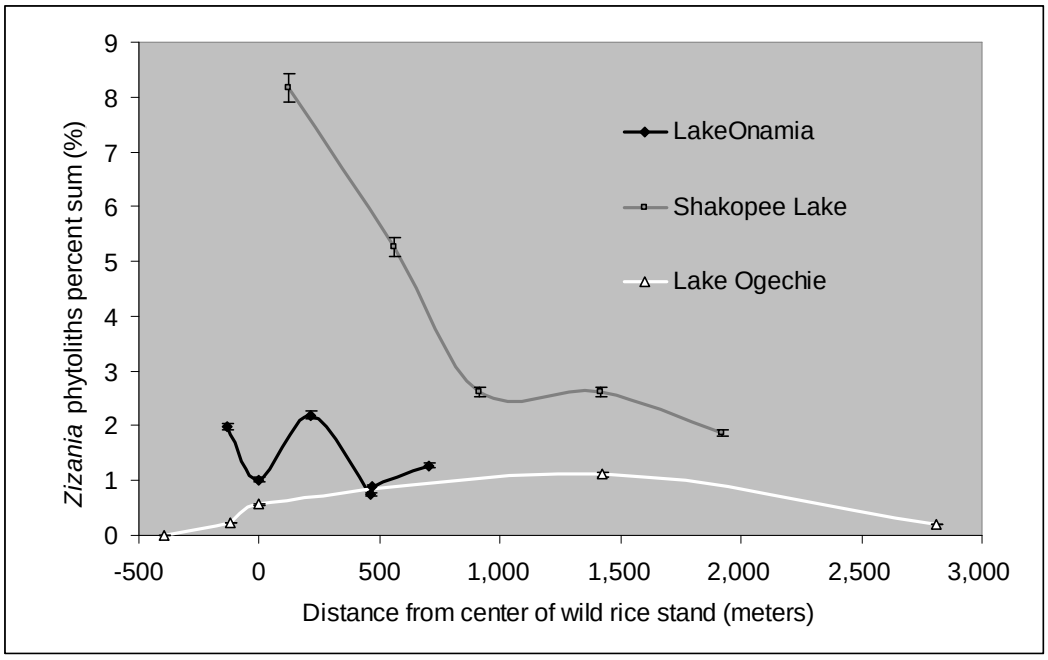


Figure 51

*Zizania* Phytoliths Percent Sum of Total Poaceae Short Cell Abundance

Lake Ogechie, with its struggling and intermittent wild rice stand, had the weakest wild rice phytolith signal. It was somewhat surprising to see that a sample point nearly 1,500 meters down current from the stand had a stronger signal than the

point from the center of the stand. The first three points (from left to right in Figures 50 & 51) also suffer from an overabundance error, so the actual value is likely even smaller. This can be explained by the moderate current that flows through Lake Ogechie, and the prevailing winds that often blow from Lake Mille Lacs, generally north to south, in the same direction. Wild rice plants are often seen uprooted and floating with algae in small flotsam mats, thus potentially spreading *Zizania* phytoliths south, across the length of the lake. These mats may be a byproduct of muskrat lodge building near the wild rice stand. The sample point with the highest *Zizania* phytolith abundance (OGT1P4) was collected near the constriction in the lake and is possibly a zone of accumulation and submersion of flotsam from the north.

Figure 52

*Zizania* and Algae Flotsam Mat on Lake Ogechie

### General Phytolith Depositional Patterns

Although rarely discussed in palynology, sediment focusing is the non-uniform distribution of particles in lake sediments and usually refers specifically to pollen deposition. Because total short cell phytolith abundance is strongly correlated with percent organic content, phytolith focusing *sensu* sediment focusing may be a factor only as much as percent organic content seems to vary within lakes. Because Lake Ogechie and Lake Onamia are shallow lakes and their sediments are easily affected by wind turbulence and resuspension of particles, *Zizania* phytolith deposition may be more homogeneous than in Shakopee Lake, where phytolith abundance decreases as distance from the stand increases.

## CONCLUSION

This chapter presents possibly the first ever analysis of phytolith depositional patterns across modern lake sediments. This study is also the first to reveal that wild rice phytolith deposition is spatially correlated with stand location and density of wild rice; and that, lake morphology and bathymetry can have an effect on the exact nature of the depositional pattern. Further, because wild rice phytolith deposition is fairly localized, the center of a lake basin may not be the best coring location for detection of a wild rice phytolith signal. Any estimates of abundance from the paleoecological record will have to take into account proximity to past wild rice stand location.

Also revealed in this chapter is the interestingly strong correlation between lake sediment percent organic matter (OM) and the total amount of grass phytoliths

recovered ($r^2$=0.852), which illustrates the significant contribution of lake margin plant debris to lake sediments. Quantification of tree and shrub leaf debris phytoliths and phytoplankton contributions to lake sediment OM may allow percent OM to serve as a proxy for very local vegetation fuel loading.

Main Conclusion Points

1) Poaceae (non-*Zizania*) short cell phytolith abundance is well correlated with the percent organic matter of lake sediment ($r^2$ = .852).

2) Most Poaceae short cell phytoliths appear to be derived locally, with little evidence for regional inheritance vectors such as eolian and alluvial processes.

3) Because of anatomical differences in plant debris decay, *Zizania* Inflorescence Type 1 rondels are most abundant; however, morphotypes from other plant parts are rarely recovered.

4) *Zizania* phytolith deposition is spatially correlated with stand location and density of wild rice; however, lake morphology and bathymetry can have an effect on the exact nature of the depositional pattern.

5) The modern lake sediment record suggests that the interpretability of *Zizania* presence and abundance in the paleo lake sediment record should be unambiguous; however, the overall percent of *Zizania* diagnostic phytoliths are at best, 5 to 10% of the total phytolith assemblage. Therefore, a sufficient number of phytoliths, typically around 500 for this study, should be counted.

# Chapter V

# PHYTOLITH DEPOSITION IN PALEO LAKE SEDIMENTS

## INTRODUCTION

The ultimate goal of this chapter was to determine the presence and abundance of wild rice (*Zizania*) through the use of phytoliths recovered from the paleo lake sediment for Lake Ogechie, located in Mille Lacs Kathio State Park. Local Native American tribes have oral histories that recount the harvesting of large quantities of wild rice from the lake (Vennum, 1998, p. 27; Rothaus, 2005) presently, wild rice has almost completely disappeared from Lake Ogechie. Understanding past wild rice populations on Lake Ogechie will assist with planning and preparations for potential future restoration efforts.

Also of importance here is that in developing a new method of wild rice paleoecological analysis, the field of phytolith analysis is advanced by demonstrating that multiplicity and redundancy of basic phytolith typologies in the Poaceae does not limit the establishment of locally diagnostic phytolith morphotypes to genus and possibly species level (e.g., Twiss and others, 1969; Brown, 1984; Mulholland, 1989). Further, in conjunction with pollen derived regional signals, phytoliths can provide a highly localized vegetation signal and enhance paleoenvironmental interpretation.

The data presented in this chapter are the result of methodologies detailed in Chapter 2 and Appendix B, but will be briefly summarized next in the methodology section

## METHODOLOGY

Two lake cores from Lake Ogechie were processed and analyzed for phytoliths (Chapter 4, Figure 46). The first core (OGMC) was lifted by J.H. McAndrews in 1968 and was dated and reanalyzed for pollen in 2000 (McAndrews, 2000). A total of 19 dry subsamples from the core, spanning the top 700 cm, were provided by McAndrews. In addition to *Zizania* phytolith morphotypes (Chapter 3, Table 19) and micro charcoal particles, all Poaceae silica short cell phytoliths observed were categorized into the same typological categories as for the modern study, except that concave rondels typical of *Phragmites* and the other rondels were lumped into a single non-*Zizania* rondel category (Table 22, Figure 42).

Subsample dry weights ($W_d$) were converted to wet volume ($V_t$) using the regression equation: $W_d / V_t = e^{(-0.296-3.719 * OM)}$ (Chapter 2, Figure 17 and Table 6). Once extracted from core subsamples, phytolith concentration was calculated by using an exotic diatom spike and is expressed as the number of phytoliths per cubic centimeter. McAndrews' original $^{14}C$ radiocarbon ages were recalibrated using CALIB 5.0.2 (Stuiver and Reimer, 1993; Stuiver and others, 2005) and are listed in Table 32.

Sedimentation rates were then calculated from the calibrated ages (Figure 53) and used to calculate phytolith influx (accumulation rates) expressed as the number of phytoliths per $cm^2$ of sediment per year (Figures 54 & 55).

The second Lake Ogechie core (OGI-1) was lifted in April of 2006 and spanned 389 cm. A total of 30 wet 1 cubic centimeter subsamples, spanning the top 360 cm were processed and analyzed for phytoliths. Only *Zizania* phytolith morphotypes (Chapter 3, Table 19) were counted. Because of time constraints, other Poaceae short cell morphotypes were not counted for the OGI-1 core. Since $^{210}Pb$ and $^{14}C$ dates have not been returned yet from OGI-1, only *Zizania* phytolith concentration was calculated (Figure 56).

## RESULTS

McAndrews (2000) originally reported $^{14}C$ radiocarbon dates for OGMC are listed in column 2 of Table 32. They were recalibrated using CALIB 5.0.2. (Stuiver and Reimer, 1993; Stuiver and others, 2005) and are reported in the last column of Table 32. The average sedimentation rates for each dated interval in Figure 53 were calculated from the median probability calibrated age and the median depth for each bulk sediment interval (see Table 32 for data). The calibrated age Y axis year of 0 = 1950 AD. The McAndrews core was lifted from Lake Ogechie in 1968.

Table 32

McAndrews' Original $^{14}C$ Ages Recalibrated Using CALIB 5.0.2. (cal yr BP)

| Depth | $^{14}C$ age yr BP† | Lab No. | 95.4% (2σ) cal age ranges [1] | Relative probability | Median Prob. (cal yr BP†) |
|---|---|---|---|---|---|
| 20-40 | 505±35 | BGS-1983 | 557-501 | 0.931 | 529 |
| | | | 625-606 | 0.069 | |
| 260-280 | 2905±105 | BGS-1984 | 3337-2842 | 0.977 | 3063 |
| | | | 2827-2796 | 0.023 | |
| 560-580 | 3895±100 | BGS-1985 | 4782-4770 | 0.004 | 4318 |
| | | | 4607-4604 | 0.001 | |
| | | | 4582-4066 | 0.966 | |
| | | | 4049-3988 | 0.029 | |
| 1180-1200 | 7410±180 | BGS-1986 | 8582-8569 | 0.004 | 8222 |
| | | | 8561-7925 | 0.985 | |
| | | | 7899-7868 | 0.011 | |

[1] McAndrews' original radiocarbon ages recalibrated using CALIB 5.0.2 (Stuiver and Reimer, 1993; Stuiver and others, 2005) and the intcal04.14c curve (Reimer and others, 2004).
† yr BP = years before 1950 AD

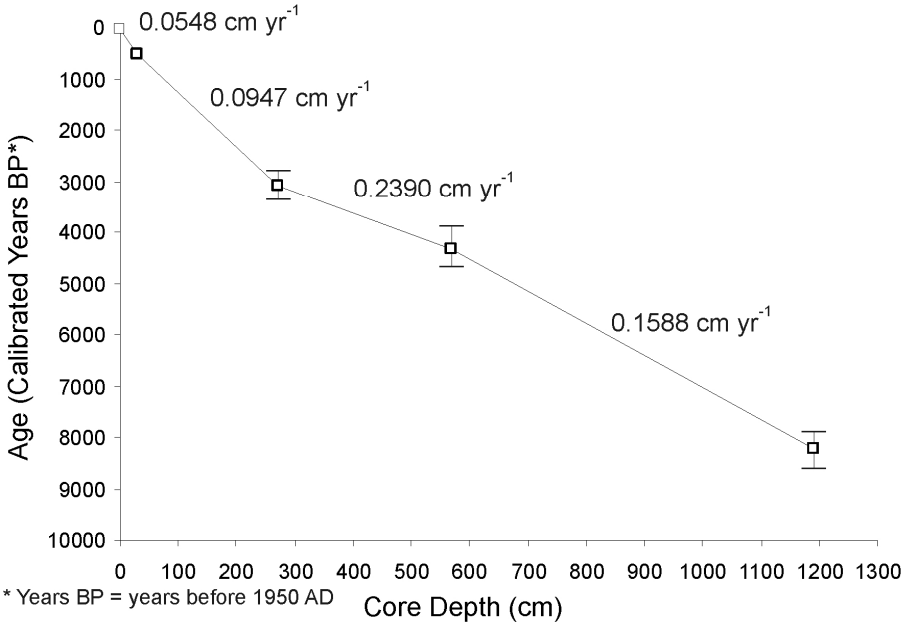


Figure 53

Age vs. Depth and Sedimentation Rates for the McAndrews Core (OGMC)

The stratigraphic phytolith and pollen diagrams in Figures 54, 55 and 56 were graphed using the program C2 written by Steve Juggins, Newcastle University, UK (Juggins, 2006). Phytolith influx values graphed in these Figures were derived from the sedimentation rates illustrated in Figure 53.

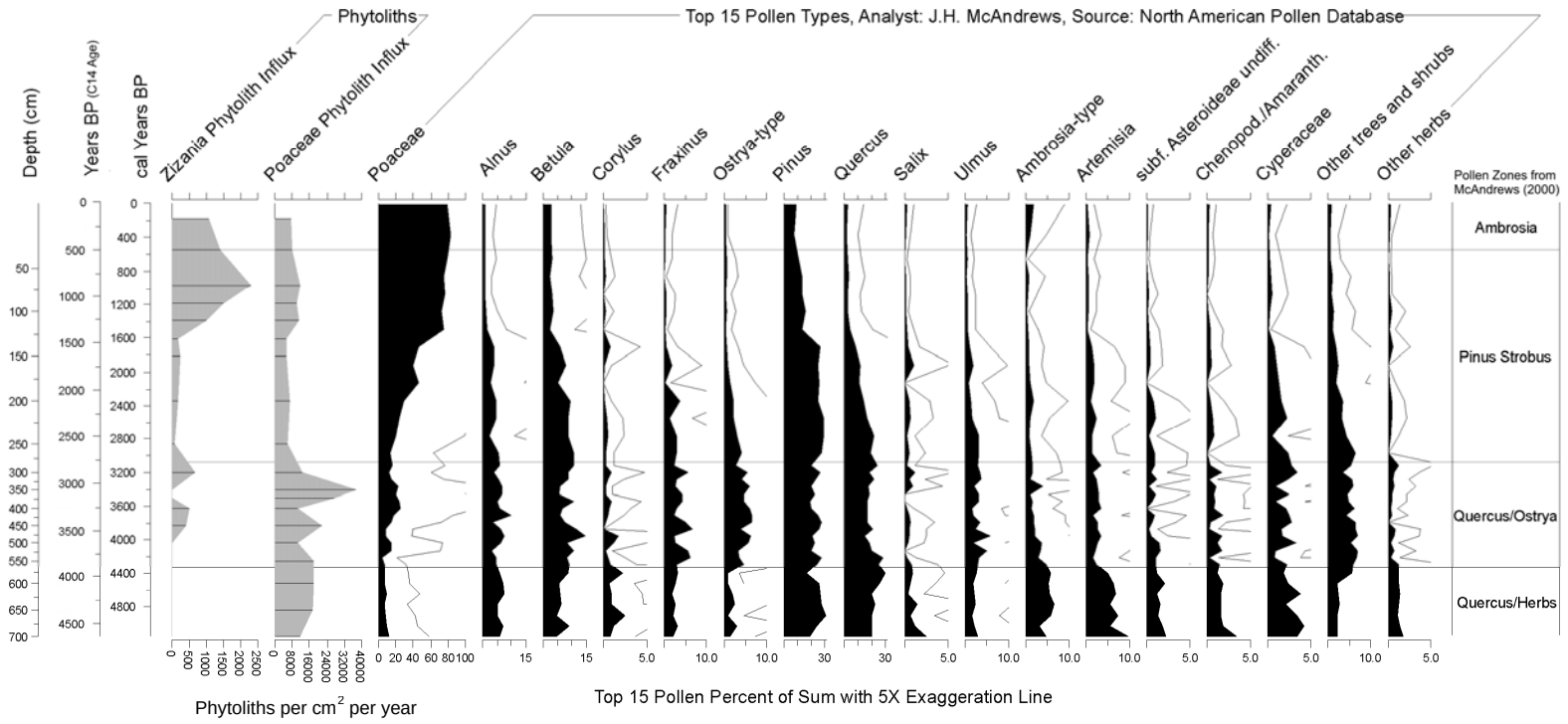


Figure 54

McAndrews Core (OGMC) Phytolith Influx and Pollen Relative Abundance Profile for Lake Ogechie

Phytolith influx data from this study is graphed together with pollen relative abundance data from McAndrews (2000). Top 15 pollen data was downloaded from North American Pollen Database. Calibrated years BP age model (linear interpolation) is the primary y axis, with Depth (cm) as the secondary y axis. For comparison, original uncalibrated $^{14}C$ radiocarbon age model (linear interpolation) is displayed next to the calibrated age model. Years BP = years before 1950 AD. The top-most phytolith sample is from a core depth of 10 cm. Younger levels were no longer available for phytolith analysis. The top-most pollen sample is from a core depth of 1 cm.

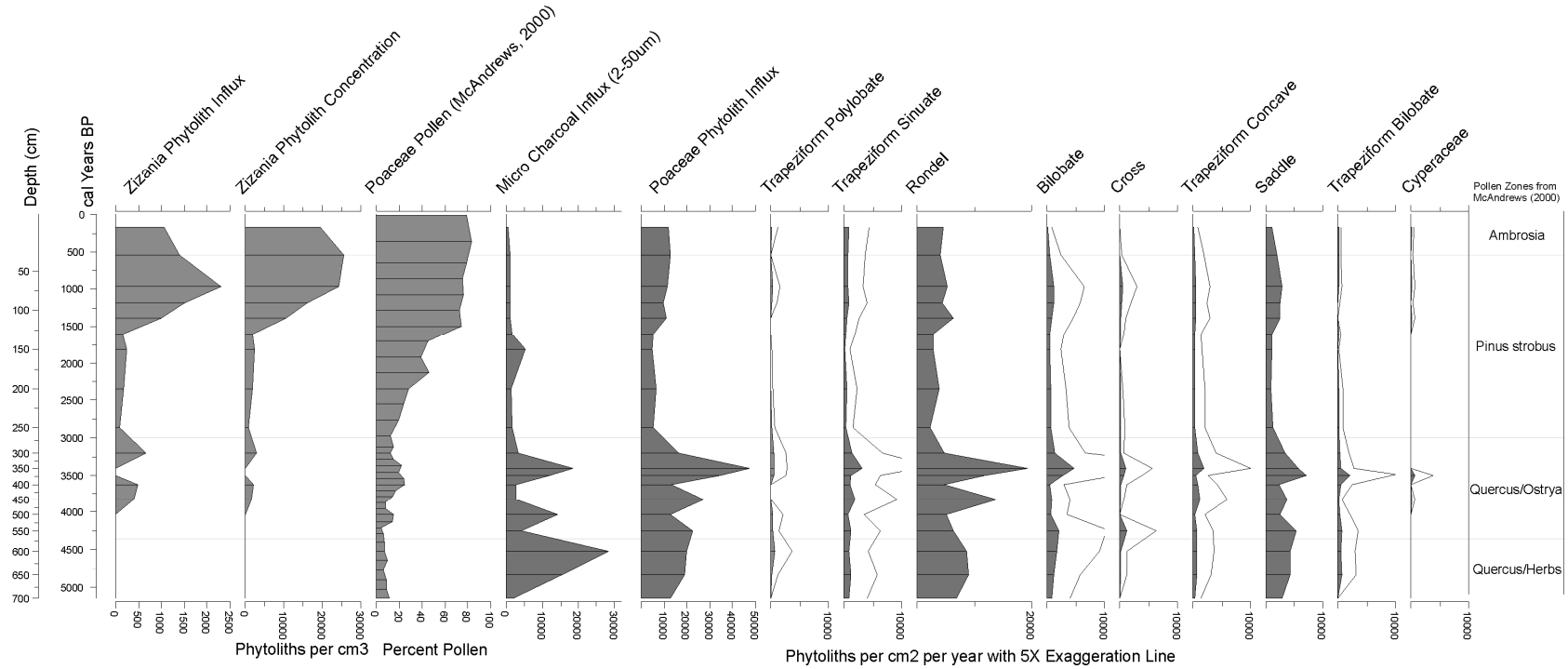


Figure 55

McAndrews' Core (OGMC) *Zizania* and Non-*Zizania* Phytolith Influx Profile for Lake Ogechie

All graphs expressed as phytoliths per cm $^2$ per year except *Zizania* phytolith concentration (phytoliths per cm$^3$) and Poaceae pollen (percent relative abundance of total sum from McAndrews, 2000). Calibrated years BP age model (linear interpolation) is the primary y axis, with Depth (cm) as the secondary y axis. Years BP = years before 1950 AD. The top-most phytolith sample is from a core depth of 10 cm. Younger levels were no longer available for phytolith analysis. The top-most pollen sample is from a core depth of 1 cm.

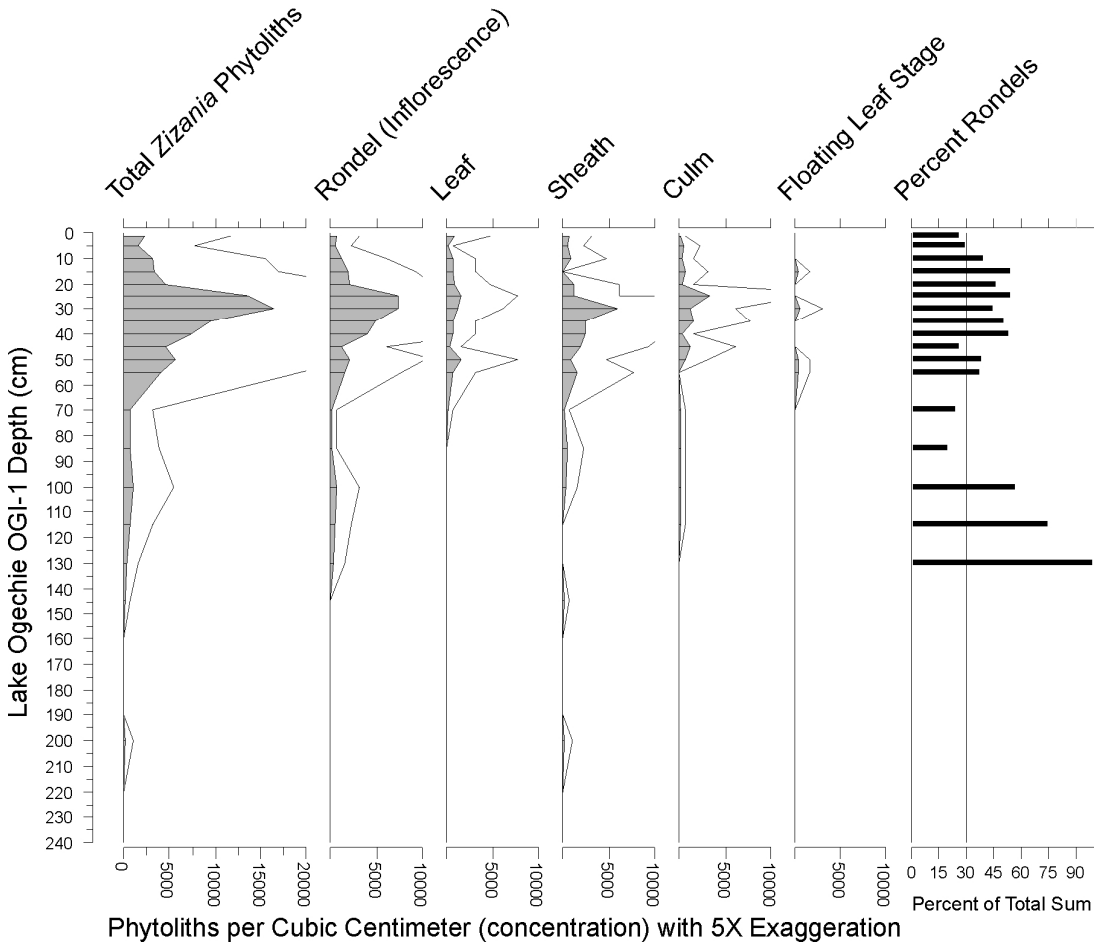


Figure 56

Vibracore (OGI-1) *Zizania* Phytolith Concentration Profile for Lake Ogechie

Since $^{210}$Pb and $^{14}$C dates have not been returned yet for the OGI-1 core, only phytolith concentration is reported here; however, from the McAndrews core (OGMC) data in Figure 54, it appears that wild rice phytolith concentration is well correlated with phytolith influx as long as sedimentation rates are fairly constant. By comparing the *Zizania* spike here with that for OGMC (Figure 55), and considering the time difference in core extraction, it appears that the sedimentation rates for OGI-1 may be approximately ½ of that experienced up at the north end for the McAndrews core.

# DISCUSSION

The results of Chapter 3 indicate that *Zizania palustris* produces 23 locally diagnostic phytolith morphotypes that can be used to determine the presence and abundance of wild rice in modern and paleo lake sediments. The results of Chapter 4 indicate that *Zizania* phytolith deposition is spatially correlated with stand location and density of wild rice; also, the interpretability of *Zizania* phytolith presence and abundance in the paleo lake sediment record should be unambiguous. Based on these findings, it is assumed that wild rice phytolith average yearly influx values derived from concentration values are directly related to actual wild rice population abundance. Thus, an increase in wild rice phytolith influx values at a fixed location (e.g. OGI-1 or OGMC) can be interpreted as being an increase in the abundance of wild rice at or near the core location.

## Recalibration and Old Carbon Error

The OGMC sedimentation rates in Figure 53 were derived from the median probability calibrated age listed in the last column of Table 32 and the median depth of each bulk sediment sample listed in the first column of Table 32. The one exception to this is the top-most sedimentation rate (0.0548 cm $yr^{-1}$) which was calculated from an age of 547 cal years BP. An age of 547 was used instead of 529 to reflect the actual time interval elapsed since core capture (AD 1968). The calibrated age for the 20-40 cm level bulk sediment sample of 529 years BP was based on years before AD 1950. The core was lifted in 1968, so 18 years was added to the age estimate for the

median level of the bulk sediment sample. This correction resulted in a sedimentation rate change of only 0.002 cm $yr^{-1}$; however, given the loose flocculent nature of the sediments, the integrity and accuracy from a 30 cm level sample is questionable anyway. In fact, McAndrews (2000) felt that the original radiocarbon age of 505±30 years BP for the bulk sediment sample from 20-40 cm was too old and suffered from an "old carbon error of 400 years". This type of error is also known as the reservoir effect. This type of dating error can stem from the residence time of organic matter in lake sediments or the incorporation of coal, lignite or carbon-containing shale into younger sediments. Humic acids and humins, isolated for dating from bulk sediment, can easily contain this "older" carbon. The reservoir effect is typically greatest for lakes with low productivity and slow decomposition (cold climate sites), and can add hundreds to even thousands of years to bulk sediment derived ages. From south central Minnesota, Grimm (1983) reports a reservoir effect of 530 years for dates from Wolsfeld Lake and 290 years for dates from French Lake.

The old carbon error is typically subtracted from $^{14}C$ radiocarbon dates before they are calibrated. The correction is usually determined by dating the base of the *Ambrosia* pollen rise, a weedy species that marks deforestation and agricultural practices by European settlement approximately 125 to 150 years ago. Complicating the correction is the fact that there is no evidence that this error is constant throughout a lake core (Grimm, 1983).

McAndrews (2000) assertion of a 400 year old carbon error for Lake Ogechie bulk sediments is based on the 505±30 years BP date for the bulk sediment sample

from the 20-40 cm level, which marks the start of an apparent, although fairy subtle, *Ambrosi*a rise. The main assumption here is that Europeans were the cause of the *Ambrosia* rise. In their study of mortuary populations and archaeological sites from the Lake Mille Lacs and Lake Ogechie area, Aufderheide and others (1994) assert that starting around 1200 years ago (800 AD), exploitation of wild rice caused major lifeway changes for native populations. Further, Lofstrum (1987) argues that exploitation and storage of wild rice for winter use permitted a several-fold increase in population to occur for Minnesota Woodland Period cultures. The start of the subtle *Ambrosia* rise coincides relatively close with a possibly dramatic decrease in wild rice abundance between the 30 and 70 cm levels (Figure 54). Additional OGMC samples between the 30 and 70 cm levels would help determine whether the decrease was a steady decline or a sudden crash. Instead of marking European settlement, the *Ambrosia* rise may actually indicate a change in land use and subsistence patterns for native populations as once dependably high wild rice yield decreased in frequency of occurrence.

Because of the uncertainty and subtlety of the *Ambrosia* rise, nothing was subtracted from the original $^{14}C$ radiocarbon dates before I recalibrated them. McAndrews subtracted 400 years from all of his radiocarbon dates before calibration of the dates that he reported (McAndrews, 2000). With some degree of reservoir effect likely for Lake Ogechie sediments, the Y axis age model for Figures 54 and 55 may be a bit too old. Macrofossil $^{14}C$ and sediment $^{210}Pb$ dates from OGI-1 may help to determine the magnitude of the old carbon reservoir effect for Lake Ogechie.

## Interpreting Micro Carbon Particles

Since they are extracted along with phytoliths from lake sediments and easily identified (Chapter 4, Figure 43 E) during phytolith counts, micro charcoal particles were counted for both OGI-1 and OGMC core samples. Micro charcoal with a diameter of 5 to 50 µm can be transported hundreds of km or more from the source fire; where as, particles 50 µm or larger are likely derived from local sources (Clark and Royall, 1995, 1996; Clark, 1998a, 1988b). All of the charcoal particles examined were in the 5 to 50 µm diameter range. It is possible that larger particles are broken into smaller particles during treatment of lake sediments; also, gravity settling and heavy liquid floatation steps may differentially bias different sized particles. Despite these shortcomings, micro charcoal particles were counted and seem to correlate well on a regional scale with climate and vegetation change. Specific examples will cited in the next section.

## Phytolith and Pollen Correlations for OGMC Core

There is generally good, complementary agreement between phytolith morphotype abundance and pollen zones from the McAndrews core (OGMC). It should be pointed out that the top 15 pollen diagram is based on the percent sum relative abundance for all of the taxa. Typically, local sources of Gramineae pollen such as wetland grasses and sedges are removed from the total sum so that changes in regional vegetation are more easily detected. In Figure 54, all taxa are summed; therefore, when grass pollen, presumably from the local wild rice population, is

relatively high, all other taxa see a relative decrease whether or not they actually do decrease. This is especially pronounced in the *Pinus* graph, where there is a sudden decrease as Poaceae values rise. For ease of display I simply used the top 15 taxa percent sum data downloaded from the North American Pollen Database.

Starting at the bottom of the OGMC core, the *Quercus* (oak)/herb pollen zone reflects an oak savanna biome that dominated the area until around 4,400 cal years BP during a warm and dry hypsithermal climate (Winkler and others, 1985; McAndrews, 2000). As expected, non-*Zizania* Poaceae values and micro carbon particles are at very high levels; suggesting a landscape with open grassy areas sustained by frequent wild fires. Although not quantified, the rondel forms present were more panicoid than *Phragmites*-like. Likewise, saddles were more elongated and not dominated by the square-tabular *Muhlenbergia* saddles. Although not the goal of this thesis, greater separation of general phytolith typologies would yield valuable upland grass vegetation signals to at least the genus level for possibly *Andropogon, Schizachyrium, Festuca, Panicum* and other dominant prairie and woodland grass taxa.

The Quercus/Ostrya (oak/ironwood) pollen zone reflects a deciduous forest dominated by xeric oak but also containing mesic species, thus indicating warm, but with more moisture than the oak savanna zone (McAndrews, 2000). This is the zone where wild rice phytoliths are first observed at approximately 3,800 cal years BP. This is also a time of dramatic fluctuations (disturbance?), with both pollen and phytolith data exhibitng major spikes and crashes. Of particular interest is the major spike in phytoliths and charcoal at the OGMC 350 cm and 370 cm level, concomitant

with a complete disappearance of *Zizania* from the lake sediment record. Based on this information and the presence of large quantities of benthic diatoms, I hypothesize that at approximately 3,500 cal years BP, lake levels were dramatically higher and that Lake Ogechie was basically a bay connected to Lake Mille Lacs for a brief period (around 100 years), thus causing the complete disappearance of wild rice. The dramatic spike in grass phytoliths may not actually be real, but is instead caused by a dramatic increase in sedimentation rates at that time. With no sediment dates from within this zone, there is no way to catch this dramatic sedimentation rate change; therefore, the average sedimentation rate for the entire age interval is used, resulting in an overabundance error for the high water event. Regardless of the cause of the spikes and crashes, this is the pollen zone where *Zizania* becomes established in Lake Ogechie.

The *Pinus strobus* pollen zone began about 3,000 cal years BP and marks the expansion of white pine and regional climatic cooling. Micro charcoal is greatly reduced from the previous zones, and wild rice appears to be present in relatively low numbers for most of the zone. However, between 1,300 and 1600 cal years BP, there was a dramatic increase in wild rice phytolith abundance that continued until around 1000 cal years BP, at which time, wild rice phytolith abundance appears to crash almost as dramatically as it rose (Figures 54 & 55). Concomitant with the dramatic *Zizania* rise is a subtle rise in: trapeziform sinuates (cf. *Calamagrostis* and *Glyceria*); saddles (cf. *Muhlenbergia*); and Cyperaceae phytoliths (Figure 55). This likely indicates a lowering of lake levels and the establishment of the sedge and *Typha*

floating mat around the Lake Ogechie margin. Lowering lake levels may have had an extremely positive effect upon wild rice abundance as well. It should be emphasized that the ultimate shape of the wild rice phytolith curve between the 10 and 70 cm level is highly dependent on the age of the OGMC core bulk sediment sample from the 20 to 40 cm level. If there is an old carbon reservoir effect, then the 505 ±35 radiocarbon years BP age is too old and the calculated sedimentation rate too low, resulting in a greater wild rice phytolith influx value. This would reduce the rate of the wild rice decline after the 70 cm level, or even stabilize it, but overall, there would likely be a net reduction in wild rice phytoliths at the 30 cm and 10 cm levels. If the *Zizania* correlation between OGI-1 (Figure 56) and OGMC (Figures 54 & 55) is as strong as it appears, then the evidence for a dramatic rice and subsequent, dramatic crash is very real. Once dated, OGI-1 will provide valuable old carbon reservoir data and provide a second set of wild rice influx values from the south end of the lake. This will greatly assist in interpreting lake-wide wild rice presence and abundance.

### ~~*Zizania* Rondel Ratios as Indicators of~~ Stand Proximity to Core

*Zizania palustris* produces a wide variety of phytolith morphotypes; many of which are only found in certain parts of the plant (Chapter 3, Table 19). Perhaps the most interesting example of a morphotype that is plant-part diagnostic is the *Zizania* Inflorescence Type 1 rondel from the spikelet lemma and palea (also called the husk or hull). Although contributing just a fraction of the dry weight and phytolith extract weight overall, the inflorescence contributes the highest number of silica short cell

morphotypes. This is likely due to the high concentration of reniform rondels densely arrayed over the entire spikelet surface (Chapter 3, Figure 31 N-P). These Inflorescence Type 1 rondels, with the distinctive deep sinus, are found almost exclusively on the inflorescence spikelet (Figure 31 A-C, E-G); with only 5.2% occurrence in sheath material (Sheath Type 2) and 6.9% occurrence in culm material (Culm Type 4). When total plant contributions are considered, occurrence outside of the inflorescence drops to 1.8% for sheath material and 0.8% for culm material (Chapter 3, Table 19). Overall, inflorescence rondels contribute an impressive 37% of the total silica short cell morphotype contribution; with the locally diagnostic Inflorescence Type 1 contributing 29%.

When wild rice seed is mature within the spikelet (hull), the entire hull with the enclosed seed falls into the surrounding water and quickly sinks to the bottom. Since Inflorescence Type 1 rondels are basically exclusive to the spikelet, they are being directly deposited within or very near to the wild rice stand, and not as likely as other morphotypes to be transferred further from the stand. After seeds are dropped, plants loose vigor and eventually collapse. Either low or high water levels in the Fall can contribute to plants being uprooted and floated away from the stand. Plants that remain rooted and frozen in place during the winter are usually pulled out of the sediment during Spring thaw ice-movements. Thus, since rondel laden material quickly sinks to the bottom of a wild rice stand, and plant material largely devoid of rondels floats away, the ratio of rondel to non-rondel wild rice phytoliths from within-stand sediments is expected to be higher than from sediments outside of the stand. It

was anticipated that this relationship would have been observed in modern sediment transects; however, since inflorescence material degrades and disarticulates its phytoliths faster than other parts of the plant, modern sediments are biased towards rondels. Paleo sediments from the zone of accumulation do not suffer from rondel bias and appear to more closely reflect entire plant morphotype assemblages. Paleo lake sediments from OGI-1 and OGMC may exhibit evidence for rondel ratios being spatially influenced by proximity to stand. Rondel ratios, defined as % of rondels to all other short cell forms for OGI-1 and OGMC are displayed next in Figure 57.

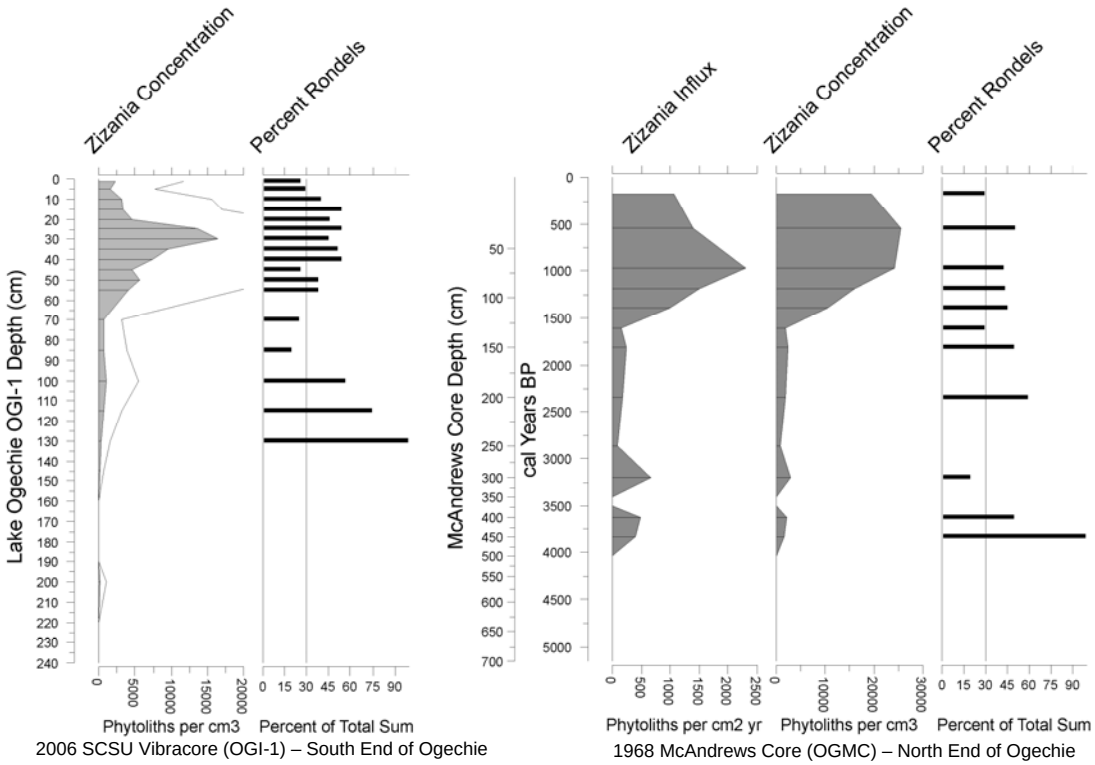


Figure 57

Comparison of *Zizania* Inflorescence Type 1 Rondel Ratios for OGI-1 and OGMC
A reference line at 30 percent rondels has been placed on the graphs for both cores and marks the approximate contribution of *Zizania* Inflorescence Type 1 rondels in an entire *Zizania* plant. The sedimentation rate for OGI-1 is possibly ½ that of OGMC.

In Figure 57, the OGI-1 and OGMC graphs were positioned side-by-side with the wild rice phytolith concentration peaks approximately juxtaposed. Once $^{14}C$ ages are returned for OGI-1, a direct correlation can be made between the two cores based on age estimates.

It's hypothesized that sediments from within wild rice stands may have a minimum rondel ratio between 30 and 45 percent. As distance from the stand increases, the rondel ratio for sediments should decrease. An analysis of a paleo lake sediment core transects across Lake Ogechie would help to determine if such a relationship exists. With four additional Lake Ogechie vibracores already lifted, additional analysis is quite feasible.

## Preservation of Phytoliths in the Paleo Lake Sediment Record

Preservation of grass silica short cell phytoliths from Lake Ogechie paleo lake sediments appear to be good across the entire span of the two cores analyzed. However, lightly silicified short cells do exhibit evidence of dissolution. In particular, lightly silicified *Zizania* Inflorescence Type 1 rondels appear to be vulnerable to dissolution, as evidenced by overall pitting and breakage of some parts of the rondel. This type of degradation was fairly common for *Zizania* Inflorescence Type 1 rondels, but did not interfere with correct identification.

Tabular square saddles associated with *Muhlenbergia* were commonly dissolved all the way through at the very center of the saddle; thus, in outline view, giving the appearance of a square with a circular opening in the center. This was

actually a convenient way to separate tabular saddles from Phragmites-type concave rondels.

It should also be noted that lightly silicified epidermal long cells were rarely encountered, even in modern lake sediments. This is possibly due to rapid dissolution in lake sediments and is the reason that these phytoliths were not emphasized and counted during comparative studies. Epidermal long cell phytoliths do appear to preserve better in dry loess (Blinnikov and others, 2002; Stromberg, 2004).

With diatoms, sponge spicules and many phytoliths showing no signs of dissolution, it is unlikely that various steps in sediment processing, such as treatment with sodium hexametaphosphate and potassium hydroxide, are responsible for the dissolution; however, elongated non-Zizania bilobates were almost always broken at half-shaft. This may be the result of automatic shaker treatment during defloccuation steps (see Chapter 2 and Appendix B).

## Presence of Wild Rice as Interpreted from the Paleo Lake Sediment Record

The presence and abundance of wild rice in paleo sediments from Lake Ogechie is interpreted from the *Zizania* phytolith record illustrated in Figures 54 through 57. Wild rice phytoliths first appear approximately 4,000 cal years BP and a depth of 500 cm in the McAndrews core (OGMC). This appears to correlate with first wild rice evidence at a depth of 220 cm in vibracore sediments (OGI-1). Because the north end of the lake has water depths more suitable for wild rice than the south end, and assuming that the influx of sediments from Lake Mille Lacs has maintained this

north to south depth gradient over time, the north end of Lake Ogechie is likely to have always contained more wild rice that the south end. Absolute abundance values from OGMC (north end) and OGI-1 (south end) support this claim, with OGMC Zizania concentration values consistently higher than OGI-1 values.

Wild rice apparently disappears during a likely high water event at approximately 3,500 cal years BP and then reappears about 100 years later. The wild rice population was likely low at this time and perhaps only occurring up at the north end of the lake and along lake margins towards the south end. This population density seems to have maintained itself until approximately 1,600 cal years BP, when the wild rice population suddenly and dramatically exploded and continued to expand for approximately 400 years, peaking at around 1,000 cal years BP, possibly filling the lake completely with wild rice. The high *Zizania* Inflorescence Type 1 ratios (see percent rondel graphs in Figure 57) at both the north and south ends of Lake Ogechie suggest that wild rice was growing throughout the lake basin. It appears that this massive wild rice population may have been sustained for a few hundred years or more; however, the lack of dated and phytolith sampled sediments throughout the peak *Zizania* zone make pinpointing the exact nature of the eventual wild rice decline only speculative at this point. Nevertheless, the more tightly sampled OGI-1 core, when dated, should be able to better resolve the timing and rate of the apparent wild rice population crash on Lake Ogechie.

# CONCLUSION

North American wild rice (*Zizania* sp.) phytolith bodies from lake sediment samples are virtually unstudied, with apparently not a single peer-reviewed journal article on the subject. By developing a methodology specific to lacustrine wild rice phytolith analysis, the results presented in this chapter are the first to provide direct, unequivocal evidence for both the presence and abundance of a wild rice population from Holocene lake sediments. This methodology can now be used to better understand the spatial and temporal paleodistribution of wild rice across the Great Lakes region and beyond.

This is also one of the first applications of phytolith analysis to interpret lake margin grass vegetation change in North America, and may be the first from northern North America. Phytolith analysis in a paleolimnological context is somewhat rare, especially in North America. Although there have been a few lake core sediment phytolith studies in Central and South America (e.g., Piperno, 1993b), Fearn's (1998) phytolith study of an estuarine sediment core from Louisiana is one of the only peer-reviewed accounts for North America.

This chapter also illustrates the complementary nature of phytolith and pollen analysis from the same core by improving the resolution of Poaceae taxa and by providing a strong local signal, thus improving overall interpretability of the core.

Main Conclusion Points

1) The ambrosia rise at circa 30 cm for the McAndrews core (OGMC) may not be a marker for European settlement as suggested by McAndrews (2000). As a result, 400 years was not subtracted from the radiocarbon ages before calibration.

2) Because some level of "old carbon" may exist in the dated OGMC bulk sediment samples, age models may be slightly too old.

3) Micro carbon particles extracted with phytoliths during processing of sediments may be useful indicators of regional fire regime.

4) Although phytoliths are much more localized than pollen, general changes in the abundance of grass phytolith morphotypes appear to correlate well with changes in the relative abundance of certain pollen taxa for OGMC.

5) *Zizania* phytolith concentration calculations for both OGI-1 and OGMC correlate very well; differences that do exist are likely the result of differing stand densities for the north (OGMC) and south (OGI-1) ends of Lake Ogechie.

6) *Zizania* Inflorescence Type 1 rondels are likely to be much more abundant in sediments within the wild rice stand than in sediments away from the stand; thus, as distance from the stand increases, the ratio of *Zizania* Inflorescence Type 1 rondels to all other *Zizania* morphotypes should decrease.

7) Dissolution of grass silica short cell phytoliths does not appear to be a problem in paleo lake sediments for the vast majority of phytoliths observed.

8) Abundance of wild rice phytoliths in paleo lake sediments appear to be directly related to actual abundance of past wild rice populations.

# Chapter VI

# CONCLUSION

This study has successfully demonstrated that plant opal phytoliths can be used to reconstruct the paleodistribution of North American wild rice (*Zizania* sp. L.) from paleo lake sediments. Further, in developing a new method of wild rice paleoecological analysis, the field of phytolith analysis was advanced by demonstrating that multiplicity and redundancy of basic phytolith typologies in the Poaceae did not limit the establishment of locally diagnostic phytolith morphotypes when three-dimensional observation is used. Phytoliths from lake sediments, in conjunction with pollen derived regional signals, can provide a highly localized vegetation signal.

## Methodology

With the majority of phytolith studies taking place within a terrestrial context, this study developed methodologies useful in the extraction and concentration of the phytolith fraction from highly organic lake sediments. With the help of Dr. Matthew Julius, Department of Biology, St. Cloud State University, a novel method of phytolith quantification was established by using extinct diatoms from a Japanese Pleistocene diatomite deposit as an exotic spike to quantify absolute abundance of phytoliths.

Since fossil diatoms and phytoliths are both comprised of biogenic opal silica, the diatom spike can be subjected to phytolith extraction steps without degradation or dissolution. This technique may allow researchers to better assess recovery and loss of phytoliths during extraction treatments.

Also, the use of a Battarbee evaporation tray to quantify absolute abundance of phytoliths is a novel approach in phytolith analysis. Although a standard technique in limnology, application of this technique is not mentioned in the phytolith literature and may prove useful for other phytolith researchers.

Modern Plant Comparative Collection

Thorough examination of phytolith production in common plant taxa from the study area determined that wild rice produces 23 locally diagnostic phytolith morphotypes that can be used to determine the presence and abundance of wild rice in modern and paleo lake sediments. Possible wild rice confusers can be identified through three dimensional rotation and surface features on the type-face. *Leersia oryzoides*, with its co-tribe Oryzeae affiliation, produces many similar phytolith morphotypes; however, clear distinctions can be made between potential wild rice confusers through three dimensional rotation and surface features. Also of interest is the fact that *Zizania palustris* produces a wide variety of phytolith morphotypes, many of which are only found in certain parts of the plant (e.g. Inflorescence Type 1 from the spikelet).

## Phytolith Deposition in Modern Lake Sediments

The establishment of a modern plant phytolith comparative collection and designation of locally diagnostic *Zizania* phytoliths allowed for examination of phytolith taphonomy in modern lake sediments. Most Poaceae short cell phytoliths appear to be derived locally, with little evidence for inheritance from long distance vectors such as eolian and alluvial processes. Because of anatomical differences in plant debris decay, *Zizania* Inflorescence Type 1 rondels are most abundant; morphotypes from other plant parts are less commonly observed.

Perhaps the most important outcome of the modern study is the determination that *Zizania* phytolith deposition in lakes is spatially correlated with stand location and density of wild rice; Furthermore, lake morphology and bathymetry can have an effect on the exact nature of the depositional pattern. Interpretations derived from lake sediment cores will need to take into consideration the proximity of the core location to the likely paleo wild rice stand location; however, modern phytolith abundance data suggests that even small wild rice populations are detectable when influences on plant debris distribution and prevailing winds and current are considered.

## ~~Phytolith Deposition in Paleo~~ Lake Sediments

Results of the modern deposition study indicate no potential difficulty in the integrity and interpretability of phytolith abundance from paleo lake sediments. Although phytoliths are much more localized than pollen, general changes in the abundance of grass phytolith morphotypes appear to correlate well with changes in the

relative abundance of certain pollen taxa, thus demonstrating the complementary nature of phytolith and pollen analysis. Further, phytolith analysis can better resolve paleoenvironmental conditions inferred from Poaceae ecological requirements than that which can be achieved from pollen analysis alone.

Since two cores from different locations were analyzed for Lake Ogechie, a comparison and contrast in quantification of phytoliths in absolute terms was possible. *Zizania* phytolith concentration calculations for both OGI-1 and OGMC correlate very well; differences that do exist are likely the result of differing stand densities for the north (OGMC) and south (OGI-1) ends of Lake Ogechie. Thus, the abundance of wild rice phytoliths in paleo lake sediment appears to be directly related to actual abundance of past wild rice populations. Further, the paleo sediment data suggests that *Zizania* Inflorescence Type 1 rondels are likely to be much more abundant in sediments within the wild rice stand than in sediments away from the stand; thus, as distance from the stand increases, the ratio of *Zizania* Inflorescence Type 1 rondels to all other *Zizania* morphotypes decreases. This is only a preliminary assertion and additional data are needed to fully resolve the relationship between the rondel ratio and lake core proximity to stand.

~~Further Research~~

The logical next step is the development of a transfer function to calculate the density of wild rice populations in terms of culms per square meter or perhaps some type of seed index, based on phytolith abundance. A lake such as Big Rice Lake in northern St. Louis County, Minnesota may be a very good system to study. Since the

750 hectare lake is of simple morphology and has possibly been completely covered with wild rice for at least 2,000 years ( Valppu and Rapp, 2000; Huber, 2001a), a short ½ meter core with a few $^{210}$Pb dates would make for a good initial transfer function study. Analysis of the other four Lake Ogechie vibracores would be a valuable application of a transfer function since exact acreage of past wild rice is unknown and has apparently fluctuated dramatically in recent times.

An equally imperative task to complete would be an analysis and consultation with the comparative collections of other phytolith analysts to better determine the diagnostic level of the 23 *Zizania palustris* morphotypes used in this study. Related to this would be a morphological and morphometric analysis of phytolith production in all species of *Zizania* to determine any species-specific phytolith traits. Such a study would be useful in understanding the antiquity and speciation of *Zizania* in North America and Asia. This would not only be a value to the field of phytogeography, but also to anthropology; specifically, the study of possible anthropogenic influences on the dispersal and speciation of *Zizania*.

# REFERENCES

# REFERENCES


Arriagada, J.E., 2006. *Plant communities of Lake Ogechie, Mille Lacs Co., MN*. Unpublished report. Saint Cloud State University, St. Cloud MN. 7 p.

Anderson, H., 1998. *A summary of the surficial geology of Mille Lacs Kathio State Park, MN*. Unpublished report. Department of Natural Resources Minerals Division, St. Paul, MN.

Ashworth, A.C., Schwert, D.P., Watts, W.A., and Wright, H.E. Jr., 1981. Plant and insect fossils at Norwood in south-central Minnesota: a record of late glacial succession. *Quaternary Research 16*, 66-79.

Aufderheide, A.C., Johnson, E., Langsjoen, O., 1994. Health, demography, and archaeology of Mille Lacs Native American mortuary populations. *Plains Anthropology 39*, 249-375.

Avnimelech, Y., Ritvo, G., Meijer, L.E., Kochba, M., 2001.Water content, organic carbon and dry bulk density in flooded sediments. *Aquacultural Engineering 25*, 25-33.

Battarbee, R.W., 1973. A new method for the estimation of absolute microfossil numbers, with reference especially to diatoms. *Limnology and Oceanography 18*(4), 647-653.

Birks, H.J.B., 1976. Late-Wisconsinian vegetational history at Wolf Creek, central Minnesota. *Ecological Monographs 46*, 395-429.

Birks, H.J.B., Birks, H.H., 2000. Future uses of pollen analysis must include plant macrofossils. *Journal of Biogeography 27*, 31-35.

Blackman, E., 1971. Opaline silica bodies in the range grasses of southern Alberta. *Canadian Journal of Botany 49*, 769-781.

Blais, J.M., Kalff, J., 1995. The influence of lake morphometry on sediment focusing. *Limnology and Oceanography 40*(3), 582-588.

Blinnikov, M.S., 2005. Phytoliths in plants and soils of the interior Pacific Northwest, USA. *Review of Palaeobotany and Palynology 135*, 71-98

Blinnikov, M.S., Busacca, A., Whitlock, C., 2001. A new 100,000-yr. record from the Columbia Basin, Washington, USA. In: Meunier, J.D. & Colin, F. (Eds.), *Phytoliths: Applications in earth sciences and human history*. A. A. Balkema, Rotterdam, the Netherlands.

Blinnikov, M.S., Busacca, A., Whitlock, C., 2002. Reconstruction of the late Pleistocene grassland of the Columbia basin, Washington, USA, based on phytolith records in loess. *Palaeogeography, Palaeoclimatology, Palaeoecology 177*, 77-101.

Bois Forte Tribal Council, 2001. *Wild rice management at Bois Forte Indian Reservation: History and current perspectives*. Report, Department of Natural Resources, Bois Forte Tribal Council, Nett Lake, MN.

Bombin, M., 1984. *On phytoliths, late quaternary ecology of Beringia, and information evolutionary theory*. Ph.D. Thesis, University of Alberta, Edmonton, Canada.

Bozarth, S.R., 1993. Biosilicate assemblages of boreal forests and aspen parklands. In: Pearsall, D.M., Piperno, D.R. (Eds.), *Current Research in Phytolith Analysis: Applications in Archaeology and Paleoecology*. MASCA Research Papers in Science and Archaeology, University of Pennsylvania, Philadelphia, PA, pp. 95-105.

Brown, D.A., 1984. Prospects and limits of a phytolith key for grasses in the Central United States. *Journal of Archaeological Science 11*, 345-368.

Carter, J.A., 2002. Phytolith analysis and paleoenvironmental reconstruction from Lake Poukawa Core, Hawkes Bay, New Zealand. *Global and Planetary Change 33*, 257-267.

Clark, J.S., 1988a. Particle motion and the theory of charcoal analysis: source area, transport, deposition, and sampling. *Quaternary Research 30*, 67-80.

Clark, J.S., 1988b. Stratigraphic charcoal analysis on petrographic thin sections: Applications to fire history in northwestern Minnesota. *Quaternary Research 30*, 81-91.

Clark, J.S., 1990. Fire and climate change during the last 750 yr in northwestern Minnesota. *Ecological Monographs 60*(2), 135-159.

Clark, J.S., Royall, P.D., 1995. Particle-size evidence for source areas of charcoal accumulation in Late Holocene sediments of eastern North American lakes. *Quaternary Research 43*, 80-89.

Clark, J.S., Royall, P.D., 1996. Local and regional sediment charcoal evidence for fire regimes in presettlement north-eastern North America. *Journal of Ecology 84*, 365-382.

Clayton, W.D., Renvoize, S.A., 1986. *Genera Graminium: Grasses of the World*. Her Majesty's Stationary Office, London.

Cushing, E.J., 1967. Late-Wisconsin pollen stratigraphy and the glacial sequence in Minnesota. In: Cushing, E.J., and Wright, H.E., Jr., (Eds.), *Quaternary Paleoecology*, Yale University Press, New Haven, pp. 59-88.

Darbyshire, S.J., Aiken, S.G., 1986. *Zizania aquatica* var. *brevis* (Poaceae): A 1983 distribution survey and a scanning electron microscope study of epidermal features. *Annual Review of Ecology and Systematics 113*, 355-360.

Davidson, D., 2003. *The use of phytolith analysis to detect wild rice (Zizania aquatica) in fossil sediment cores at Cootes Paradise in southern Ontario* [undergraduate thesis]. Department of Geography, University of Toronto. 63 p.

Davis, M.B., 1973. Redeposition of pollen grains in lake sediment. Limnology and *Oceanography 18*(1), 44-52.

Dean, W.E. Jr., 1974. Determination of carbonate and organic matter in calcareous sediments and sedimentary rocks by loss on ignition: Comparison with other methods. J*ournal of Sedimentary Petrology 44*(1), 242-248.

Dore, W.G., 1969. *Wild rice*. Canada, Department of Agriculture, Research Branch, Publication 1393. Information Canada, Ottawa. 84 p.

Downing, J.A, Rath, L.C., 1988. Spatial patchiness in the lacustrine sedimentary environment. *Limnology and Oceanography 33*(3), 447-458.

Duvall, M.R., Biesboer, D.D., 1988. Anatomical distinctions between the pistillate spiklets of the species of wild rice (*Zizania*, Poaceae). *American Journal of Botany 75*(1), 157-159.

Duvall, M.R., Peterson, P.M., Terrell, E.E., Christensen, A.H., 1993. Phylogeny of North American Oryzoid grasses as construed from maps of plastid DNA restriction sites. *American Journal of Botany 80*(1), 83-88.

Farnham, R.S., McAndrews, J.H., Wright, H.E. Jr., 1964. A late-Wisconsin buried soil near Aitkin, Minnesota, and its paleobotanical setting. *American Journal of Science 262,* 393-412.

Fassett, N.C., 1924. A study of the genus *Zizania*. *Rhodora 26*, 153-160.

Fearn, M.L., 1998. Phytoliths in sediment as indicators of grass pollen source. *Review of Palaeobotany and Palynology 103,* 75-81.

Ford, R.I., Brose, D.S., 1975. Prehistoric wild rice from the Dunn Farm Site, Leelanau County, Michigan. *Wisconsin Archaeologist 56*(1), 9-15.

Fredlund, G.G., Tieszen, L.T., 1994. Modern phytolith assemblages from the North American Great Plains. *Journal of Biogeography 21,* 321-335.

Geisen, Amy., 2004. Minnesota Department of Natural Resources, Shallow Lakes Program. Personal Communication.

Gibbon, G., 1976. The old Shakopee bridge site: A late Woodland ricing site on Shakopee Lake, Mille Lacs County, Minnesota. *Minnesota Archaeologist 35*(2), 2-56.

Glew, J.R., 1991. Miniature gravity corer for recovering short sediment cores. *Journal of Paleolimnology 5,* 285-287.

[GPWG] (Grass Phylogeny Working Group), 2001. Phylogeny and subfamilial classification of the grasses (Poaceae). *Annals of the Missouri Botanical Gardens 88,* 373-457.

Grimm, E.C., 1983. Chronology and dynamics of vegitation change in the prairie-woodland region of southern Minnesota, U.S.A. *New Phytologist 93*(2), 311-350.

Grimm, E.C., 2001. Trends and palaeoecological problems in the vegetation and climate history of the northern Great Plains, U.S.A. *Proceedings of the Royal Irish Academy 101B*(1-2), 47-64.

Hart, J.P., Thompson, R.G., Brumbach, H.J., 2003. Phytolith evidence for early maize (*Zea Mays*) in the northern Finger Lakes region of New York. *American Antiquity 68*(4), 619-640.

Hawthorn, W.R., Stewart, J.M., 1970. Epicuticular wax forms on leaf surfaces of *Zizania aquatica*. *Canadian Journal of Botany 48*(2), 201-205.

Heiri, O., Lotter, A.E., Lemcke, G., 2001. Loss on ignition as a method for estimating organic and carbonate content in sediments: reproducibility and comparability of results. *Journal of Paleolimnology 25*, 101-110.

Hodson, M.J., Sangster, A.G., Wynn Parry, D., 1985. An ultrastructural study on the developmental phases and silicification of the glumes of *Phalaris canariensis*. *Annals of Botany 55*, 649-665.

Horne, F., Kahn, A.B., 1997. Phylogeny of North American wild rice, a theory. *Southwestern Naturalist 42*(4), 423-434.

Hsu, J., 1983. Late Cretaceous and Cenozoic vegetation in China, emphasizing their connections with North America. *Annals of the Missouri Botanical Gardens 70*, 490-508.

Huber, J.K., 1996. A postglacial pollen and nonsiliceous algae record from Gegoka Lake, Lake County, Minnesota. *Journal of Paleolimnology 16*, 23-35.

Huber, J.K., 2001a. *Palynological investigations related to archaeological sites and the expansion of wild rice (Zizania aquatica L.) in northeast Minnesota*. Ph.D. Thesis, Univ. of Minnesota.

Huber, J.K., 2001b. *A palynological investigation in the Superior National Forest, northeast Minnesota: Results of a palaeoecological study of Shannon Lake, St. Louis Co., MN*: Duluth, Archaeometry Laboratory, University of Minnesota-Duluth. Report submitted to Heritage Resources, Superior National Forest, Duluth Minnesota, Archaometry Report Number 01-18.

Huber, J.K., 2006. Poaceae pollen grain size frequency data infers the probable presence of wild rice in northeast Minnesota during the Late-Paleoindian period. *Current Research in the Pleistocene 23*, In press.

Janssen, C.R., 1966. Recent pollen spectra from the deciduous and coniferous-deciduous forests of northeastern Minnesota: A study in pollen dispersal. *Ecology 47*(5),804-825.

Jenks, A.E., 1900. The wild rice gatherers of the Upper Lakes: A study in American primitive economics. In: *Nineteenth Annual Report of the Bureau of American Ethnology, 1897-98, part 2*. Washington, D.C.: GPO, 1900.

Johnson, E., 1969a. Archaeological evidence for the utilization of wild rice. *Science 163*(3864), 276-277.

Johnson, E., 1969b. Preliminary notes on the prehistoric use of wild rice. *Minnesota Archaeologist 30*(2), 31-43.

Juggins, S., 2006. C2 Version 1.4.3 (Build 1) <http://www.campus.ncl.ac.uk/staff/Stephen.Juggins/software/c2home.htm> Accessed 2006 May 13.

Julius, M.L., Curtin, M., Tanaka, H., 2006. *Stephanodiscus kusuensis*, sp. nov a new Pleistocene diatom from southern Japan. *Phycological Research 54,* 294-301.

Lee, G-A., Davis, A.M., Smith, D.G., McAndrews, J.H., 2004. Identifying fossil wild rice (*Zizania*) pollen from Cootes Paradise, Ontario: a new approach using scanning electron microscopy. *Journal of Archaeological Science 31*, 411-412.

Lentfer, C.J., Cotter, M.M., Boyd, W.E., 1999. An assessment of techniques for the deflocculation and removal of clays from sediments used in phytolith analysis. *Journal of Archaeological Science 26*, 31-44.

Lentfer, C.J., Boyd, W.E., 2003. Particle settling times for gravity sedimentation and centrifugation: a practical guide for palynologists. *Journal of Archaeological Science 30*, 149-168.

[LMIC] Land Management Information Center, Minnesota Department of Administration, Office of Geographic and Demographic Analysis. NAIP 2003-04 Air Photo County Mosaics. 2006. <http://www.lmic.state.mn.us/chouse/naip03mrsid.html> Accessed 2007 Mar 1.

Lofstrom, T., 1987. The rise of wild rice exploitation and its implications for population size and social organization in Minnesota Woodland Period cultures. *Minnesota Archaeologist 46*, 3-16.

Lu, H.Y., Liu, K.B., 2003a. Morphological variations of lobate phytoliths from grasses in China and the south-eastern United States. *Diversity and Distributions 9*, 73-87.

Lu, H.Y., Liu, K.B., 2003b. Phytoliths of common grasses in the coastal environments of southeastern USA. Estuarine, *Coastal and Shelf Science 58*, 587-600.

Lu, H.Y., Wu, N.Q., Yang, X.D., Jiang, H., Liu, K.B., Liu, T.S., 2006. Phytoliths as quantitative indicators for the reconstruction of past environmental conditions in China I: phytolith-based transfer functions. *Quaternary Science Reviews 25*, 945-959.

Madella, M., Alexandre, A., Ball, T., 2005. International code for phytolith nomenclature 1.0. *Annals of Botany 96*, 253-260.

Maki, J.B., 1970. *A survey of certain limnological aspects of the Rum River* [Master's Thesis]. Saint Cloud State University, MN.

Mehra, P.N., Sharma, O.P., 1965. Epidermal silica cells in the *Cyperaceae*. *Botanical Gazette 126*(1), 53-58.

McAndrews, J.H., 1969. Paleobotany of a wild rice lake in Minnesota. *Canadian Journal of Botany 47*, 1671-1679.

McAndrews, J.H., 2000. Wild rice and upland vegetation history near Lake Mille Lacs, Minnesota. In: *The Lake Onamia - Trunk Highway 169 Data Recovery Project, Mille Lacs County, Minnesota*, by D. Mather and E. Abel. Loucks & Associates, Inc., Maple Grove. Report prepared for the Department of Transportation, St. Paul.

McAndrews, J.H., 2005. Geese fouled Crawford Lake 700 years ago: Iroquoian cornfields led to guanotrophy. *Newsletter of the Ontario Field Ornithologists 23*(2), 5.

Metcalfe, C.R., 1960. *Anatomy of the monocotyledons: I. Gramineae*. Clarendon Press of Oxford University Press, London.

[MGS] Minnesota Geological Survey, 1997. *Minnesota at a glance: Quaternary glacial geology*. Minnesota Geological Survey, St. Paul, MN.

[MNDNR] Minnesota Department of Natural Resources Shallow Lakes Program. 2007. Wild rice management. <http://www.dnr.state.mn.us/wildlife/shallowlakes/wildrice.html> Accessed 2007 Mar 1.

[MNDNR Data Deli] Minnesota Department of Natural Resources Data Deli. 2007 Mar 1 MNDNR Data Deli homepage. <http://deli.dnr.state.mn.us/index.html> Accessed 2007 Mar 1.

Moffat, C.R., 2000. New data on the late woodland use of wild rice in northern Wisconsin. *Midcontinental Journal of Archaeology 25*(1), 49-82.

Mulholland, S.C., 1989. Phytolith shape frequencies in North Dakota grasses: A comparison to general patterns. *Journal of Archaeological Science 16*, 489-511.

Mulholland, S.C., 2000. The Arrowhead since the glaciers: the prehistory of northeastern Minnesota. *Minnesota Archaeologist 59*, 1-10.

Mulholland, S.C., Mulholland, S.L., Peters, G.R., Huber, J.K., Mooers, H.D., 1997. Paleo-Indian occupations in northeastern Minnesota: how early? *North American Archaeologist 18*(4), 371-400.

Mulholland, S.C., Rapp, G. Jr., 1992. A morphological classification of grass silica-bodies. In: Rapp, G., Mulholland, S.C. (Eds.), *Phytolith Systematics*. Plenum Press, New York.

[NRCS] Soil Survey Staff, Natural Resources Conservation Service, United States Department of Agriculture. U.S. General Soil Map (STATSGO) for State. 2006 Jul 18. <http://soildatamart.nrcs.usda.gov> Accessed 2007 Mar 1.

Ollendorf, A.L., Mulholland, S.C., Rapp, G. Jr., 1987. Phytoliths from some Israeli sedges. *Israel Journal of Botany 36*, 125-132.

Ollendorf, A.L., Mulholland, S.C., Rapp, G. Jr., 1988. Phytolith analysis as a means of plant identification: *Arundo donax* and *Phragmites communis*. *Annals of Botany 61*, 209-214.

Orson, R.A., Simpson, R.L., Good, R.E., 1992. The paleoecological development of a late Holocene, tidal freshwater marsh of the Upper Delaware River Estuary. *Estuaries 15*(2), 130-146.

Parr, J.F., Dolic, V., Lancaster, G., Boyd, W.E., 2001a. A microwave digestion method for the extraction of phytoliths from herbarium specimens. *Review of Palaeobotany and Palynology 116*, 203-212.

Parr, J.F., Lentfer, C.J., Boyd, W.E., 2001b. A comparative analysis of wet and dry ashing techniques for the extraction of phytoliths from plant material. *Journal of Archaeological Science 28*, 875-886.

Pastor, J., Walker, R., 2006. Delays in nutrient cycling and plant population oscillations. *Oikos 112*(3), 698-705.

Pearsall, D.M., 2000. *Paleoethnobotany: A Handbook of Procedures*. Academic Press, San Diego, CA.

Pearsall, D.M., Piperno, D.R., Dinan, E.H., Umlauf, M., Zhao, Z., Benfer, R.A., 1995. Distinguishing rice (*Oryza sativa* Poaceae) from wild *Oryza* species throuth phytolith analysis: Results of preliminary research. *Economic Botany 49*(2), 183-196.

Piepgras, Steve, 2004. *Wild rice lake survey, 1999 and 2001*. Minnesota Department of Natural Resources Shallow Lakes Program (unpublished data). St Paul, MN.

Piperno, D.L., 1993a. The Nature and Status of Phytolith Analysis. In: Pearsall, D.M., and Piperno, D.L.,(Eds.), *Current research in phytolith analysis: Applications in archaeology and paleoecology*. MASCA Research Papers in Science and Archaeology, Vol. 10. MASCA, University of Pennsylvania, Philadelphia, PA, pp. 9-18.

Piperno, D.L., 1993b. Phytolith and charcoal records from deep lake cores in the American tropics. In: Pearsall, D.M., and Piperno, D.R., (Eds.), *Current research in phytolith analysis: Applications in archaeology and paleoecology*. MASCA Research Papers in Science and Archaeology, Vol. 10. MASCA, University of Pennsylvania, Philadelphia, PA, pp. 58-71.

Piperno, D.L., 2006. *Phytoliths: a comprehensive guide for archaeologists and paleoecologists*. AltaMira Press, Lanham, MD.

Piperno, D.L., Jones, J.G., 2003. Paleoecological and archaeological implications of a Late Pleistocene/Early Holocene record of vegetation and climate from the Pacific coastal plain of Panama. *Quaternary Research 59*, 79-87.

Piperno, D.L., Pearsall, D.M.,1998. The silica bodies of tropical American grasses: Morphology, Taxonomy, and implications for grass systematics and fossil phytolith identification. *Smithsonian Contributions to Botany 85*, 40 p.

Piperno, D.L., Sues, H.-D., 2005. Dinosaurs dined on grass. *Science 310*, 1126-1128.

Prasad, V., Stromberg, A.E., Alimohammadian, H., Sahni, A., 2005. Dinosaur coprolites and the early evolution of grasses and grazers. *Science 310*, 1177-1180.

Qian, H., 1999. Floristic analysis of vascular plant genera of North America north of Mexico: characteristics of phytogeography. *Journal of Biogeography 26*, 1307-1321.

Rajnovich, G., 1984. A study of possible prehistoric wild rice gathering on Lake of the Woods, Ontario. *North American Archaeologist. 5*(3), 197-215.

Reimer, P. J., Baillie, M. G. L., Bard, E., Bayliss, A., Beck, J. W., Bertrand, C. J. H., and others, 2004. IntCal04 Terrestrial radiocarbon age calibration, 26 - 0 ka BP. *Radiocarbon 46*, 1029-1058.

Rogosin, A., 1954. *An ecological history of wild rice*. University of Minnesota Department of Botany Research Report, reproduced by Minnesota Department of Conservation, Division of Game and Fish, St. Paul, 1-29.

Rothaus, R.M., 2000. *The Ogechie Dam in Mille Lacs Kathio State Park*. Unpublished Report, Saint Cloud State University, Saint Cloud, MN.

Schuyler, A.E., 1971. Scanning electron microscopy of achene epidermis in species of *Scirpus* (Cyperaceae) and related genera. *Proceedings of the Academy of Natural Sciences of Philadelphia 123*(2), 29-52.

Serpa, K., Phil, M., 2005. Cultigens of the American Northeast: A phytolith study. *Phytolitharien 17*(3), 1-9.

Smith, J.B., Clausner, J.E., 1993. *An inexpensive method for vibracoring sands and fine-grained sediments in shallow water*. Dredging Research Technical Notes, DRP-2-06, April, US Army Engineer Waterways Experiment Station, Vicksburg, MS.

Stover, E.L., 1928. The roots of wild rice, *Zizania aquatica*. *Ohio Journal of Science 28*(1), 43-49.

Stromberg, C.A.E., 2004. Using phytolith assemblages to reconstruct the origin and spread of grass-dominated habitats in the great plains of North America during the late Eocene to early Miocene. *Palaeogeography, Palaeoclimatology, Palaeoecology 207*, 239-275.

Stromberg, C.A.E., 2005. Decoupled taxonomic radiation and ecological expansion of open-habitat grasses in the Cenozoic of North America. *Proceedings of the National Academy of Sciences U.S.A. 102*(34): 11980-11984.

Stuiver, M., Reimer, P. J., 1993. Extended 14C database and revised CALIB radiocarbon calibration program. *Radiocarbon 35*, 215-230.

Stuiver, M., Reimer, P. J., Reimer, R. W., 2005. CALIB 5.0.2. <http://calib.qub.ac.uk/calib/calib.html> Accessed 2007 April 8.

Teller, J.T., 1987. Proglacial lakes and the southern margin of the Laurentide ice sheet. In: Ruddiman, W.F., Wright, H.E., (Eds.), *Geology of North America: North American and adjacent oceans during the last deglaciation*. Geological Society of America, Boulder, K-3, pp. 39-69.

Terrell, E.E., Emery, W.H.P., Beaty, H.E., 1978. Observations on *Zizania texana* (Texas wildrice), an endangered species. *Bulletin of the Torrey Botanical Club 105*(1), 50-57.

Terrell, E.E., Peterson, P.M., Reveal, J.L., Duvall, M.R., 1997. Taxonomy of North American species of *Zizania* (Poaceae). *SIDA Contributions to Botany 17*(3), 533-549.

Terrell, E.E., Robinson, H., 1974. Luziolinae, a new subtribe of oryzoid grasses. *Bulletin of the Torrey Botanical Club 101*(5), 235-245.

Terrell, E.E., Wergin, W.P., 1981. Epidermal features and silica deposition in lemmas and awns of *Zizania* (Gramineae). *American Journal of Botany 68*(5), 697-707.

Terrell, E.E., Wergin, W.P., Renvoize, S.A., 1983. Epidermal features of spikelets in *Leersia* (Poaceae). *Bulletin of the Torrey Botanical Club 110*(4), 423-434.

Thompson, R.G., Kluth, R.A., Kluth, D.W., 1994. Tracing the use of Brainerd ware through opal phytolith analysis of food residues. *Minnesota Archaeologist 53*, 86-95.

Valppu, S.H., Rapp, G., 2000. Paleoethnobotanical context and dating of the laurel use of wild rice: the Big Rice site. *Minnesota Archaeologist. 59*, 81-87.

Vennum, T. Jr., 1998. *Wild rice and the Ojibway people*. Minnesota Historical Society Press, St. Paul. 357 p.

Wang, S.S., Kim, K., Hess, W.M., 1998. Variation of silica bodies in leaf epidermal long cells within and among seventeen species of Oryza (Poaceae).*American Journal Botany 85*(4), 461-466.

Watson, L., Dallwitz, M.J., 1992. *The Grass Genera of the World*. CAB International, Wallingford, UK.

Warner, B.G., Karrow, P.F., Morgan, A.V., Morgan, A., 1987. Plant and insect fossils from Nipissing sediments along the Goulais River, southeastern Lake Superior. C*anadian Journal of Earth Sciences 24*, 1526-1536.

Weatherwax, P., 1929. The morphology of the spiklets of six genera of Oryzeae. *American Journal of Botany 16*(7), 547-555.

White, B.M., 2000. The regional context of the removal order of 1850. In: McClurken, J.M., (Eds.), *Fish in the lakes, wild rice, and game in abundance*. Michigan State University Press 282-289.

Winkler, M.G., Swain, A.M., Kutzbach, J.E., 1985. Middle Holocene dry period in the Northern Midwestern United States: lake levels and pollen stratigraphy. *Quaternary Research 25*, 235-250.

Wrenn, J.H., Tedford, R.A., 2004. *Phytolith atlas, Catahoula Lake, Louisiana*. Prepared for the Assistant Vice Chancellor, Office of Research & Graduate Studies as part of the outcomes for 2003-2004 Faculty Research Grant No. 115-40-9101. 79 p.

Wright, H.E. Jr., 1990. An improved Hongve sampler for surface sediments. *Journal of Paleolimnology 4*, 91-91.

Wright, H.E. Jr., Stefanova, I., Tian, J., Brown, T.E., Hu, F.S., 2004. A cronological framwork for the Holocene vegetational history of central Minnesota: the Steel Lake pollen record. *Quaternary Science Reviews 23*, 611-626.

Yarnell, R.A., 1964. Aboriginal relationships between culture and plant life in the upper Great Lakes region. *University of Michigan, Museum of Anthropology, Anthropological Papers No. 23*. Ann Arbor, MI. 218 p.

Yourd, W.J., 1988. *The antiquity and distribution of wild rice in Lake Marquette, north-central Minnesota: implications for regional archaeology and the natural history of wild rice.* M.S. Plan B Thesis, University of Minnesota, Minneapolis, Minnesota.

Yu, Z., Wright, H.E. Jr., 2001. Response of interior North America to abrupt climate oscillations in the North Atlantic region during the last deglaciation. *Earth-Science Reviews 52*, 333-369.

Zhao, Z., Pearsall, D.M., 1998. Experiments for improving phytolith extraction from soils. *Journal Archaeological Science 25*, 587-598.

Zhao, Z., Pearsall, D.M., Benfer, R.A., Piperno, D.R., 1998. Distinguishing rice (*Oryza sativa* Poaceae) from wild *Oryza* species through phytolith analysis, II: finalized method. *Economic Botany 52*(2), 134-145.

Zhao, Z., Piperno, D.R., 2000. Late Pleistocene/Holocene environments in the Middle Yangtze River Valley, China and rice (*Oryza sativa* L.) domestication: The phytolith evidence. *Geoarchaeology 15*(2), 203-222.

# APPENDICES

# APPENDIX A

## List of Comparative Plant Phytolith Samples

List of Comparative Plant Phytolith Samples

| Sample | Plant or Soil Sample Processed | Plant Part Processed | Provenience | Wt (g) |
|---|---|---|---|---|
| 001 | *Zizania palustris* var. *palustris* | seed | Shakopee Lake, Mille Lacs Co. MN | 0.1129 |
| 002 | *Zizania palustris* var. *palustris* | seed | Shakopee Lake, Mille Lacs Co. MN | 0.1013 |
| 003 | *Zizania palustris* var. *palustris* | primary & advent. root | Shakopee Lake, Mille Lacs Co. MN | 1.0000 |
| 004 | *Zizania palustris* var. *palustris* | leaf, entire | Shakopee Lake, Mille Lacs Co. MN | 1.0000 |
| 005 | *Zizania palustris* var. *palustris* | rachis | Shakopee Lake, Mille Lacs Co. MN | 0.1036 |
| 006 | *Zizania palustris* var. *palustris* | pistillate lemma & awn | Shakopee Lake, Mille Lacs Co. MN | 0.1013 |
| 007 | *Zizania palustris* var. *palustris* | pistillate awn | Shakopee Lake, Mille Lacs Co. MN | 0.0271 |
| 008 | *Zizania palustris* var. *palustris* | awn, lower section | Shakopee Lake, Mille Lacs Co. MN | 0.0300 |
| 009 | *Zizania palustris* var. *palustris* | leaf midrib | Shakopee Lake, Mille Lacs Co. MN | 0.1296 |
| 010 | *Zizania palustris* var. *palustris* | leaf blade | Shakopee Lake, Mille Lacs Co. MN | 0.1669 |
| 011 | *Zizania palustris* var. *palustris* | adventitious root | Shakopee Lake, Mille Lacs Co. MN | 0.0952 |
| 012 | *Zizania palustris* var. *palustris* | primary root | Shakopee Lake, Mille Lacs Co. MN | 0.1424 |
| 013 | *Zizania palustris* var. *palustris* | upper leaf sheath | Shakopee Lake, Mille Lacs Co. MN | 0.1040 |
| 014 | *Zizania palustris* var. *palustris* | lower leaf sheath | Shakopee Lake, Mille Lacs Co. MN | 0.1292 |
| 015 | *Zizania palustris* var. *palustris* | upper culm | Shakopee Lake, Mille Lacs Co. MN | 0.1261 |
| 016 | *Zizania palustris* var. *palustris* | lower culm | Shakopee Lake, Mille Lacs Co. MN | 0.1648 |
| 017 | *Zizania palustris* var. *palustris* | pistillate lemma | Shakopee Lake, Mille Lacs Co. MN | 0.0914 |
| 018 | *Zizania palustris* var. *palustris* | seed ($HNO_3$ digested) | Shakopee Lake, Mille Lacs Co. MN | N/A |
| 019 | *Leersia oryzoides* | lemma | Boot Lake, BWCAW, St. Louis Co. MN | 0.0726 |
| 020 | *Leersia oryzoides* | rachis | Boot Lake, BWCAW, St. Louis Co. MN | 0.0280 |
| 021 | *Leersia oryzoides* | culm | Boot Lake, BWCAW, St. Louis Co. MN | 0.1652 |
| 022 | *Leersia oryzoides* | midrib | Boot Lake, BWCAW, St. Louis Co. MN | 0.0194 |
| 023 | *Leersia oryzoides* | leaf blade | Boot Lake, BWCAW, St. Louis Co. MN | 0.0899 |
| 024 | *Leersia oryzoides* | roots | Boot Lake, BWCAW, St. Louis Co. MN | 0.0127 |
| 025 | *Typha angustifolia* | Inflorescence | Shakopee Lake, Mille Lacs Co. MN | 0.0492 |

| Sample | Plant or Soil Sample Processed | Plant Part Processed | Provenience | Wt (g) |
|---|---|---|---|---|
| 026 | *Typha angustifolia* | Inflorescence stem | Shakopee Lake, Mille Lacs Co. MN | 0.4367 |
| 027 | *Typha angustifolia* | seed | Shakopee Lake, Mille Lacs Co. MN | 0.0928 |
| 028 | *Typha angustifolia* | leaf | Shakopee Lake, Mille Lacs Co. MN | 0.3505 |
| 029 | *Typha angustifolia* | sheath | Shakopee Lake, Mille Lacs Co. MN | 0.2967 |
| 030 | *Typha angustifolia* | stem | Shakopee Lake, Mille Lacs Co. MN | 0.4679 |
| 031 | *Typha angustifolia* | root crown | Shakopee Lake, Mille Lacs Co. MN | 0.3035 |
| 032 | *Typha angustifolia* | roots | Shakopee Lake, Mille Lacs Co. MN | 0.0701 |
| 033 | *Scirpus validus* | Inflorescence | Rum River, Mille Lacs Co. MN | 0.2291 |
| 034 | *Scirpus validus* | stem | Rum River, Mille Lacs Co. MN | 0.2408 |
| 035 | *Glyceria canadensis* | lemma | Big Rice Lake, St. Louis Co. MN | 0.2003 |
| 036 | *Glyceria canadensis* | rachis | Big Rice Lake, St. Louis Co. MN | 0.0420 |
| 037 | *Glyceria canadensis* | leaf | Big Rice Lake, St. Louis Co. MN | 0.1589 |
| 038 | *Glyceria canadensis* | stem | Big Rice Lake, St. Louis Co. MN | 0.2041 |
| 039 | *Phragmites australis* | leaf | Little Trout Lake, BWCAW, St. Louis Co. MN | 0.4144 |
| 040 | *Phragmites australis* | culm | Little Trout Lake, BWCAW, St. Louis Co. MN | 0.6000 |
| 041 | *Phragmites australis* | Inflorescence | Little Trout Lake, BWCAW, St. Louis Co. MN | 0.2602 |
| 042 | *Calamagrostis canadensis* | leaf | Big Rice Lake, St. Louis Co. MN | 0.4183 |
| 043 | *Calamagrostis canadensis* | culm | Big Rice Lake, St. Louis Co. MN | 0.6904 |
| 044 | *Calamagrostis canadensis* | Inflorescence | Big Rice Lake, St. Louis Co. MN | 0.2895 |
| 045 | *Phalaris arundinacea* | Inflorescence | Tomahawk Trail, S.N.F., St. Louis Co. MN | 0.0177 |
| 046 | *Phalaris arundinacea* | leaf & sheath | Tomahawk Trail, S.N.F., St. Louis Co. MN | 0.0496 |
| 047 | *Phalaris arundinacea* | culm | Tomahawk Trail, S.N.F., St. Louis Co. MN | 0.0499 |
| 048 | *Dulichium arundinaceum* | Inflorescence | Big Rice Lake, St. Louis Co. MN | 0.0308 |
| 049 | *Dulichium arundinaceum* | leaf & sheath | Big Rice Lake, St. Louis Co. MN | 0.0388 |
| 050 | *Dulichium arundinaceum* | culm | Big Rice Lake, St. Louis Co. MN | 0.0288 |
| 051 | *Equisetum pratense* | entire plant | Kraft Lake, BWCAW, Cook Co., MN | 0.0612 |
| 052 | *Zizania palustris* var. *palustris* | culm | Little Indian Sioux River, BWCAW, St. Louis Co. MN | 0.2480 |
| 053 | *Zizania palustris* var. *palustris* | staminate lemma | Little Indian Sioux River, BWCAW, St. Louis Co. MN | 0.0652 |
| 054 | *Zizania palustris* var. *palustris* | leaf, entire | Little Indian Sioux River, BWCAW, St. Louis Co. MN | 0.1379 |
| 055 | *Zizania palustris* var. *palustris* | rachis | Little Indian Sioux River, BWCAW, St. Louis Co. MN | 0.1854 |

| Sample | Plant or Soil Sample Processed | Plant Part Processed | Provenience | Wt (g) |
|---|---|---|---|---|
| 056 | *Zizania palustris* var. *palustris* | pistillate lemma | Little Indian Sioux River, BWCAW, St. Louis Co. MN | 0.1417 |
| 057 | *Zizania palustris* var. *palustris* | leaf sheath | Little Indian Sioux River, BWCAW, St. Louis Co. MN | 0.1571 |
| 058 | *Pinus strobus* | needles | Mille Lacs Kathio State Park, Mille Lacs Co. MN | 0.2157 |
| 059 | *Pinus strobus* | bark | Mille Lacs Kathio State Park, Mille Lacs Co. MN | 0.5895 |
| 060 | *Acer rubrum* | leaf | Mille Lacs Kathio State Park, Mille Lacs Co. MN | 0.1069 |
| 061 | *Phragmites australis* | Inflorescence | Lake Ogechie, Mille Lacs Co. MN | 0.1220 |
| 062 | *Phragmites australis* | leaf | Lake Ogechie, Mille Lacs Co. MN | 0.2376 |
| 063 | *Phragmites australis* | culm | Lake Ogechie, Mille Lacs Co. MN | 0.4465 |
| 064 | *Pinus resinosa* | bark | Lake Ogechie, Mille Lacs Co. MN | 0.4512 |
| 065 | *Pinus resinosa* | needles | Lake Ogechie, Mille Lacs Co. MN | 0.2557 |
| 066 | *Calamagrostis canadensis* | Inflorescence | central Minnesota | 0.0096 |
| 067 | *Calamagrostis canadensis* | leaf | central Minnesota | 0.1595 |
| 068 | *Calamagrostis canadensis* | culm | central Minnesota | 0.3494 |
| 069 | *Panicum virgatum* | Inflorescence | central Minnesota | 0.0800 |
| 070 | *Panicum virgatum* | leaf | central Minnesota | 0.2180 |
| 071 | *Panicum virgatum* | rachis | central Minnesota | 0.0360 |
| 072 | *Panicum virgatum* | culm | central Minnesota | 0.1110 |
| 073 | *Glyceria grandis* | Inflorescence | central Minnesota | 0.0760 |
| 074 | *Glyceria grandis* | leaf | central Minnesota | 0.1220 |
| 075 | *Glyceria grandis* | rachis | central Minnesota | 0.0450 |
| 076 | *Glyceria grandis* | culm | central Minnesota | 0.1220 |
| 077 | *Poa palustris* | Inflorescence | central Minnesota | 0.0090 |
| 078 | *Poa palustris* | leaf | central Minnesota | 0.0180 |
| 079 | *Poa palustris* | culm (some rachis) | central Minnesota | 0.0670 |
| 080 | *Calamagrostis canadensis* | Inflorescence | Lake Ogechie, Mille Lacs Co. MN | 0.0780 |
| 081 | *Calamagrostis canadensis* | leaf | Lake Ogechie, Mille Lacs Co. MN | 0.1030 |
| 082 | *Calamagrostis canadensis* | culm | Lake Ogechie, Mille Lacs Co. MN | 0.1370 |
| 083 | *Poa pratensis* | Inflorescence | Lake Ogechie, Mille Lacs Co. MN | 0.0370 |
| 084 | *Poa pratensis* | leaf | Lake Ogechie, Mille Lacs Co. MN | 0.0190 |
| 085 | *Poa pratensis* | culm | Lake Ogechie, Mille Lacs Co. MN | 0.0380 |

| Sample | Plant or Soil Sample Processed | Plant Part Processed | Provenience | Wt (g) |
|---|---|---|---|---|
| 086 | *Quercus sp.* | acorn, whole | Mille Lacs Kathio State Park, Mille Lacs Co. MN | 0.6410 |
| 087 | *Quercus sp.* | acorn, shell | Mille Lacs Kathio State Park, Mille Lacs Co. MN | 0.5790 |
| 088 | *Populus grandidentata* | leaf | Mille Lacs Kathio State Park, Mille Lacs Co. MN | 0.1820 |
| 089 | *Quercus alba* | leaf | Mille Lacs Kathio State Park, Mille Lacs Co. MN | 0.1550 |
| 090 | *Ceratophyllum demersum* | leaflets | Lake Ogechie, Mille Lacs Co. MN | 0.3100 |
| 091 | *Ceratophyllum demersum* | stem | Lake Ogechie, Mille Lacs Co. MN | 0.3150 |
| 092 | *Myriophyllum verticillatum* | entire plant | Lake Ogechie, Mille Lacs Co. MN | 0.4350 |
| 093 | *Zizania palustris* var. *palustris* | awn | Shakopee Lake, Mille Lacs Co. MN | 0.0130 |
| 094 | *Zizania palustris* var. *palustris* | lemma | Shakopee Lake, Mille Lacs Co. MN | 0.1030 |
| 095 | *Zizania palustris* var. *palustris* | rachis | Shakopee Lake, Mille Lacs Co. MN | 0.0750 |
| 096 | *Zizania palustris* var. *palustris* | leaf | Shakopee Lake, Mille Lacs Co. MN | 0.1170 |
| 097 | *Zizania palustris* var. *palustris* | sheath | Shakopee Lake, Mille Lacs Co. MN | 0.2360 |
| 098 | *Zizania palustris* var. *palustris* | culm | Shakopee Lake, Mille Lacs Co. MN | 0.4190 |
| 099 | *Typha cf (may be nympha rhizome)* | rhizome | Lake Ogechie, Mille Lacs Co. MN | 5.6290 |
| 100 | *Elodea canadensis* | entire plant | Lake Ogechie, Mille Lacs Co. MN | 0.3610 |
| 101 | *Elodea canadensis* | leaf | Lake Ogechie, Mille Lacs Co. MN | 0.0510 |
| 102 | *Elodea canadensis* | stem | Lake Ogechie, Mille Lacs Co. MN | 0.1530 |
| 103 | *Ceratophyllum demersum* | leaf | Lake Ogechie, Mille Lacs Co. MN | 0.1980 |
| 104 | *Ceratophyllum demersum* | stem | Lake Ogechie, Mille Lacs Co. MN | 0.1580 |
| 105 | *Myriophyllum verticillatum* | entire plant | Lake Ogechie, Mille Lacs Co. MN | 0.2450 |
| 106 | *Larch laricina* | needles | Lake Ogechie, Mille Lacs Co. MN | 0.1162 |
| 107 | *Larch laricina* | braches | Lake Ogechie, Mille Lacs Co. MN | 0.5462 |
| 108 | *Larch laricina* | cones | Lake Ogechie, Mille Lacs Co. MN | 0.6285 |
| 109 | *Larch laricina* | bark | Lake Ogechie, Mille Lacs Co. MN | 0.6437 |
| 110 | *Cornus stolonifera* | Inflorescence | Lake Ogechie, Mille Lacs Co. MN | 0.5456 |
| 111 | *Cornus stolonifera* | leaf | Lake Ogechie, Mille Lacs Co. MN | 0.2735 |
| 112 | *Cornus stolonifera* | braches | Lake Ogechie, Mille Lacs Co. MN | 0.4405 |
| 113 | *Alnus rugosa* | female catkins | Lake Ogechie, Mille Lacs Co. MN | 0.5794 |
| 114 | *Alnus rugosa* | leaf | Lake Ogechie, Mille Lacs Co. MN | 0.5470 |
| 115 | *Alnus rugosa* | braches | Lake Ogechie, Mille Lacs Co. MN | 0.9041 |

| Sample | Plant or Soil Sample Processed | Plant Part Processed | Provenience | Wt (g) |
|---|---|---|---|---|
| 116 | *Alnus rugosa* | male catkins | Lake Ogechie, Mille Lacs Co. MN | 0.1393 |
| 117 | *Betula pumila* | leaf | Lake Ogechie, Mille Lacs Co. MN | 0.3837 |
| 118 | *Betula pumila* | stem | Lake Ogechie, Mille Lacs Co. MN | 0.4209 |
| 119 | *Carex stricta* | Inflorescence | Lake Ogechie, Mille Lacs Co. MN | 0.1480 |
| 120 | *Carex stricta* | leaf & stem | Lake Ogechie, Mille Lacs Co. MN | 0.4556 |
| 121 | *Carex sterilis* | Inflorescence | Lake Ogechie, Mille Lacs Co. MN | 0.3034 |
| 122 | *Carex sterilis* | leaf & stem | Lake Ogechie, Mille Lacs Co. MN | 0.3557 |
| 123 | *Carex lacustris* | Inflorescence | Lake Ogechie, Mille Lacs Co. MN | 0.2311 |
| 124 | *Carex lacustris* | leaf & stem | Lake Ogechie, Mille Lacs Co. MN | 0.2666 |
| 125 | *Carex comosa* | Inflorescence | Lake Ogechie, Mille Lacs Co. MN | 0.3551 |
| 126 | *Carex comosa* | leaf & stem | Lake Ogechie, Mille Lacs Co. MN | 0.4604 |
| 127 | *Thelypteris palustris* | blade | Lake Ogechie, Mille Lacs Co. MN | 0.1942 |
| 128 | *Thelypteris palustris* | petiole | Lake Ogechie, Mille Lacs Co. MN | 0.1854 |
| 129 | *Sparganium eurycarpum* | Inflorescence | Lake Ogechie, Mille Lacs Co. MN | 0.3294 |
| 130 | *Sparganium eurycarpum* | leaf & stem | Lake Ogechie, Mille Lacs Co. MN | 0.7603 |
| 131 | *Potentilla palustris* | flower & peduncle | Lake Ogechie, Mille Lacs Co. MN | 0.5295 |
| 132 | *Potentilla palustris* | stem, leaf & peduncle | Lake Ogechie, Mille Lacs Co. MN | 0.7125 |
| 133 | *Lysimachia thyrsiflora* | flower | Lake Ogechie, Mille Lacs Co. MN | 0.0877 |
| 134 | *Lysimachia thyrsiflora* | stem, leaf & roots | Lake Ogechie, Mille Lacs Co. MN | 0.3901 |
| 135 | *Iris versicolor* | flower | Lake Ogechie, Mille Lacs Co. MN | 0.2407 |
| 136 | *Iris versicolor* | stem, leaf & roots | Lake Ogechie, Mille Lacs Co. MN | 0.7352 |
| 137 | *Typha latifolia* | Inflorescence | Lake Ogechie, Mille Lacs Co. MN | 1.7522 |
| 138 | *Typha latifolia* | stem & leaves | Lake Ogechie, Mille Lacs Co. MN | 2.7078 |
| 139 | *Phalaris arundinacea* | Inflorescence | Lake Ogechie, Mille Lacs Co. MN | 0.4096 |
| 140 | *Phalaris arundinacea* | stem & leaves | Lake Ogechie, Mille Lacs Co. MN | 0.5344 |
| 141 | *Calamagrostis inexpansa* | Inflorescence | Lake Ogechie, Mille Lacs Co. MN | 0.2316 |
| 142 | *Calamagrostis inexpansa* | stem & leaves | Lake Ogechie, Mille Lacs Co. MN | 0.4041 |
| 143 | *Zizania palustris* var. *palustris (floating)* | entire plant | Lake Ogechie, Mille Lacs Co. MN | 0.5166 |
| 144 | *Zizania palustris* var. *palustris (floating)* | roots | Lake Ogechie, Mille Lacs Co. MN | 0.0881 |
| 145 | *Zizania palustris* var. *palustris (floating)* | entire plant | Lake Ogechie, Mille Lacs Co. MN | 0.5174 |

| Sample | Plant or Soil Sample Processed | Plant Part Processed | Provenience | Wt (g) |
|---|---|---|---|---|
| 146 | *Zizania palustris* var. *palustris (floating)* | roots | Lake Ogechie, Mille Lacs Co. MN | 0.1167 |
| 147 | *Zizania palustris* var. *palustris (floating)* | entire plant | Lake Ogechie, Mille Lacs Co. MN | 0.5924 |
| 148 | *Zizania palustris* var. *palustris (floating)* | roots | Lake Ogechie, Mille Lacs Co. MN | 0.0722 |
| 149 | *Zizania palustris* var. *palustris (floating)* | leaf | Lake Ogechie, Mille Lacs Co. MN | 0.0937 |
| 150 | *Zizania palustris* var. *palustris (floating)* | stem & sheath | Lake Ogechie, Mille Lacs Co. MN | 0.1339 |
| 151 | *Zizania palustris* var. *palustris (floating)* | roots | Lake Ogechie, Mille Lacs Co. MN | 0.1012 |
| 152 | *Phragmites australis* | Inflorescence | Lake Ogechie, Mille Lacs Co. MN | 0.6526 |
| 153 | *Phragmites australis* | stem | Lake Ogechie, Mille Lacs Co. MN | 2.8419 |
| 154 | *Phragmites australis* | leaf & sheath | Lake Ogechie, Mille Lacs Co. MN | 0.8277 |
| 155 | *Leersia oryzoides* | Inflorescence | Lake Ogechie, Mille Lacs Co. MN | 0.2913 |
| 156 | *Leersia oryzoides* | leaf & sheath | Lake Ogechie, Mille Lacs Co. MN | 0.5772 |
| 157 | *Leersia oryzoides* | stem | Lake Ogechie, Mille Lacs Co. MN | 0.4308 |
| 158 | *Calamagrostis canadensis* | Inflorescence | Lake Ogechie, Mille Lacs Co. MN | 0.3035 |
| 159 | *Calamagrostis canadensis* | stem | Lake Ogechie, Mille Lacs Co. MN | 0.8192 |
| 160 | *Calamagrostis canadensis* | leaf & sheath | Lake Ogechie, Mille Lacs Co. MN | 0.5194 |
| 161 | *Muhlenbergia glomerata* | Inflorescence | Lake Ogechie, Mille Lacs Co. MN | 0.0487 |
| 162 | *Muhlenbergia glomerata* | entire plant | Lake Ogechie, Mille Lacs Co. MN | 0.3358 |
| 163 | *Andropogon gerardii* | Inflorescence | SCSU campus native prairie demo planting | 0.1400 |
| 164 | *Andropogon gerardii* | entire plant | SCSU campus native prairie demo planting | 2.5078 |
| 165 | *Schizachyrium scoparium* | Inflorescence | SCSU campus native prairie demo planting | 0.0453 |
| 166 | *Schizachyrium scoparium* | entire plant | SCSU campus native prairie demo planting | 0.4217 |
| 167 | Soil from sedge mat (pinch sample) | N/A | Lake Ogechie, Mille Lacs Co. MN | 0.0027 |
| 168 | Soil from Oak/Maple stand (pinch sample) | N/A | Lake Ogechie, Mille Lacs Co. MN | 0.0222 |
| 169 | Goose Scat | N/A | Lake Ogechie, Mille Lacs Co. MN | 0.0028 |
| 170 | Muskrat Scat | N/A | Lake Ogechie, Mille Lacs Co. MN | 0.0157 |
| 171 | Soil from *Andropogon* stand (pinch sample) | N/A | Sand Prairie WMA, Stearns Co., MN | 0.0102 |
| 172 | Soil from Indian grass stand (pinch sample) | N/A | Sand Prairie WMA, Stearns Co., MN | 0.2980 |
| 173 | *Zizania palustris* var. *palustris* | entire plant | Lake Ogechie, Mille Lacs Co. MN | 0.7370 |
| 174 | *Zizania palustris* var. *palustris* | entire plant | Little Indian Sioux River, BWCAW, St. Louis Co. MN | 0.2091 |
| 175 | *Zizania palustris* var. *palustris* | 100 spikelets | Little Indian Sioux River, BWCAW, St. Louis Co. MN | 0.0267 |

# APPENDIX B

## Phytolith Lake Sediment Extraction Procedure

# PHYTOLITH LAKE SEDIMENT EXTRACTION PROCEDURE

This procedure was developed by the author over a year-long trial and error period and is optimized for extraction of wild rice phytoliths from shallow depth, highly organic lake sediments (Figure 15). Although intended for extraction from lacustrine environments, this procedure may have applications in terrestrial soils where a significant fraction of humic colloidal particles and hydrophobic long-chain humic compounds are present

## DEFLOCCULATION (DISAGGREGATION)

Step 1: wet sediment. Label six 50 ml centrifuge tubes. Weigh 1 ml scoop (1 ml = 1 $cm^3$), tare scale to zero (with scoop on), and using a metal spoon-end spatula, fill scoop with exactly 1 $cm^3$ of wet lake sediment. Record weight of sediment and transfer to 50 ml tube using spatula and squeeze bottle with 5% calgon solution (sodium hexametaphosphate: $[NaPO_3]_6$). Repeat for all samples. Fill 50 ml tubes to the 25 ml level with 5% calgon, vortex and place on shaker overnight.

Step 1: dry sediment. Label six 50 ml centrifuge tubes. Weigh 0.10 grams of dry sediment and place in 50 ml tube. If sediment has hardened, break-up before weighing. A razor blade or other sharp-edged object can be used to scrape-off fine grains from a hardened mass of sediment. Repeat for all samples. Fill 50 ml tubes to the 25 ml level with 5% calgon, vortex and place on shaker overnight.

Step 2. Next day, obtain six tall 200 ml boiling beakers numbered 1 through 6 and place in fume hood. Remove samples from shaker, fill with $H_2O$ to the 45 ml level, vortex, centrifuge (10 min, 3000 RPM), and carefully decant. Particles in calgon solution do not form a very cohesive pellet. Stop decanting if pellet falls apart. Some organics may be floating. Scoop these out before decanting and place them in the appropriately numbered, tall 200 ml boiling beakers. Fill 50 ml tubes with $H_2O$ to the 45 ml level, vortex, centrifuge (8 min, 3000 RPM) and decant. If supernatant was discolored, repeat rinse cycles until clear. Otherwise proceed to carbonate procedure.

PHYTOLITH LAKE SEDIMENT EXTRACTION PROCEDURE

CARBONATE REMOVAL AND ACID OXIDATION

Step 1. Samples should now be in a minimal amount of water. Working with gloves under the fume hood, fill a 150 ml beaker with a little over 100 ml of full strength hydrochloric acid (˜36% HCl). Fill the first tube to approximately the 5 ml level with HCl, gently swirl by hand to break up sediment and then quickly pour into the appropriate beaker. If the pellet is not breaking up by hand, place cap on tube and vortex on the lowest setting (Vortex Genie®). Fill tube again to the 5 ml level with HCl, swirl by hand and pour into beaker. Fill tube to the 5 ml level with HCl, place cap on and vortex on highest setting for a few seconds and then pour in beaker. Repeat this with 5 ml HCl one more time. Thus, about 20 ml of HCl has been used to transfer sediment sample from tube to beaker. Some particles may remain adhering to the centrifuge tube and will be rinsed in later with nitric acid. Repeat this entire process for the remaining samples. If any HCl remains in the 150 ml beaker, dilute with an excess amount of water and pour down drain.

Note on HCl reaction. HCl is added to remove carbonates, mostly calcium carbonate, from sediment. HCl is also used to remove iron (Fe); sample solution will be partially colored by Fe going into solution. The reaction is: $CaCO_3 + 2HCl \rightarrow CaCl_2 + H_2O + CO_2$. The calcium chloride goes into solution and carbon dioxide is emitted as gas.

Step 2. Place all six beakers on the hotplate in a horseshoe pattern, with the opening at the back. The hottest part of hotplate is set back slightly from the center. This will allow samples to evaporate at about the same rate. Do not use a watch glass. Set hotplate heat dial to 4 which is just under boiling (36% HCl boiling point ~110º C) and heat for 1 hour. Periodically check reaction and gently swirl beaker to break up clumps that may form in center. Do not allow samples to dry out. Sample solution color will change from light green to yellow. Remove beakers from heat.

Step 3. Set the re-pipetter on the concentrated nitric acid bottle ($HNO_3$) to 30 ml, dispense into a small beaker, and slowly pour into the first sample. An initial foaming reaction will start, but will soon subside; however, brown $NO_2$ gas will continue to be emitted. If the reaction is too vigorous and in danger of boiling over (this has never happened), use a squirt bottle with $H_2O$ to cool down reaction. When 30 ml $HNO_3$ has been added to all samples, place beakers back onto the hotplate, add a watch glass to each, and set heat to 4, which is just under boiling (69% $HNO_3$ boiling point ~120º C). After about 2.5 hours, sample solution will turn a dull yellow. Remove watch glass and evaporate off to about the 20 ml level. This evaporation will take approximately 1.5 hours. Remove samples from heat.

Step 4. When beakers have cooled slightly, pick up the first beaker, gently swirl by hand for a few seconds and pour back into its respective 50 ml centrifuge tube. Use a distilled water squirt bottle to rinse beaker and aid in transfer. Some hydrophobic humic acid materials may adhere to the inside beaker wall. These can

remain in the beaker and will be dealt with later. Fill tube to the 45 ml level and cap. Repeat for remaining samples. Keep the inside threads of caps and the outside surface of centrifuge tubes completely clean of extraneous nitric acid. Even one drop left will migrate to the bottom of the Vortex Genie cup and dissolve the rubber, leaving black marks on the bottom of the centrifuge tubes. Further, these acids (and all other liquids used) will track to the inside of the centrifuge tube holders and the inside wall of the centrifuge. If this happens, clean all of these areas with water. Vortex, centrifuge (8 min, 3000 RPM), and decant into sink. Repeat the vortex, centrifuge, decant cycle two more times with $H_2O$. Nitric acid will react with hydrogen peroxide, so samples must be well rinsed. Finally, add 35% hydrogen peroxide ($H_2O_2$) to about the 5 or 7 ml level in each centrifuge tube, swirl by hand to loosen pellet, cap, and set aside until ready to start the next procedure. Samples can remain in the $H_2O_2$ as long as necessary; however, $H_2O_2$ will eventually change to non-reactive $H_2O$ and $O_2$.

A note on nitric acid. Nitric acid is not a strong enough oxidizing agent by itself to completely convert organic molecules to $CO_2$ and $H_2O$, but it does help to partially decompose organic compounds. Typically a catalyst such as potassium chlorate is used with $HNO_3$ to aid in oxidation. Without a catalyst added to concentrated nitric acid, $NO_2$ (brown gas) and $H_2O$ are emitted during a reaction with organics. The addition of hydrogen peroxide during the next step will finish the organic compound oxidation.

PHYTOLITH LAKE SEDIMENT EXTRACTION PROCEDURE

OXIDATION WITH HYDROGEN PEROXIDE

Step 1. If samples in 50 ml tubes did not have approximately 5 ml of $H_2O_2$ previously added, add now to all six. Swirl first sample by hand and pour into respective 200 ml boiling beaker. Add another 5 ml $H_2O_2$, swirl by hand and pour into beaker. Add 5 ml $H_2O_2$, put on cap, vortex a few seconds and pour into beaker. Repeat once more with 5 ml $H_2O_2$. Try to transfer all material. If some particles remain in 50 ml centrifuge tube, invert tube over beaker and use a minimal amount of distilled water from squeeze bottle to rinse into beaker. Repeat this procedure for the remaining samples and place beakers in a horseshoe formation on hotplate. Add enough $H_2O_2$ to raise solution to the 50 ml level. Place watch glass on all beakers, set heat to 2 (~85º C), and keep on heat until no more oxidation reaction is visible.

A reaction is indicated by foam around edge of solution surface and vigorous bubble effervescence from sediment. Highly organic sediments can take over 6 hours to completely oxidize. Sediments should be almost completely white when fully oxidized. If after 5 hours of heat, samples are still producing foam and bubbles, proceed to step 2. If after 5 hours, no foam is formed and no vigorous effervescence is present, evaporate off excess liquid to the 25 ml level and proceed to step 3.

A note on hydrogen peroxide. The boiling point of 35% $H_2O_2$ is 108º C. It is best to keep the reaction below the boiling point to avoid disassociation of $H_2O_2$ into

hydrogen gas and water. Complete oxidation of organics to $CO_2$ requires a high ratio of $H_2O_2$ to organic carbon.

Step 2. Take watch glasses off, turn heat to 4 (˜100º C) and evaporate off excess liquid to at least the 25 ml level. Add fresh $H_2O_2$ to the 50 ml level, turn off heat, and let samples in beakers sit overnight. Next day, turn heat to 4 (˜100º C) and evaporate off excess liquid to the 25 ml level.

Step 3. Turn off hotplate heat, gently swirl beakers by hand and transfer samples to their respective centrifuge tubes; while beaker is inverted over tube, use a distilled water squeeze bottle to rinse beaker walls and bottom. Fill 50 ml centrifuge tubes to the 45 ml level. It is OK if some hydrophobic humic compounds are still adhering to beaker walls. They will be dissolved with the upcoming potassium hydroxide (KOH) step. If humic compounds are floating on surface of liquid in centrifuge tubes, scoop into respective beaker with a metal spoon-end spatula and rinse off with water. Turn hotplate to 1 and place glass reagent jar with 10% KOH on hotplate to warm. Do not over heat KOH. Vortex samples, centrifuge (8 min at 3000 RPM) and decant. Add $H_2O$ to the 45 ml level, vortex, centrifuge (8 min at 3000 RPM) and decant.

Step 4. Take the first sample and fill tube to about the 5 ml level with warm (not hot) 10% potassium hydroxide (KOH), swirl tube by hand and empty back into respective 200 ml boiling beaker. Fill with KOH again to the 5 ml level, swirl by hand and empty into beaker. Fill KOH to 5 ml level, put cap on and vortex on highest

setting for a few seconds and empty into beaker. Repeat again with another 5 ml KOH and place beaker off to the side (not on hotplate). Repeat the entire step for all remaining samples.

Step 5. There should be approximately 20 ml of KOH in each sample beaker. Pick up the first beaker and tilt on about a 45º angle. Gently and slowly, while maintaining the 45º angle, rotate beaker to wash the sides with KOH solution. This action will dissolve sticky, hydrophobic humic compounds adhering to the sides of the beaker. For a persistent chunk, use a glass rod to help break them up. Do not loose any solution while rotating beaker. As a back up, place a large watch glass on the counter and rotate the beaker over the watch glass to catch any solution. When sides are clean, transfer solution back to its respective 50 ml centrifuge tube. Using a distilled water squeeze bottle, rinse sample from inverted beaker to centrifuge tube, filling with $H_2O$ to the 45 ml level. The 200 ml boiling beakers should now be completely clean of all sample particles and can be thoroughly cleaned at sink with distilled water and put in storage.

Step 6. Vortex, centrifuge (10 minutes, 3000 RPM), and decant samples. Add 10% HCl to the 45 ml level (to return samples from basic to acidic), vortex, centrifuge (8 minutes, 3000 RPM) and decant. Add $H_2O$ to the 45 ml level, vortex, centrifuge (8 minutes, 3000 RPM) and decant. If the still-settling procedure is to be preformed the next day, then fill tubes to the 25 ml level with 5% calgon solution and place on shaker overnight. Otherwise, store without calgon until ready to shake.

A note on potassium hydroxide (KOH). Potassium hydroxide is very alkaline (strong base), and can potentially etch (pit) and dissolve phytoliths. The current stock solution of 10% KOH has a measured pH close to 14. Phytoliths with prolonged exposure to a pH above 9 have been known to dissolve. KOH in the glass reagent jar should be buffered to a pH of 10. Steps 4 through 6 should proceed as quickly as possible to minimize exposure to KOH. The addition of 10% HCL in step six is intended to return the sample to acidic conditions, as repeating $H_2O$ rinses did not adequately lower pH to a phytolith safe range.

## PHYTOLITH SEDIMENT EXTRACTION PROCEDURE

### GRAVITY SETTLING

Step 1. Shake samples overnight with 25 ml of 5% calgon. Set up six 100 ml glass graduated cylinders and fill them to the 60 ml level with 5% calgon. Remove first sample from overnight shaker, swirl by hand to get all particles into suspension and pour directly into first graduated cylinder. Using the 5% calgon squeeze bottle, rinse cap into cylinder, then rinse 50 ml tube into cylinder. Do not allow calgon solution to go past the 100 ml level in the graduated cylinder. Set automatic timer to 1 hour and start. Repeat the aforementioned procedure for all remaining samples.

The gravity settling day is also the best day to prepare the exotic diatom spike for latter addition to phytolith samples. This first round of gravity settling is the best time to start the exotic diatom preparation (see Exotic Diatom Spike Preparation procedure).

Step 2. Just before 1 hour of settling is complete, set up the vacuum pump to aspirate the top ten centimeters of supernatant in each graduated cylinder. Connect hose from pump to a 1000 ml Erlenmeyer filtering flask with a side arm hose attachment (moisten side arm with water to allow easy removal of hose from flask). Affix stopper fitted with tygon tubing with a Pasteur pipette end. Fill a tall 600 ml beaker with water (used to wash pipette between samples).

Step 3. When 1 hour has expired, turn on pump, and with one hand on the tubing and the other guiding the pipette tip, lower to the 10 centimeter level and aspirate. Remove pipette, dip completely in 600 ml beaker of $H_2O$ to wash, remove, wipe excess water off with Kim-wipe, and aspirate the next graduated cylinder sample. Repeat until all samples have been aspirated. It may be helpful to move aspirated cylinders to the side to avoid accidentally knocking over. When finished, unhook filtering flask, pour contents and rinse with distilled water at the sink.

Step 4. Set out 6 metal spatulas on brown paper towels. Add calgon to all cylinders to the 100 ml level. Insert the first spatula into the first cylinder so that the spoon-end is as close to the settled particles as possible. Vigorously stir to lift all particles into suspension, then gradually swirl and raise spatula to lift sediment higher up into the calgon solution column. Raise spatula above top of liquid and rinse spoon-end briefly using 5% calgon squirt bottle. Set timer to 1 hour and start. Repeat this step for all remaining samples. When 1 hour has expired, aspirate all samples as outlined in step 3. Two rounds of gravity settling have now been completed.

The goal is to reach a state where after 1 hour, the top 10 centimeters are completely clear (all clay-sized particles have been removed). For lake sediments examined thus far, this typically takes five rounds of settling for the upper, highly organic portion of a lake core and 4 rounds for the lower portions of a lake core. Thus, repeat step 4 at least two more times, with one change for the final gravity settling; only fill the cylinders to the 75 ml level and aspirate 10 centimeters down from there. This should leave 20 ml of solution at the bottom of each cylinder.

Step 5. Pick up first sample cylinder, swirl by hand to fully suspend particles and quickly pour into its respective 50 ml centrifuge tube. Keep cylinder inverted while using the distilled water squeeze bottle to thoroughly rinse all sediments off of surrounding walls and into centrifuge tube. Don't let water go past the 45 ml level in the tube. Repeat for all remaining samples. Vortex, centrifuge (10 minutes, 3000 RPM), and carefully decant. Pellets at this stage are fairly loose and easily disintegrate. Stop decanting when meniscus reaches the pellet; however, enough needs to be decanted to allow subsequent transfer and rinse into a 15 ml tube.

Step 6. Label six new 15 ml centrifuge tubes. Pick up the first sample in the 50 ml tube, swirl by hand to completely loosen pellet and pour into its respective 15 ml tube. Keep 50 ml tube inverted and use distilled water squeeze bottle to rinse its side walls until the 15 ml tube is at the 14 ml level with water. Vortex, centrifuge (8 minutes, 3000 RPM), and decant. Repeat once more with 14 ml of $H_2O$. After decanting, samples should now be in a miniscule amount of $H_2O$. Read the beginning of the heavy liquid flotation procedure for more information on why this is important. Swirl samples by hand to loosen up the sediment pellet and store until ready for heavy liquid flotation.

PHYTOLITH LAKE SEDIMENT EXTRACTION PROCEDURE

EXOTIC DIATOM SPIKE PREPARATION

Diatom spike preparation is best conducted simultaneously with gravity settling procedure and is usually started just after the first round of settling has started. Since this procedure makes quantification of phytolith abundance possible, extra care must be taken to perform this procedure consistently and flawlessly. Inconsistent technique will result in erroneous results and interpretations.

Step 1. In the fume hood, place calibrated exotic diatom spike jar on stir plate and vigorously stir for 30 minutes (do not use heat). Obtain six 50 ml beakers, fill with 30 ml of 69% nitric acid ($HNO_3$) and place in a line. Obtain the P-200 (0.2 ml) Pipeteman and set to 200. Obtain seven P-100/200 plastic tips and place on a brown paper towel positioned in front of the six beakers.

Step 2. Remove diatom spike from stir plate and place near beakers. Put first tip on Pipeteman, insert into spike solution 2 cm, extract 0.2 ml (62,031 +/- 8505 diatoms at 95% CI) and withdraw. Expel solution into sink and discard tip. This is just a “dry run” to make sure everything is working and the motions are familiar. The main point is that all diatom extractions for the entire core, not just this set, need to be executed in a consistent manner. Replace tip and extract first spike aliquot exactly as

stated above, expel into the first 50 ml beaker and cover with a small watch glass. Pipeteman tip can be discarded. Repeat for the remaining samples.

Step 3. Place beakers on hotplate, set temperature to 4 and keep on heat for at least 4 hours. After the first 3 hours, remove watch glasses and allow $HNO_3$ solution to evaporate to about the 8 ml level. Do not allow samples to evaporate dry. If this happens, add 20 ml $HNO_3$ to beaker, sonicate for a few seconds and return to heat for a few hours. When finished heating samples, turn off heat, remove from hotplate, place watch glasses back on, and set aside in the hood until called for during the heavy liquid flotation procedure.

PHYTOLITH LAKE SEDIMENT EXTRACTION PROCEDURE

HEAVY LIQUID FLOTATION

At this point, samples should be in 15 ml centrifuge tubes with a miniscule amount of water (less than 0.1 ml). Too much water will dilute heavy liquid solution ($ZnI_2$) and reduce specific gravity to lower than 2.3 g/cm$^3$, causing some phytoliths to sink. Phytoliths have a specific gravity of 1.5 to 2.3 g/cm$^3$. If sample is in too much water, centrifuge and decant. Alternatively, let sample settle a few hours or overnight and then carefully use a Pasteur pipette fitted with bulb to extract excess water. Zinc Iodide is a very corrosive substance and will quickly tarnish and rust metal objects. Keep work area clean and all metal surfaces free from exposure to $ZnI_2$. All equipment soiled with $ZnI_2$ should first be rinsed-off into the $ZnI_2$ waist container before being rinsed at the sink.

Step 1. Using gloves, place magnetic stir bar in bottom of a 300 ml glass beaker. Using the 3-place scale and a large plastic weigh boat, weigh a total of 400 g of $ZnI_2$ and place in beaker. Immediately cover $ZnI_2$ bucket and clean any excess $ZnI_2$ from the work area. Place scoop and weigh boat on a paper towel. In the fume hood, add 119 ml of $H_2O$ and then add 28 ml of HCl. Stir with glass rod for about 30 seconds and then use large hotplate to gently heat and stir (heat setting at 1, stir setting 4 or 5). Once all $ZnI_2$ is in solution, turn off heat and stop stirring. Pour approximately 40 or 45 ml of $ZnI_2$ into a 50 ml glass graduated cylinder. Use paper towel to clean

any $ZnI_2$ that may be on the outside of the 300 ml beaker. Gently place heavy liquid gravity float into 50 ml cylinder and make sure it is floating freely and not stuck to the side of the cylinder. The bottom of the $ZnI_2$ meniscus should be at the line midway between 20 and 40 (i.e. 30), indicating that the heavy liquid is set to 2.3 $g/cm^3$. Lift float directly above the cylinder, allow to drip for a few seconds, wipe with paper towel, rinse with water directly into $ZnI_2$ waist container, and then dry with paper towel. Pour 50 ml cylinder contents back into 300 ml beaker. If the specific gravity is at 2.3 $g/cm^3$, then this step is finished. If the meniscus is reading less than 30 (i.e. closer to 20), the liquid is too light, and additional $ZnI_2$ will be needed to increase liquid density. Try adding $ZnI_2$ in increments of 5 grams to the beaker until desired specific gravity is achieved. This means that for each incremental addition, stir solution, pour 45 ml back into the cylinder and recheck with the float. If the meniscus is reading greater than 30 (i.e. closer to 40), then the liquid is too heavy (dense), and will need to be thinned. Try adding 5 ml increments of distilled $H_2O$ to the beaker until desired specific gravity is achieved. Repeat aforementioned stirring and floating steps for each incremental addition of $H_2O$.

Step 2. Once the heavy liquid is set, add $ZnI_2$ solution to the 14 ml mark in each sample centrifuge tube. Pouring heavy liquid from the beaker directly into each sample can be very messy. This is easily avoided by using the P-5000 Pipeteman fitted with a 5 ml plastic tip. Important, make sure there is no excess $ZnI_2$ solution on the outside of the sample tubes. Extraneous $ZnI_2$ solution can track onto the Vortex Genie cup and then onto the inside of the centrifuge carriages and walls. Place caps on the 15

ml centrifuge tubes, and using the Vortex Genie, thoroughly mix each sample for at least 30 seconds, inverting once to check for complete mixing of the sample from the bottom of each tube. Centrifuge samples for 5 minutes at 3000 RPM.

Step 3. While samples are spinning, acquire six 50 ml centrifuge tubes. Either re-use clean and dry tubes from the end of the still-settling procedure or label 6 new tubes. A desktop lamp is recommended for additional light (floating phytoliths will shimmer in bright light). When samples are done spinning, very slowly and carefully remove samples from centrifuge and place on work bench. Any perturbation of samples can cause floating phytoliths to sink slightly in the heavy liquid. Using two hands, one on the tube and one on the cap, slowly and gently twist caps off. Decant each sample from its 15 ml tube to its respective 50 ml tube. Decant only to the point on the 15 ml tube where it begins to taper to the base. While decanting, some phytoliths will remain adhering to the side wall of the tube. These will lessen as additional steps below are taken (especially during step 7). Do not let the meniscus reach the heavier particle pellet at the bottom. Wipe off any extraneous heavy liquid from the outside of centrifuge tubes. When all samples have been decanted into 50 ml tubes, fill each tube to the 45 ml level with $H_2O$, vortex and centrifuge for 15 minutes at 3000 RPM. This step will dilute the heavy liquid and pull the phytoliths to the bottom of the 50 ml centrifuge tube. While the 50 ml tubes are spinning, fill the 15 ml tubes with the heavy particle fraction to the 14 ml level with additional $ZnI_2$. Place caps on, and using the Vortex Genie, thoroughly mix each sample for at least 30

seconds, inverting once to check for complete mixing of the sample from the bottom of each tube. Centrifuge samples for 5 minutes at 3000 RPM.

Step 4. By this time, the 50 ml tubes should be done spinning, with the phytolith fraction now in a loose pellet at the bottom. Slowly, but steadily, decant 1st sample into a tall 600 ml beaker, but do not let the meniscus hit the loose pellet at the bottom. Use the desktop lamp for extra light and make sure no phytoliths have left the bottom of the 50 ml tube. When the phytolith pellet disintegrates, stop decanting. Pouring into the 600 ml beaker allows for backup recovery if phytolith material is accidentally decanted off (this has never been a problem, it's just a safeguard). Discard heavy liquid in the 600 ml beaker and rinse into waist container. Repeat this for all remaining samples.

Step 5. By this time, the 15 ml tubes spinning with heavy liquid for the 2nd time should be done spinning. Slowly and carefully decant 1st sample into its respective 50 ml tube from Step 4, stopping when the meniscus reaches the beginning of the tapering base. This 50 ml tube will have approximately 5 to 7 ml of diluted heavy liquid and phytolith fraction from the previous step and will now hold additional liquid. Repeat for the other samples. When this is finished, do not fill the 50 ml tubes with $H_2O$ as in Step 3. This is because there will be enough room for one more addition of decanted floating phytolith material (the 3rd and final floatation). The basic principle here is that heavy liquid needs to be diluted at a ratio of 2.5 to 1 in order for phytoliths to be pulled down at 3000 RPM. If the 50 ml tube is filled too

high with heavy liquid, there will not be enough room to add 2.5 times that volume in $H_2O$.

Step 6. Fill each 15 ml tube containing the heavy fraction with additional $ZnI_2$ heavy liquid to the 14 ml level. Place caps on, and using the Vortex Genie, thoroughly mix each sample for at least 30 seconds, inverting once to check for complete mixing of the sample from the bottom of each tube. Centrifuge samples for 5 minutes at 3000 RPM. This will be the third and last round of heavy liquid flotation. While samples are spinning obtain 6 long metal spatulas, fill a 300 ml beaker with water and place near work area. When samples are done spinning, carefully remove from centrifuge and remove caps.

Step 7. At this point, there should be little to no phytolith grains visibly floating; however, often there is a thin ring of phytoliths adhering at the liquid surface/side wall interface (around the 14 ml level or just under). These phytoliths can often be seen by tilting the 15 ml tube on an angle and rotating under bright light. Using a metal spatula, insert the wide-spoon end and gently scrape the side wall at around the 13.5 to 14 ml level using a circular motion for a few seconds. The spoon-end will fit almost exactly in the 15 ml tube and touch the side wall tangentially. Remove the spatula, hold over its respective 50 ml tube, rinse off with distilled water bottle and place in the beaker of water. Decant this sample into its respective 50 ml tube as previously done. Repeat this step for all remaining samples.

Step 8. All of the phytolith extracts are now in the 50 ml centrifuge tubes. Fill these tubes to the 45 ml level, vortex and centrifuge for 15 minutes at 3000 RPM. The 15 ml tubes contain material that sank during the floatation process. Decant the supernatant into a beaker and transfer to the $ZnI_2$ waist container. Fill each tube to the 14 ml level, vortex, centrifuge (5 minutes, 3000 RPM), and decant as above. If saving the sink material to look for unfloated phytoliths, rinse, vortex, centrifuge and decant one more time, otherwise, these tubes can now be discarded.

Step 9. When the 50 ml tubes are done spinning, carefully decant exactly as stated in step 4. There should be about 5 ml of liquid left in each tube. Obtain six new 15 ml centrifuge tubes and label accordingly. Carefully transfer contents of the 50 ml tubes into the new 15 ml tubes, fill to 14 ml level with $H_2O$, vortex, centrifuge 8 minutes at 3000 RPM, and decant into beaker. Repeat this process three more times. It is very important to completely remove all $ZnI_2$ from the phytolith samples. The supernatant should be completely clear with no discoloration. If all of the $ZnI_2$ is not removed, the addition of the exotic diatom spike/$HNO_3$ solution in the next step will cause a purple/red precipitate to form.

Step 10 A. Add $H_2O$ to each exotic diatom spike/$HNO_3$ solution that was boiled for 4 hours and evaporated to around 5 ml. Add enough $H_2O$ to raise the solution meniscus to just at or over the 10 ml level. Mix each sample thoroughly until the reaction is no longer visible. Next, add one diatom spike solution to each 15 ml tube with phytolith sample. Use a distilled water squeeze bottle to rinse the 50 ml

beaker contents into each 15 ml tube to the 14 ml level. If the phytolith sample is not clean enough a precipitate will form immediately upon addition of the spike solution. If this happens, do not add anymore spike solution to the remaining samples and proceed to Step 10 B. Otherwise, vortex, centrifuge (8 min, 3000 RPM) and decant. Repeat (vortex, centrifuge, decant) three more times with $H_2O$ to ensure that phytolith samples are completely clean. Samples should now be at the bottom of each 15 ml tube with a miniscule amount of water. Proceed to Step 11.

Step 10 B. Add full strength HCl to the phytolith sample with precipitate to return the $ZnI_2$ back into solution. Sonication may be necessary to help break-up larger precipitate particles. Vortex, centrifuge (8 min, 3000 RPM) and decant. Repeat once more with HCl and then 3 times with $H_2O$. The remaining samples should be rinsed twice more with RO DI (Type 1) $H_2O$ before addition of diatom spike. Return to Step 10 A for remaining samples.

Step 11. Remove six 1-dram vials from the drying oven (vials need to be dried for 24 hours before weighing) and weigh on the analytical electronic scale (4 decimal places). Use metal tweezers or forceps to handle the vials. Do not use bare hands or gloved hands (bare hands will add oil weight to the vials and gloves will add a static charge and some weight). After weighing, record weight (number 1 through 6 in note book) and place each vial in its respective position (1 through 6) in the white dram vial holder (do not label vials with marker).

Step 12. With the 1 ml (P-1000) Pipeteman and only the water already in the bottom of the tube from step 11, transfer the first sample to the first 1 dram glass vial. If there is only a millimeter or so of water above the sample, it is OK to add a few drops of RO DI (Type 1) water before transferring. Also, it may be helpful to gently agitate the sample by hand to suspended phytoliths into the water fraction. Slowly extracting and releasing solution with the Pipeteman a few times before final extraction may also help mix the sample. After first extraction and transfer, add a few drops to the empty 15 ml tube, hold up to the light, and mix gently using the Pipeteman technique. A few phytoliths will shimmer in the light. Transfer contents to the glass vial. Repeat one more time, or until all noticeable phytoliths have been removed. The basic principle here is to use an absolutely minimal amount of water to transfer phytoliths to the glass vial. At most, the vial should be 1/3 full, preferably less. The more water added, the longer it takes to evaporate, and the greater the chance for diatoms to adhere to the glass wall of the vial. Repeat for the remaining samples.

Step 13. With all of the phytolith extracts now in glass vials, leave in a safe place overnight to allow the diatom spike to settle from solution. Next day, move vials uncapped to the drying oven (50-70º C) and dry for three or four days (exact time depends on water volume). When dry, remove from drying oven and cool for 5 to 10 minutes, then record weight on the analytical scale, using metal tweezers to handle vials. Vials can now be freely handled, capped and affixed with labels.

Note on drying samples. Through a very laborious trial and error effort, RO/DI (reverse osmosis / deionized) type 1 water was determined to be the best medium to dry samples that contain an exotic fossil centric diatom spike. The centric fossil diatoms used here have decorated silica frustules and are typically 10 to 20 µm in diameter. These are basically thin, round plates that definitely do not follow Stoke's law of settling velocity. In fact, convection currents in a drying oven that is too hot, may actually keep fossil diatoms suspended at or near the liquid surface. If liquid is evaporating faster than diatoms are settling, rings will form along the side wall of the glass vial. Although alcohol is commonly used to dry phytolith extracts, evaporation may be too rapid. Further, upon addition of 95% ETOH, diatoms, and possibly other particles, commonly clumped together and dropped out of solution. Clumping of spike diatoms and deposits of diatoms on vial walls will cause an overabundance error in estimates of phytolith absolute abundance calculations.